1

Finite Element Methods

This chapter reviews some basic concepts in the mechanics of deformable bodies that are needed as foundations for the later chapters; much of the content is abstracted from References [56, 71]. First, we introduce the concept of deformation and strain, followed by stress and the equations of motion. To complete the mechanics formulation of problems, we also describe the constitutive (or material) behavior.

The chapter then reformulates the governing equations in terms of a variational principle; in this, equilibrium is seen as the achievement of a stationary value of the total potential energy. This approach lends itself well to approximate computer methods. In particular, we introduce the finite element method (FEM).

For illustrative purposes, the discussion of the finite element method will be limited to a few standard elements, some applications of which are shown in Figure 1.1.

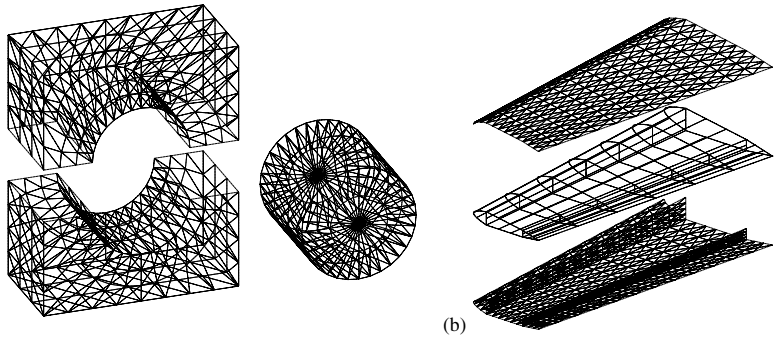

Figure 1.1: Exploded views of some FEM applications. (a) Solid bearing block and shaft modeled with tetrahedral elements (The interior edges are removed for clearer viewing). (b) Wing section modeled as a thin-walled structure discretized as collections of triangular shell elements and frame elements.

Modern Experimental Stress Analysis: completing the solution of partially specified problems. James Doyle
 ISBN 0-470-86156-8

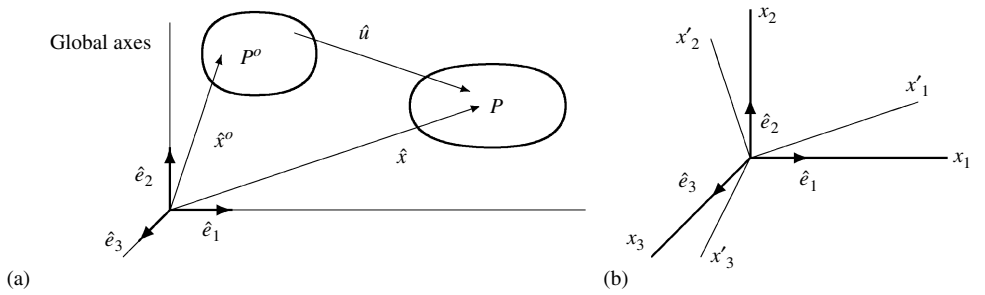

Figure 1.2: Coordinate descriptions. (a) Displacement from an undeformed to a deformed configuration. (b) Base vectors and rotated coordinate system.

More details, elaborations, and examples of FEM in general situations can be found in References [18, 45, 46, 67, 71].

1.1 Deformation and Strain

A deformation is a comparison of two states. In the mechanics of deformable bodies, we are particularly interested in the relative deformation of neighboring points because this is related to the straining of a body.

Motion and Coordinate Descriptions

Set up a common global coordinate system as shown in Figure 1.2(a) and associate x_i^o with the undeformed configuration and x_i with the deformed configuration, that is,

$$\text{initial position:} \quad \hat{x}^o = \sum\nolimits_i x_i^o \hat{e}_i \qquad\qquad \text{final position:} \quad \hat{x} = \sum\nolimits_i x_i \hat{e}_i$$

where both vectors are referred to the common set of unit vectors $\hat{e}_i$. The variables x_i^o and x_i are called the *Lagrangian* and *Eulerian* variables, respectively. A displacement is the shortest distance traveled when a particle moves from one location to another; that is,

$$\hat{u} = \hat{r} - \hat{r}^o = \sum\nolimits_i x_i \hat{e}_i - \sum\nolimits_i x_i^o \hat{e}_i \qquad \text{or} \qquad u_i = x_i - x_i^o$$

and is illustrated in Figure 1.2(a). A motion is expressed as

$$x_i = x_i(x_1^o, x_2^o, x_3^o, t) \tag{1.1}$$

which says that the trajectory of any point is uniquely identified through its original position. In this Lagrangian description, all quantities (stress, strain, and so on) are expressed in terms of the initial position coordinates and time.

The quantities we deal with (such as x_1^o, x_2^o, x_3^o, of the initial position) have components differentiated by their subscripts. These quantities are examples of what we will

begin calling *tensors*. A given tensor quantity will have different values for the components in different coordinate systems. Thus, it is important to know how these components change under a coordinate transformation.

Consider two Cartesian coordinate systems (x_1, x_2, x_3) and (x_1', x_2', x_3') as shown in Figure 1.2(b). A *base* vector is a unit vector parallel to a coordinate axis. Let $\hat{e}_1$, $\hat{e}_2$, $\hat{e}_3$ be the base vectors for the (x_1, x_2, x_3) coordinate system, and $\hat{e}_1'$, $\hat{e}_2'$, $\hat{e}_3'$ the base vectors for the (x_1', x_2', x_3') system as also shown in the figure. The transformation of components in one coordinate system into components in another is given by

$$x_i' = \sum\nolimits_j \beta_{ij} x_j \,, \qquad x_i = \sum\nolimits_j \beta_{ji} x_j' \,, \qquad \beta_{ij} \equiv \hat{e}_i' \cdot \hat{e}_j$$

where $[\,\beta_{ij}\,]$ is the matrix of *direction cosines*. This matrix is orthogonal, meaning that its transpose is its inverse.

A system of quantities is called by different tensor names depending on how the components of the system are defined in the variables x_1, x_2, x_3 and how they are transformed when the variables x_1, x_2, x_3 are changed to x_1', x_2', x_3'. A system is called a *scalar* field if it has only a single component ϕ in the variables x_i and a single component ϕ' in the variables x_i' and if ϕ and ϕ' are numerically equal at the corresponding points, that is,

$$\phi(x_1, x_2, x_3) = \phi'(x_1', x_2', x_3')$$

Temperature, volume, and mass density are examples of scalar fields. A system is called a *vector* field or a tensor field of order one if it has three components V_i in the variables x_i' and the components are related by the transformation law

$$V_i' = \sum\nolimits_k \beta_{ik} V_k \,, \qquad V_i = \sum\nolimits_k \beta_{ki} V_k'$$

As already shown, quantities such as position and displacement are first-order tensors; so also are force, velocity, and area. The tensor field of order two is a system which has nine components T_{ij} in the variables x_1, x_2, x_3, and nine components T_{ij}' in the variables x_1', x_2', x_3', and the components are related by

$$T_{ij}' = \sum\nolimits_{m,n} \beta_{im} \beta_{jn} T_{mn} \,, \qquad T_{ij} = \sum\nolimits_{m,n} \beta_{mi} \beta_{nj} T_{mn}'$$

As shown shortly, strain and stress are examples of second-order tensor fields. A special second-order tensor is the Kronecker delta, δ_{ij}, which has the same components (arranged similar to those of the unit matrix) and are the same in all coordinate systems. Tensors such as these are called isotropic tensors and are not to be confused with scalar tensors.

This sequence of defining tensors is easily extended to higher order tensors [56].

Strain Measures

As a body deforms, various points in it will translate and rotate. Strain is a measure of the "stretching" of the material points within a body; it is a measure of the relative

displacement without rigid-body motion and is an essential ingredient for the description of the constitutive behavior of materials. The easiest way to distinguish between deformation and the local rigid-body motion is to consider the change in distance between two neighboring material particles. We will use this to establish our strain measures.

There are many measures of strain in existence and we review a few of them here. Assume that a line segment of original length L_o is changed to length L, then some of the common measures of strain are the following:

$$\text{Engineering:} \quad \epsilon = \frac{\text{change in length}}{\text{original length}} = \frac{\Delta L}{L_\mathrm{o}}$$

$$\text{True:} \quad \epsilon^\mathrm{T} = \frac{\text{change in length}}{\text{final (current) length}} = \frac{\Delta L}{L} = \frac{\Delta L}{L_\mathrm{o} + \Delta L}$$

$$\text{Logarithmic:} \quad \epsilon^\mathrm{N} = \int_{L_\mathrm{o}}^{L} \text{true strain} = \int_{L_\mathrm{o}}^{L} \frac{\mathrm{d}L}{L} = \log_n \left(\frac{L}{L_\mathrm{o}} \right)$$

The relations among the measures are

$$\epsilon^\mathrm{T} = \frac{\epsilon}{1+\epsilon}, \qquad \epsilon^\mathrm{N} = \log_n(1+\epsilon)$$

An essential requirement of a strain measure is that it allow the final length to be calculated knowing the original length. This is true of each of the above since

$$\text{Engineering:} \quad L = L_\mathrm{o} + \Delta L = L_\mathrm{o} + L_\mathrm{o}\epsilon = L_\mathrm{o}(1+\epsilon)$$

$$\text{True:} \quad L = L_\mathrm{o} + \Delta L = L_\mathrm{o} + \frac{\epsilon^\mathrm{T} L_\mathrm{o}}{(1-\epsilon^\mathrm{T})} = \frac{L_\mathrm{o}}{(1-\epsilon^\mathrm{T})}$$

$$\text{Logarithmic:} \quad L = L_\mathrm{o} \exp(\epsilon^\mathrm{N})$$

The measures give different numerical values for the strain but all are equivalent in that they allow ΔL (or L) to be calculated using L_o. Because the measures are equivalent, it is a matter of convenience as to which measure is to be chosen in an analysis.

The difficulty with these strain measures is that they do not transform conveniently from one coordinate system to another. This poses a problem in developing a three-dimensional theory because the quantities involved should transform as tensors of the appropriate order. We now review a strain measure that has appropriate transformation properties.

Let two material points before deformation have the coordinates (x_i^o) and $(x_i^o + \mathrm{d}x_i^o)$; and after deformation have the coordinates (x_i) and $(x_i + \mathrm{d}x_i)$. The initial distance between these neighboring points is given by

$$\mathrm{d}S_o^2 = \sum\nolimits_i \mathrm{d}x_i^o \mathrm{d}x_i^o = (\mathrm{d}x_1^o)^2 + (\mathrm{d}x_2^o)^2 + (\mathrm{d}x_3^o)^2$$

and the final distance between the points by

$$\mathrm{d}S^2 = \sum\nolimits_i \mathrm{d}x_i \mathrm{d}x_i = \sum\nolimits_{i,j,m} \frac{\partial x_m}{\partial x_i^o} \frac{\partial x_m}{\partial x_j^o} \mathrm{d}x_i^o \mathrm{d}x_j^o$$

where $\partial x_m/\partial x_i^o$ is called the *deformation gradient* and, as per the motion of Equation (1.1), the deformed coordinates are considered a function of the original coordinates. Only in the event of stretching or straining is $\mathrm{d}S^2$ different from $\mathrm{d}S_o^2$, that is,

$$\mathrm{d}S^2 - \mathrm{d}S_o^2 = \mathrm{d}S^2 - \sum\nolimits_i \mathrm{d}x_i^o \mathrm{d}x_i^o = \sum\nolimits_{i,j,m} \left[\frac{\partial x_m}{\partial x_i^o} \frac{\partial x_m}{\partial x_j^o} - \delta_{ij} \right] \mathrm{d}x_i^o \mathrm{d}x_j^o$$

is a measure of the relative displacements. It is insensitive to rotation as can be easily demonstrated by considering a rigid-body motion. These equations can be written as

$$\mathrm{d}S^2 - \mathrm{d}S_o^2 = \sum\nolimits_{i,j} 2E_{ij} \mathrm{d}x_i^o \mathrm{d}x_j^o \,, \qquad E_{ij} \equiv \frac{1}{2} \sum\nolimits_m \left[\frac{\partial x_m}{\partial x_i^o} \frac{\partial x_m}{\partial x_j^o} - \delta_{ij} \right] \tag{1.2}$$

by introducing the strain measure E_{ij}. It is easy to observe that E_{ij} is a symmetric tensor of the second order. It is called the Lagrangian strain tensor.

Sometimes it is convenient to deal with displacements and displacement gradients instead of the deformation gradient. These are obtained by using the relations

$$x_m = x_m^o + u_m \,, \qquad \frac{\partial x_m}{\partial x_i^o} = \frac{\partial u_m}{\partial x_i^o} + \delta_{im}$$

The Lagrangian strain tensor is written in terms of the displacement by

$$E_{ij} = \frac{1}{2} \left[\frac{\partial u_i}{\partial x_j^o} + \frac{\partial u_j}{\partial x_i^o} + \sum\nolimits_m \frac{\partial u_m}{\partial x_i^o} \frac{\partial u_m}{\partial x_j^o} \right]$$

Typical expressions for E_{ij} in unabridged notations are

$$\begin{aligned}
E_{11} &= \frac{\partial u_1}{\partial x_1^o} + \frac{1}{2} \left[\left(\frac{\partial u_1}{\partial x_1^o} \right)^2 + \left(\frac{\partial u_2}{\partial x_1^o} \right)^2 + \left(\frac{\partial u_3}{\partial x_1^o} \right)^2 \right] \\
E_{22} &= \frac{\partial u_2}{\partial x_2^o} + \frac{1}{2} \left[\left(\frac{\partial u_2}{\partial x_2^o} \right)^2 + \left(\frac{\partial u_2}{\partial x_2^o} \right)^2 + \left(\frac{\partial u_3}{\partial x_2^o} \right)^2 \right] \\
E_{12} &= \frac{1}{2} \left(\frac{\partial u_1}{\partial x_2^o} + \frac{\partial u_2}{\partial x_1^o} \right) + \frac{1}{2} \left[\frac{\partial u_1}{\partial x_1^o} \frac{\partial u_1}{\partial x_2^o} + \frac{\partial u_2}{\partial x_1^o} \frac{\partial u_2}{\partial x_2^o} + \frac{\partial u_3}{\partial x_1^o} \frac{\partial u_3}{\partial x_2^o} \right]
\end{aligned} \tag{1.3}$$

Note the presence of the nonlinear terms.

Principal Strains and Strain Invariants

Consider the line segment before deformation as a vector $\mathrm{d}\hat{S}^o = \sum_i \mathrm{d}x_i^o \hat{e}_i$. We can then interpret Equation (1.2) as a vector product relation

$$\mathrm{d}S^2 - \mathrm{d}S_o^2 = 2 \sum\nolimits_j V_j \mathrm{d}x_j^o = 2\hat{V} \cdot \mathrm{d}\hat{S}^o \,, \qquad V_j \equiv \sum\nolimits_i E_{ij} \mathrm{d}x_i^o \tag{1.4}$$

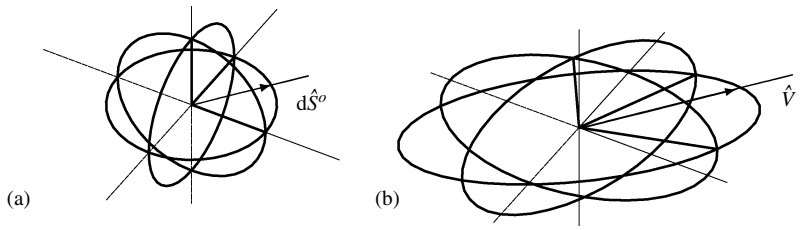

Figure 1.3: The ellipsoid of strain. (a) Traces of the vector $d\hat{S}^o$. (b) Traces of the vector $\hat{V}$.

Consider different initial vectors $d\hat{S}^o$ each of the same size but of different orientations; they will correspond to different vectors $\hat{V}$. Figure 1.3 shows a collection of such vectors where $d\hat{S}^o$ traces out the coordinate circles of a sphere. Note that $\hat{V}$ traces an ellipse and many such traces would form an ellipsoid, that is, the sphere traced by $d\hat{S}^o$ is transformed into an ellipsoid traced by $\hat{V}$.

In general, the vectors $d\hat{S}^o$ and $\hat{V}$ are not parallel. An interesting question to ask, however, is the following: are there any initial vectors that have the same orientation before and after transformation? The answer will give an insight into the properties of all second- order tensors, not just strain but also stress and moments of inertia, to name two more.

To generalize the results, we will consider the symmetric second-order tensor T_{ij}, and unit initial vectors $n_i = dx_i^o/dS^o$. Assume that there is an $\hat{n}$ such that it is proportional to $\hat{V}$, that is,

$$V_i = \sum\nolimits_j T_{ij} n_j = \lambda n_i \qquad \text{or} \qquad \sum\nolimits_j \left[T_{ij} - \lambda \delta_{ij}\right] n_j = 0$$

This is given in expanded matrix form as

$$\begin{bmatrix} T_{11} - \lambda & T_{12} & T_{13} \\ T_{12} & T_{22} - \lambda & T_{23} \\ T_{13} & T_{23} & T_{33} - \lambda \end{bmatrix} \begin{Bmatrix} n_1 \\ n_2 \\ n_3 \end{Bmatrix} = 0$$

This is an eigenvalue problem and has a nontrivial solution for n_i only if the determinant of the coefficient matrix vanishes. Expanding the determinantal equation, we obtain the characteristic equation

$$\lambda^3 - I_1 \lambda^2 + I_2 \lambda - I_3 = 0$$

where the invariants I_1, I_2, I_3 are defined as

$$\begin{aligned} I_1 &= \sum\nolimits_i T_{ii} = T_{11} + T_{22} + T_{33} \\ I_2 &= \sum\nolimits_{i,j} \frac{1}{2} [T_{ii} T_{jj} - T_{ij} T_{ji}] = T_{11}T_{22} + T_{22}T_{33} + T_{33}T_{11} - T_{12}^2 - T_{23}^2 - T_{13}^2 \\ I_3 &= \det[T_{ij}] = T_{11}T_{22}T_{33} + 2T_{12}T_{23}T_{13} - T_{11}T_{23}^2 - T_{22}T_{13}^2 - T_{33}T_{12}^2 \end{aligned} \tag{1.5}$$

The characteristic equation yields three roots or possible values for λ: $\lambda^{(1)}$, $\lambda^{(2)}$, $\lambda^{(3)}$. These are called the *eigenvalues* or *principal* values. For each principal value there is a

corresponding solution for $\hat{n}$: $\hat{n}^{(1)}$, $\hat{n}^{(2)}$, $\hat{n}^{(3)}$. The three $\hat{n}$s are called the *eigenvectors* or *principal directions*.

The principal values can be computed from the invariants [143] by first defining

$$Q = \tfrac{1}{9}[I_1^2 - 3I_2]\,, \qquad R = \tfrac{1}{54}[-2I_1^3 + 9I_1I_2 - 27I_3]\,, \qquad \theta = \cos^{-1}[R/\sqrt{Q^3}]$$

then

$$\lambda_1 = \tfrac{1}{3}I_1 - 2\sqrt{Q}\cos\left(\tfrac{1}{3}\theta\right)\,, \qquad \lambda_2, \lambda_3 = \tfrac{1}{3}I_1 - 2\sqrt{Q}\cos\left(\tfrac{1}{3}(\theta \pm 2\pi)\right) \tag{1.6}$$

For two-dimensional problems where $T_{13} = 0$ and $T_{23} = 0$, this simplifies to

$$\lambda_1, \lambda_2 = \tfrac{1}{2}[T_{11} + T_{22}] \pm \tfrac{1}{2}\sqrt{[T_{11} - T_{22}]^2 + 4T_{12}^2}\,, \qquad \lambda_3 = T_{33} \tag{1.7}$$

These can easily be obtained from the Mohr's circle [48].

It is now of interest to know what the components T_{ij} are when transformed to the coordinate system defined by the principal directions. Let the transformed coordinate system be defined by the triad

$$\hat{e}'_1 = \hat{n}^{(1)}, \qquad \hat{e}'_2 = \hat{n}^{(2)}, \qquad \hat{e}'_3 = \hat{n}^{(3)}$$

Then the transformation matrix of direction cosines is given by

$$\beta_{ij} = \hat{e}'_i \cdot \hat{e}_j = \hat{n}^{(i)} \cdot \hat{e}_j = \sum\nolimits_k n_k^{(i)} \hat{e}_k \cdot \hat{e}_j = n_j^{(i)} \qquad \text{and} \qquad \beta_{ki} = n_i^{(k)}$$

From the eigenvalue problem, we have for the k^{th} eigenmode

$$\sum\nolimits_j T_{ij} n_j^{(k)} = \lambda^{(k)} n_i^{(k)} \qquad \text{or} \qquad \sum\nolimits_j T_{ij}\beta_{kj} = \lambda^{(k)}\beta_{ki}$$

Multiply both sides by β_{li} and sum over i; recognizing the left-hand side as the transform of T_{ij} and the right-hand side as the Kronecker delta (because of the orthogonality of β_{ij}) gives

$$T'_{lk} = \lambda^{(k)}\delta_{kl} \qquad \text{or} \qquad \begin{bmatrix} T'_{11} & T'_{12} & T'_{13} \\ & T'_{22} & T'_{23} \\ sym & & T'_{33} \end{bmatrix} = \begin{bmatrix} \lambda^{(1)} & 0 & 0 \\ 0 & \lambda^{(2)} & 0 \\ 0 & 0 & \lambda^{(3)} \end{bmatrix}$$

that is, T_{ij} has a diagonal form when transformed to the principal coordinates. We can further show [56] that the $\lambda^{(i)}$s are the extremums of the associated ellipsoid surface.

The properties just established are valid for all symmetric second-order tensors.

Infinitesimal Strain and Rotation

The full nonlinear deformation analysis of problems is quite difficult and so simplifications are often sought. Three situations for the straining of a block are shown in

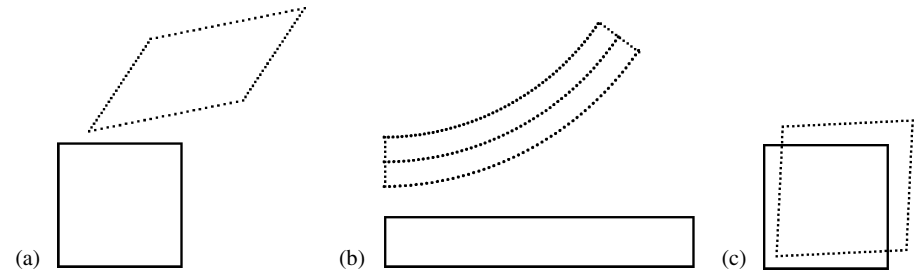

Figure 1.4: Combinations of displacements and strains. (a) Large displacements, rotations, and strains. (b) Large displacements and rotations but small strains. (c) Small displacements, rotations, and strains.

Figure 1.4. The general case is that of large displacements, large rotations, and large strains. In the chapters dealing with the linear theory, the displacements, rotations, and strains are small, and Case (c) prevails. Nonlinear analysis of thin-walled structures such as shells is usually restricted to Case (b), where the deflections and rotations can be large but the strains are small. This is a reasonable approximation because structural materials do not exhibit large strains without yielding and structures are designed to operate without yielding.

If the displacement gradients are small, that is,

$$\left| \frac{\partial u_i}{\partial x_j^o} \right| \ll 1$$

then the nonlinear product terms in the strain tensor definition can be neglected. The result is

$$E_{ij} \simeq \epsilon_{ij} = \frac{1}{2} \left(\frac{\partial u_i}{\partial x_j^o} + \frac{\partial u_j}{\partial x_i^o} \right)$$

where ϵ_{ij} is the infinitesimal strain tensor. This assumption also leads to the conclusion that the components E_{ij} are small as compared with unity.

If, in addition to the above, the following condition on the size of the displacements exists

$$\left| \frac{u_i}{L} \right| \ll 1$$

where L is the smallest dimension of the body, then

$$x_i \simeq x_i^o$$

and the distinction between the Lagrangian and Eulerian variables vanishes. Henceforth, when we use the small-strain approximations, ϵ_{ij} will be used to denote the strain tensor, and x_i will denote both Lagrangian and Eulerian variables.

1.2 Tractions and Stresses

The kinetics of rigid bodies are described in terms of forces; the equivalent concept for continuous media is stress (loosely defined as force over unit area). Actions can be exerted on a continuum through either contact forces or forces contained in the mass. The contact force is often referred to as a surface force or traction as its action occurs on a surface. We are primarily concerned with contact forces but acting inside the body.

Cauchy Stress Principle

Consider a small surface element of area ΔA on an imagined exposed surface A in the deformed configuration as depicted in Figure 1.5. There must be resultant forces and moments acting on ΔA to make it equipollent to the effect of the rest of the material, that is, when the pieces are put back together, these forces cancel each other. Let these forces be thought of as contact forces and so give rise to contact stresses (even though they are inside the body). Cauchy formalized this by introducing his concept of traction vector.

Let $\hat{n}$ be the unit vector that is perpendicular to the surface element ΔA and let $\Delta \hat{F}$ be the resultant force exerted from the other part of the surface element with the negative normal vector. We assume that as ΔA becomes vanishingly small, the ratio $\Delta \hat{F}/\Delta A$ approaches a definite limit $\mathrm{d}\hat{F}/\mathrm{d}A$. The vector obtained in the limiting process

$$\lim_{\Delta A \to 0} \frac{\Delta \hat{F}}{\Delta A} = \frac{\mathrm{d}\hat{F}}{\mathrm{d}A} \equiv \hat{t}^{(\hat{n})}$$

is called the *traction vector*. This vector represents the force per unit area acting on the surface, and its limit exists because the material is assumed continuous. The superscript $\hat{n}$ is a reminder that the traction is dependent on the orientation of the exposed area.

To give explicit representation of the traction vector, consider its components on the three faces of a cube as shown in Figure 1.6(a). Because this description is somewhat cumbersome, we simplify the notation by introducing the components

$$\sigma_{ij} \equiv t_j^{(\hat{e}_i)} \qquad \text{e.g.} \qquad \sigma_{11} \equiv t_1^{(\hat{e}_1)}, \quad \sigma_{13} \equiv t_3^{(\hat{e}_1)}, \quad \sigma_{31} \equiv t_1^{(\hat{e}_3)}, \quad \ldots$$

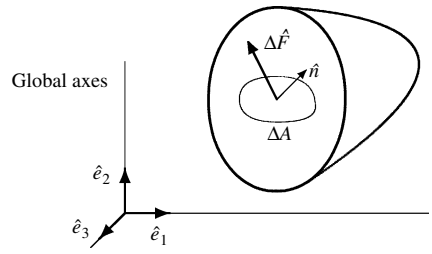

Figure 1.5: Exposed forces on an arbitrary section cut.

where i refers to the face and j to the component. The normal projections of $\hat{t}^{(\hat{n})}$ on these special faces are the normal stress components σ_{11}, σ_{22}, σ_{33}, while projections perpendicular to $\hat{n}$ are shear stress components σ_{12}, σ_{13}; σ_{21}, σ_{23}; σ_{31}, σ_{32}.

It is important to realize that while $\hat{t}$ resembles the elementary idea of stress as force over area, it is not stress; $\hat{t}$ transforms as a vector and has only three components. The tensor σ_{ij} is our definition of stress; it has nine components with units of force over area, but at this stage we do not know how these components transform.

Tractions on Arbitrary Planes

The traction vector $\hat{t}^{(\hat{n})}$ acting on an area $\mathrm{d}A\hat{n}$ depends on the normal $\hat{n}$ of the area. The particular relation can be obtained by considering a traction on an arbitrary surface of the tetrahedron shown in Figure 1.7 formed from the stressed cube of Figure 1.6. The vector acting on the inclined surface ABC is $\hat{t}$ and the unit normal vector $\hat{n}$. The equilibrium of the tetrahedron requires that the resultant force acting on it must vanish.

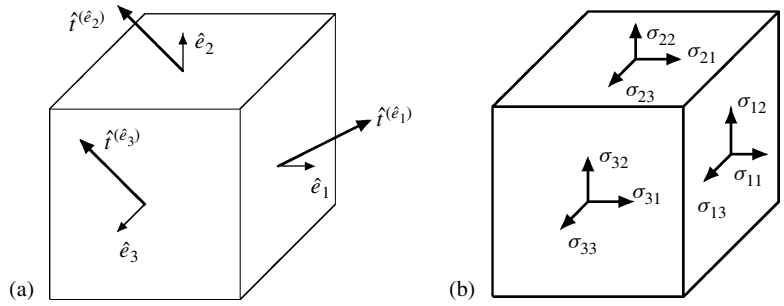

Figure 1.6: Stressed cube. (a) Traction components. (b) Stress components.

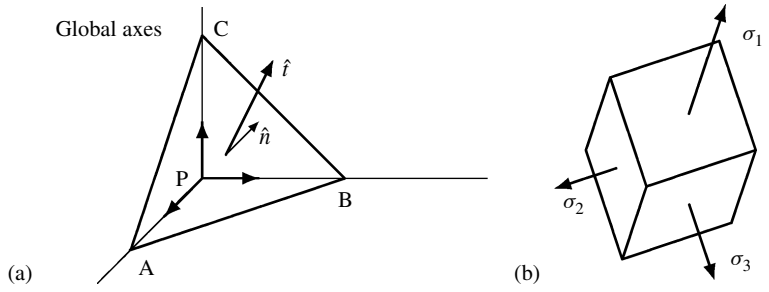

Figure 1.7: Tractions on particular planes. (a) Tetrahedron with exposed traction. (b) Cube with principal stresses.

From the equation for the balance of forces in the x_1-direction for the tetrahedron, and letting $h \to 0$, we obtain

$$t_1 = \sigma_{11} n_1 + \sigma_{21} n_2 + \sigma_{31} n_3 = \sum\nolimits_j \sigma_{j1} n_j$$

Similar equations can be derived from the consideration of the balance of forces in the x_2- and x_3-directions. These three equations can be written collectively as

$$t_i = \sum\nolimits_j \sigma_{ji} n_j \tag{1.8}$$

This compact relation says that we need only know nine numbers $[\sigma_{ij}]$ to be able to determine the traction vector on any area passing through a point. These elements are called the Cauchy stress components and form the Cauchy stress tensor. It is a second-order tensor because t_i and n_j transform as first-order tensors. Later, through consideration of equilibrium, we will establish that it is symmetric.

The traction vector $\hat{t}$ acting on a surface depends on the direction $\hat{n}$ and is usually not parallel to $\hat{n}$. Consider the normal component acting on the face

$$\sigma_n = \hat{t} \cdot \hat{n} = \sum\nolimits_i t_i n_i = \sum\nolimits_{i,j} \sigma_{ij} n_i n_j$$

If we make the associations

$$t_i \longrightarrow V_i\,, \qquad n_i \longrightarrow \mathrm{d}x_i^o\,, \qquad \sigma_{ij} \longrightarrow E_{ij}$$

then we may infer that the behavior of the normal stress component is the same as that for the stretching of Equation (1.4). In particular, the stress tensor $[\,\sigma_{ij}\,]$ has principal values (called *principal stresses*) and a corresponding set of principal directions. The principal stresses are shown in Figure 1.7(b); note that the shear stresses are zero on a principal cube. It is usual to order the principal stress according to

$$\sigma_3 < \sigma_2 < \sigma_1$$

These values can be computed according to the formulas of Equation (1.6).

Stress Referred to the Undeformed Configuration

Stress is most naturally established in the deformed configuration, but we have chosen to use the Lagrangian variables (i.e., the undeformed configuration) for the description of a body with finite deformation. For consistency, we need to introduce a measure of stress referred to the undeformed configuration. To help appreciate the new definitions of stress to be introduced, it is worthwhile to keep the following in mind:

- The traction vector is first defined in terms of a force divided by area.
- The stress tensor is then defined according to a transformation relation for the traction and area normal.

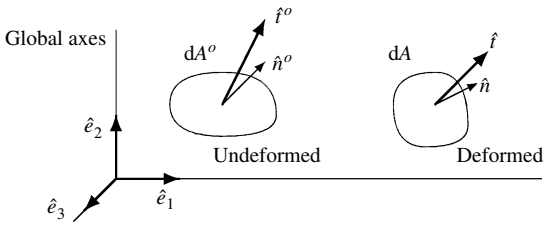

Figure 1.8: Traction vectors in the undeformed and deformed configurations.

To refer our description of tractions to the surface before deformation, we must define a traction vector $\hat{t}^o$ acting on an area dA^o as indicated in Figure 1.8. The introduction of such a vector is somewhat arbitrary, so we first reconsider the Cauchy stress so as to motivate the developments.

In the deformed state, on every plane surface passing through a point, there is a traction vector $\hat{t}_i$ defined in terms of the deformed surface area; that is, letting the traction vector be $\hat{t}$ and the total resultant force acting on dA be $d\hat{F}$, then

$$\hat{t} \equiv \frac{d\hat{F}}{dA} \qquad \text{or} \qquad t_i \equiv \frac{dF_i}{dA}$$

Let all the traction vectors and unit normals in the deformed body form two respective vector spaces. Then, the Cauchy stress tensor σ_{ij} was shown to be the transformation between these two vector spaces, that is,

$$t_i = \sum\nolimits_j \sigma_{ji} n_j$$

Defined in this manner, the Cauchy stress tensor is an abstract quantity; however, on special plane surfaces such as those with unit normals parallel to $\hat{e}_1$, $\hat{e}_2$, and $\hat{e}_3$, respectively, the nine components of $[\,\sigma_{ij}\,]$ can be related to the traction vector and thus have physical meaning; that is, the meaning of σ_{ij} is the components of stress derived from the force vector dF_i divided by the deformed area. This, in elementary terms, is called *true stress*.

We will now do a parallel development for the undeformed configuration. Let the resultant force $d\hat{F}^o$, referred to the undeformed configuration, be given by a transformation of the force $d\hat{F}$ acting on the deformed area. One possibility is to take $dF_i^o = dF_i$, and this gives rise to the so-called Lagrange stress tensor, which in simple terms would correspond to "force divided by original area." Instead, let

$$dF_i^o = \sum\nolimits_j \frac{\partial x_i^o}{\partial x_j} dF_j$$

which follows the analogous rule for the deformation of line segments. The reason for this choice will become apparent later when we consider the equations of motion. It is

important to realize that this is not a rotation transformation but that the force components are being "deformed". The Kirchhoff traction vector is defined as

$$t_i^o \equiv \frac{\mathrm{d}F_i^o}{\mathrm{d}A^o} = \sum\nolimits_j \frac{\partial x_i^o}{\partial x_j} \frac{\mathrm{d}F_j}{\mathrm{d}A^o}$$

This leads to the definition of the Kirchhoff stress tensor σ_{ij}^K:

$$t_i^o = \sum\nolimits_j \sigma_{ji}^K n_j^o$$

The meaning of σ_{pq}^K components of stress derived from the transformed components of the force vector, divided by the original area. There is no elementary equivalence to this stress. This stress is often referred to as the second Piola–Kirchhoff stress tensor; we will abbreviate it simply as the Kirchhoff stress tensor.

It can be shown [56] that the relation between the Kirchhoff and Cauchy stress tensors is

$$\sigma_{ji}^K = \sum\nolimits_{m,n} \frac{\rho^o}{\rho} \frac{\partial x_i^o}{\partial x_m} \frac{\partial x_j^o}{\partial x_n} \sigma_{mn}, \qquad \sigma_{ji} = \sum\nolimits_{m,n} \frac{\rho}{\rho^o} \frac{\partial x_i}{\partial x_m^o} \frac{\partial x_j}{\partial x_n^o} \sigma_{mn}^K \tag{1.9}$$

where ρ is the mass density. We will show that the Cauchy stress tensor is symmetric, hence these relations show that the Kirchhoff stress tensor is also a symmetric tensor.

1.3 Governing Equations of Motion

Newton's laws for the equation of motion of a rigid body will be used to establish the equations of motion of a deformable body. It will turn out, however, that they are not the most suitable form, and we look at other formulations. In particular, we look at the forms arising from the principle of virtual work and leading to stationary principles such as Hamilton's principle and Lagrange's equation.

Strong and Weak Formulations

Consider an arbitrary volume V taken from the deformed body as shown in Figure 1.9; it has tractions $\hat{t}$ on the boundary surface A, and body force per unit mass $\hat{b}$. Newton's laws of motion become

$$\int_A \hat{t}\,\mathrm{d}A + \int_V \rho\hat{b}\,\mathrm{d}V = \int_V \rho\ddot{\hat{u}}\,\mathrm{d}V$$

$$\int_A \hat{x} \times \hat{t}\,\mathrm{d}A + \int_V \hat{x} \times \hat{b}\rho\,\mathrm{d}V = \int_V \hat{x} \times \ddot{\hat{u}}\,\rho\,\mathrm{d}V$$

where ρ is the mass density. These are the equations of motion in terms of the traction. We now state the equations of motion in terms of the stress. In doing this, there is a choice between using the deformed state and the undeformed state.

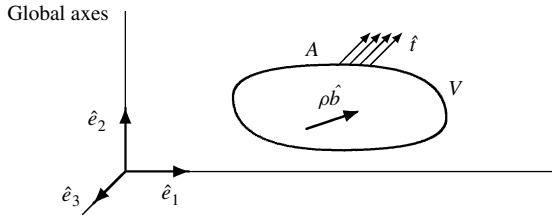

Figure 1.9: Arbitrary small volume taken from the deformed configuration.

Reference [56] shows how the stress-traction relation, $t_i = \sum_j \sigma_{ji} n_j$, combined with the integral theorem can be used to recast the first equilibrium equation into the form

$$\begin{aligned}
\frac{\partial \sigma_{11}}{\partial x_1} + \frac{\partial \sigma_{21}}{\partial x_2} + \frac{\partial \sigma_{31}}{\partial x_3} + \rho b_1 &= \rho \ddot{u}_1 \\
\frac{\partial \sigma_{12}}{\partial x_1} + \frac{\partial \sigma_{22}}{\partial x_2} + \frac{\partial \sigma_{32}}{\partial x_3} + \rho b_2 &= \rho \ddot{u}_2 \\
\frac{\partial \sigma_{13}}{\partial x_1} + \frac{\partial \sigma_{23}}{\partial x_2} + \frac{\partial \sigma_{33}}{\partial x_3} + \rho b_3 &= \rho \ddot{u}_3
\end{aligned} \tag{1.10}$$

and that the second becomes $\sigma_{ij} = \sigma_{ji}$, showing the symmetry of the stress tensor. The statement of a problem in terms of a set of differential equations plus the associated boundary conditions is called the *strong formulation* of the problem. The equations of motion in terms of the Kirchhoff stress are more complicated than those using the Cauchy stress because they explicitly include the deformed state. We will not state them here because the finite element formulation can be done more simply in terms of a variational form.

Let $u_i(x_i^o)$ be the displacement field, which satisfies the equilibrium equations in V. On the surface A, the surface traction t_i is prescribed on A_t and the displacement on A_u. Consider a variation of displacement δu_i (we will sometimes call this the virtual displacement), then

$$\overline{u}_i = u_i + \delta u_i$$

where u_i satisfy the equilibrium equations and the given boundary conditions. Thus, δu_i must vanish over A_u but be arbitrary over A_t. Let δW_e be the virtual work done by the body force b_i and traction t_i; that is,

$$\delta W_e = \sum_i \int_V \rho b_i \delta u_i \, \mathrm{d}V + \sum_i \int_{A_t} t_i \delta u_i \, \mathrm{d}A + \sum_i \int_{A_u} t_i \delta u_i \, \mathrm{d}A \tag{1.11}$$

After some manipulation and substitution for the traction vector, we can write the virtual work form of equilibrium as [71]

$$\delta W = \delta W_e - \sum_{m,n} \int_V \sigma_{mn} \delta \epsilon_{mn} \, \mathrm{d}V = \delta W_e - \sum_{p,q} \int_{V^o} \sigma_{pq}^K \delta E_{pq} \, \mathrm{d}V^o = 0 \tag{1.12}$$

Hence, the Cauchy stress/small-strain combination is energetically equivalent to the Kirchhoff stress/Lagrangian strain combination. In contrast to the differential equations of motion, there are no added complications using the undeformed state as reference. This formulation of the problem is known as the *weak formulation*.

The virtual work formulation is completely general, but there are further developments that are more convenient to use in some circumstances. We now look at some of these developments.

Stationary Principles

The internal virtual work is associated with the straining of the body and therefore we will use the representation

$$\delta \mathcal{U} = \sum\nolimits_{i,j} \int_V \sigma_{ij} \delta \epsilon_{ij} \, \mathrm{d}V = \sum\nolimits_{i,j} \int_{V^o} \sigma_{ij}^K \delta E_{ij} \, \mathrm{d}V^o$$

and call $\mathcal{U}$ the strain energy of the body.

A system is *conservative* if the work done in moving the system around a closed path is zero. We say that the external force system is conservative if it can be obtained from a potential function. For example, for a set of discrete forces, we have

$$P_i = -\frac{\partial \mathcal{V}}{\partial u_i} \qquad \text{or} \qquad \mathcal{V} = -\sum\nolimits_i P_i u_i$$

where u_i is the displacement associated with the load P_i, and $\mathcal{V}$ is the potential. The negative sign in the definition of $\mathcal{V}$ is arbitrary, but choosing it so gives us the interpretation of $\mathcal{V}$ as the capacity (or potential) to do work. The external work term now becomes

$$\delta W_e = \sum\nolimits_i P_i \delta u_i = -\sum\nolimits_i \frac{\partial \mathcal{V}}{\partial u_i} \delta u_i = -\delta \mathcal{V}$$

We get almost identical representations for conservative body forces and conservative traction distributions. The principle of virtual work can be rewritten as

$$\delta \mathcal{U} + \delta \mathcal{V} = 0 \qquad \text{or} \qquad \delta \Pi \equiv \delta[\mathcal{U} + \mathcal{V}] = 0 \tag{1.13}$$

The term inside the brackets is called the *total potential energy*. This relation is called the *principle of stationary potential energy*. We may now restate the principle of virtual work as follows: *For a conservative system to be in equilibrium, the first-order variation in the total potential energy must vanish for every independent admissible virtual displacement*. Another way of stating this is as follows: among all the displacement states of a conservative system that satisfy compatibility and the boundary constraints, those that also satisfy equilibrium make the potential energy stationary. In comparison to the conservation of energy theorem, this is much richer, because instead of one equation it leads to as many equations as there are degrees of freedom (independent displacements).

To apply the idea of virtual work to dynamic problems, we need to account for the presence of inertia forces, and the fact that all quantities are functions of time. The inertia leads to the concept of *kinetic energy*, defined as

$$\mathcal{T} \equiv \frac{1}{2}\sum\nolimits_i \int_V \rho \dot{u}_i \dot{u}_i \, \mathrm{d}V \qquad \text{such that} \qquad \delta\,\mathcal{T} \equiv \sum\nolimits_i \int_V \rho \dot{u}_i \, \delta\dot{u}_i \, \mathrm{d}V$$

Hamilton refined the concept that a motion can be viewed as a path in configuration space; he showed [89] that, for a system with given configurations at times t_1 and t_2, of all the possible configurations between these two times the actual that occurs satisfies a stationary principle. Hamilton integrated the equation over time and since by stipulation, the configuration has no variations at the extreme times, the virtual work relation becomes

$$\int_{t_1}^{t_2} [\delta W^s + \delta W^b + \delta\,\mathcal{T} - \delta\,\mathcal{U}] \, \mathrm{d}t = 0 \tag{1.14}$$

This equation is generally known as the *extended Hamilton's principle*. In the special case when the applied loads, both body forces and surface tractions, can be derived from a scalar potential function $\mathcal{V}$, the variations become complete variations and we can write

$$\delta \int_{t_1}^{t_2} [\,\mathcal{T} - (\mathcal{U} + \mathcal{V})] \, \mathrm{d}t = 0 \tag{1.15}$$

This equation is the one usually referred to as *Hamilton's principle*.

When we apply these stationary principles, we need to identify two classes of boundary conditions, called *essential* and *natural* boundary conditions, respectively. The essential boundary conditions are also called *geometric* boundary conditions because they correspond to prescribed displacements and rotations; these geometric conditions must be rigorously imposed. The natural boundary conditions are associated with the applied loads and are implicitly contained in the variational principle.

Lagrange's Equations

Hamilton's principle provides a complete formulation of a dynamical problem; however, to obtain solutions to some problems, the Hamilton integral formulation must be converted into one or more differential equations of motion. For a computer solution, these must be further reduced to equations using discrete unknowns; that is, we introduce some generalized coordinates (or degrees of freedom with the constrained degrees removed). At present, we will not be explicit about which coordinates we are considering but accept that we can write any function (the displacement, say) as

$$u(x, y, z) = u(u_1 g_1(x, y, z), u_2 g_2(x, y, z), \ldots, u_N g_N(x, y, z))$$

where u_i are the generalized coordinates and $g_i(x, y, z)$ are prescribed (known) functions of (x, y, z). The generalized coordinates are obtained by the imposition of *holonomic*

constraints—the constraints are geometric of the form $f_i(u_1, u_2, \ldots, u_N, t) = 0$ and do not depend on the velocities.

Hamilton's extended principle now takes the form

$$\int_{t_1}^{t_2} \sum_{j=1}^{N} \left\{ -\frac{\mathrm{d}}{\mathrm{d}t}\left(\frac{\partial \mathcal{T}}{\partial \dot{u}_j}\right) + \frac{\partial \mathcal{T}}{\partial u_j} - \frac{\partial(\mathcal{U}+\mathcal{V})}{\partial u_j} + Q_j \right\} \delta u_j \, \mathrm{d}t = 0$$

where Q_j are a set of nonconservative forces. Because the virtual displacements δu_j are independent and arbitrary, and because the time limits are arbitrary, each integrand is zero. This leads to the *Lagrange's equation of motion*:

$$\mathcal{F}_i \equiv \frac{\mathrm{d}}{\mathrm{d}t}\left(\frac{\partial \mathcal{T}}{\partial \dot{u}_i}\right) - \frac{\partial \mathcal{T}}{\partial u_i} + \frac{\partial}{\partial u_i}(\mathcal{U}+\mathcal{V}) - Q_i = 0 \tag{1.16}$$

for $i = 1, 2, \ldots, N$. The expression, $\mathcal{F}_i = 0$, is our statement of (dynamic) equilibrium. It is apparent from the Lagrange's equation that, if the system is not in motion, then we recover the principle of stationary potential energy expressed in terms of generalized coordinates.

It must be emphasized that the transition from Hamilton's principle to Lagrange's equation was possible only by identifying u_i as generalized coordinates; that is, Hamilton's principle holds true for constrained as well as generalized coordinates, but Lagrange's equation is valid only for the latter. A nice historical discussion of Hamilton's principle and Lagrange's equation is given in Reference [176].

Consider the Lagrange's equation when the motions are small. Specifically, consider small motions about an equilibrium position defined by $u_i = 0$ for all i. Perform a Taylor series expansion on the strain energy function to get

$$\mathcal{U}(u_1, u_2, \ldots) = \mathcal{U}(0) + \sum\nolimits_i \left.\frac{\partial \mathcal{U}}{\partial u_i}\right|_0 u_i + \frac{1}{2}\sum\nolimits_{i,j} \left.\frac{\partial^2 \mathcal{U}}{\partial u_i \partial u_j}\right|_0 u_i u_j + \cdots$$

The first term in this expansion is irrelevant and the second term is zero, since, by assumption, the origin is an equilibrium position. We therefore have the representation of the strain energy as

$$\mathcal{U}(u_1, u_2, \ldots) \approx \frac{1}{2}\sum\nolimits_{i,j} K_{ij} u_i u_j, \qquad K_{ij} \equiv \left.\frac{\partial^2 \mathcal{U}}{\partial u_i \partial u_j}\right|_0$$

We can do a similar expansion for the kinetic energy; in this case, however, we also assume that the system is linear in such a way that $\mathcal{T}$ is a function only of the velocities $\dot{u}_j$. This leads to

$$\mathcal{T}(\dot{u}_1, \dot{u}_2, \ldots) \approx \frac{1}{2}\sum\nolimits_{i,j} M_{ij} \dot{u}_i \dot{u}_j, \qquad M_{ij} \equiv \left.\frac{\partial^2 \mathcal{T}}{\partial \dot{u}_i \partial \dot{u}_j}\right|_0$$

The potential of the conservative forces also has an expansion similar to that for $\mathcal{U}$, but we retain only the linear terms in u_j such that

$$\mathcal{V} = -\sum\nolimits_j P_j u_j, \qquad P_j \equiv -\left.\frac{\partial \mathcal{V}}{\partial u_j}\right|_0$$

Finally, assume that the nonconservative forces are of the viscous type such that the virtual work is

$$\delta W^d = Q^d \delta u = -c\dot{u}\,\delta u$$

This suggests the introduction of a function analogous to the potential for the conservative forces

$$Q_j^d = -\frac{\partial \mathcal{D}}{\partial \dot{u}_j} \qquad \text{where} \qquad \mathcal{D} = \mathcal{D}(\dot{u}_1, \dot{u}_2, \ldots, \dot{u}_N)$$

For small motions, this gives

$$\mathcal{D}(\dot{u}_1, \dot{u}_2, \ldots, \dot{u}_N) \approx \frac{1}{2}\sum\nolimits_{i,j} C_{ij}\dot{u}_i\dot{u}_j, \qquad C_{ij} \equiv \left.\frac{\partial^2 \mathcal{D}}{\partial \dot{u}_i \partial \dot{u}_j}\right|_0$$

The function $\mathcal{D}$ is called the *Rayleigh dissipation function*.

Substitute these forms for $\mathcal{U}$, $\mathcal{V}$, $\mathcal{T}$, and $\mathcal{D}$ into Lagrange's equation to get

$$\sum\nolimits_j \{K_{ij}u_j + C_{ij}\dot{u}_j + M_{ij}\ddot{u}_j\} = P_i\,, \qquad i = 1, 2, \ldots, N$$

This is put in the familiar matrix form as

$$[\ K\ ]\{u\} + [\ C\ ]\{\dot{u}\} + [\ M\ ]\{\ddot{u}\} = \{P\} \tag{1.17}$$

By comparison with a single spring–mass system, we have the meaning of $[\ K\ ]$, $[\ M\ ]$, and $[\ C\ ]$ as the (generalized) structural stiffness, mass, and damping matrices, respectively. As yet, we have not said how the actual coefficients can be obtained or the actual meaning of the generalized coordinates; this is the subject of a later section where we consider some specific finite elements.

In this system of equations, $\{u\}$ is the vector of all the free degrees of freedom and is of size $\{M_u \times 1\}$, $[\ K\ ]$ is the $[M_u \times M_u]$ stiffness matrix, $[\ C\ ]$ is the $[M_u \times M_u]$ damping matrix, $\{P\}$ is the $\{M_u \times 1\}$ vector of all applied loads (some of which are zero).

1.4 Material Behavior

The concepts of stress, on the one hand, and strain, on the other, were developed independently of each other and apart from the assumption of a continuum, the development placed no restrictions on the material; that is, the concepts developed so far apply whether the material is elastic or plastic, isotropic or anisotropic. Indeed, they apply even if the material is a fluid. This section makes the material behavior explicit.

Types of Materials

There is a wide range of materials available, but engineering structures are made from relatively few. (Reference [86] gives an enjoyable account of a variety of structures and

the types of materials used for their construction.) Most structures are designed to sustain only elastic loads and are fabricated from isotropic and homogeneous materials (steel and aluminum, for instance); and therefore a discussion of these materials will suffice for most situations (see Table 1.1 and Table 1.2). Analysis of structural components fabricated with composite materials, on the other hand, requires the use of anisotropic elasticity theory. Analysis of problems in metal-forming and ductile fracture are based on the inelastic and plastic responses of materials, particularly those under large deformation. Polymeric materials require knowledge of their time-dependent stress relaxation and creep properties. We consider these latter behaviors only briefly.

While the behavior of a real material is very complicated, most structural materials can be divided into a limited number of classes; four of the main classes will be considered briefly here. To simplify the following relations, only small deformations will be considered.

We begin the discussion by considering the ubiquitous stress/strain diagram of a tensile test. Load (P) and extension (ΔL) are the typical data collected in the performance of a tensile test; when these are plotted as stress (P/A) against strain ($\Delta L/L$) they may look like one of the plots in Figure 1.10. A number of terms are used to describe these plots. The *Proportionality Limit* is the last point where stress and strain are linearly related (Point a). The *Elastic Limit* is the last point from which, after removal of load, there is no permanent strain (Point b). The *Yield Point* is technically the same as the elastic limit but is usually associated with the gross onset of permanent strain. Many materials do not exhibit a clearly defined yield point and so this point is often taken to correspond to a certain offset of strain. Point c is the yield point for 0.2% (.002 strain) offset. The *Yield Strength* is the stress at the yield point, σ_Y. The *Tensile Strength*, or sometimes called the Ultimate Tensile Strength (UTS), is the maximum stress reached during loading (Point d). The *Rupture Strain* is the maximum strain reached during loading (Point $\times$).

The unloading curve is usually parallel to the elastic loading curve and results in a permanent set or a plastic strain at complete unloading. The difference in yield stresses between the virgin and plastically deformed material is caused by its strain-hardening response.

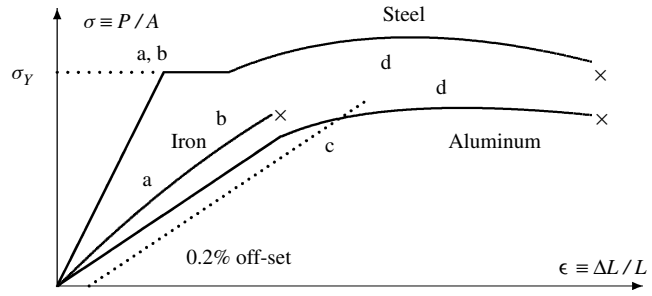

Figure 1.10: Some stress/strain diagrams.

Table 1.1: Typical structural material properties in SI units.

Material	ρ [kg/m^3]	E [GPa]	G [GPa]	σ_Y [MPa]	σ_U [MPa]	K_{1c} [MPa$\sqrt{\text{m}}$]	α [$\mu\epsilon$/°C]
Aluminum:							
2024	2768	73	27.6	276	414	26	22.5
7075		71	27.6	483	538	24	22.5
Titanium:							
6AL-4 V	4429	110	41	924	924	115	9.4
Steel:							
4340	7832	200	27.6	1170	1240	–	11.9
AMS6520	183	27.6	1720	1730	–	11.9	
Stainless		200	27.6	1117	1241	(−)	11.9
300 M		200	27.6	165	193	(−)	11.9
Plastic:							
PMMA	1107	4.1	–	76	–	–	90
Epoxy		3.5	–	–	–	–	90
Wood:							
Spruce	443	9.0	(−)	65	–	–	–
Fir		11	–	47	55	–	–

Table 1.2: Typical structural material properties in common units.

Material	ρ [lb/in^3]	E [msi]	G [msi]	σ_Y [ksi]	σ_U [ksi]	K_{1c} [ksi$\sqrt{\text{in}}$]	α [$\mu\epsilon$/°F]
Aluminum							
2024	0.10	10.6	4.00	40	60	29.0	12.5
7075		10.3	3.9	70	78	22.0	12.5
Titanium							
6AL-4 V	0.16	16.0	6.0	130	134	105	5.2
Steel							
4340	0.283	29.0	12.0	170	180	–	6.6
AMS6520		26.5	12.0	250	252	–	6.6
17-7 PH		29.0	12.0	162	180	40.0	6.6
300 M		29.0	12.0	240	280	47.0	6.6
Plastic							
PMMA	0.04	0.6	–	11	–	–	50
Epoxy		0.475	–	–	–	–	50
Wood							
Spruce	0.016	1.3	–	9.4	–	–	–
Fir		1.6	–	6.8	8	–	–

If there is a one to one relation between the stress and strain, and, on unloading, all the strain is instantaneously recovered, then the material is said to be elastic. Most structural materials in common use are adequately described by this type of material. In linear elasticity, the deformation is a linear function of the stress

$$\sigma = E\epsilon$$

where E is called the Young's modulus.

For some materials, it is found that beyond a certain stress level large deformations occur for small increments in load, and furthermore, much of the deformation is not recovered when the load is removed. On the load/unload cycle, if $\sigma > \sigma_Y$ (σ_Y is the yield stress), this material cannot recover the deformation caused after yielding. This remaining deformation is called the permanent or plastic strain. The total strain is considered as composed of elastic and plastic parts

$$\epsilon = \epsilon^e + \epsilon^p$$

and constitutive relations are written for the separate parts. An explicit constitutive relation is considered later in this chapter.

The mechanical properties of all solids are affected to varying degrees by the temperature and rate of deformation. Although such effects are not measurable (for typical structural materials) at ordinary temperatures, they become noticeable at high temperatures relative to the glassy transition temperature for polymers or the melting temperature for metals. Above the glassy transition temperature, many amorphous polymers flow like a Newtonian fluid and are referred to as *viscoelastic* materials; that is, they exhibit a combination of solid and fluid effects. Viscoelastic materials are time-dependent and the relation must be written in terms of the time derivatives; the standard linear solid, for example, is described by

$$\frac{\mathrm{d}\epsilon}{\mathrm{d}t} + \frac{E_2}{\eta}\epsilon = \frac{1}{E}\frac{\mathrm{d}\sigma}{\mathrm{d}t} + \frac{1}{\eta}\left[1 + \frac{E_2}{E_1}\right]\sigma$$

In addition to the time dependence, there is also a dependence on more material coefficients. This material exhibits a residual strain after the load is removed, but over time it recovers this strain to leave the material in its original state.

The structural properties of some base materials can be improved by combining them with other materials to form composite materials. A historical survey is given in Reference [86]. For a sandwich material such as plywood, the cross-grain weakness of the wood is improved by alternating directions of the lamina. Concrete is an example of particulate materials with cement as the bonding agent. Reinforced concrete uses steel bars to improve the tensile strength of the base concrete. Sheets of glass are stiff but prone to brittle failure because of small defects. Glass-fiber-reinforced composites combine the stiffness of glass in the form of fibers with the bonding of a matrix material such as epoxy; in this way, a defect in individual fibers does affect the overall behavior. It is possible to describe these structured materials through their constituent behavior, but for structural analyses this is very rarely done because it is computationally prohibitive. It is more usual

to treat these materials as homogeneous materials and establish average properties based on a representative volume. The variety of behaviors from these structured materials is much richer than that of traditional homogeneous materials and not easily summarized in a brief discussion; by way of example, we will consider their anisotropic properties.

Failure Criteria

In broad terms, failure refers to any action that leads to an inability on the part of a structure to function as intended. Common modes of failure include permanent deformation (yielding), fracture, buckling, creep, and fatigue. The successful use of a material in any application requires assurance that it will function safely. Therefore, the design process must involve steps where the predicted in-service stresses, strains, and deformations are limited to appropriate levels using failure criteria based on experimental data.

The basic assumption underlying all failure criteria is that failure is predicted to occur at a particular point in a material only when the value of a certain measure of stress reaches a critical value. The critical level of the selected measure is obtained experimentally, usually by a uniaxial test similar to that of Figure 1.10; that is, the goal of such criteria is to predict failure in multiaxial states of stress using uniaxial failure stress as the only input parameter. We discuss some of the more common criteria below.

The stress state of a body is characterized in terms of the principal stresses because they are the extremum values. In the following, we assume the principal stresses are ordered according to $\sigma_3 < \sigma_2 < \sigma_1$.

The maximum principal stress theory predicts that failure will occur at a point in a material when the maximum principal normal stress becomes equal to or exceeds the uniaxial failure stress for that material; that is, this criterion predicts failure to occur at a point when

$$\sigma_1 \geq \sigma_f \qquad \text{or} \qquad \sigma_3 \leq -\sigma_f$$

where σ_f is the magnitude of the uniaxial failure stress in tension and an equal but opposite failure stress is assumed in compression. This theory provides a generally poor prediction of yield onset for most metals and is not typically used for materials that behave in a ductile fashion. It has, however, been applied successfully to predict fracture of some brittle materials in multiaxial stress states.

The maximum shear stress theory states that the yield is predicted to occur at a point in a material when the absolute maximum shear stress at that point becomes equal to or exceeds the magnitude of the maximum shear stress at yield in a uniaxial tensile test. On the basis of the stress transformation equations, this critical yielding value of the maximum shear stress during a uniaxial test is $\tau_Y = \frac{1}{2}\sigma_Y$. Thus, yield failure is predicted to occur in a multiaxial state of stress if

$$\tau_{\max} \geq \tfrac{1}{2}\sigma_Y$$

In terms of the principal stresses, this can be recast into the form

$$\sigma_1 - \sigma_3 \geq \sigma_Y$$

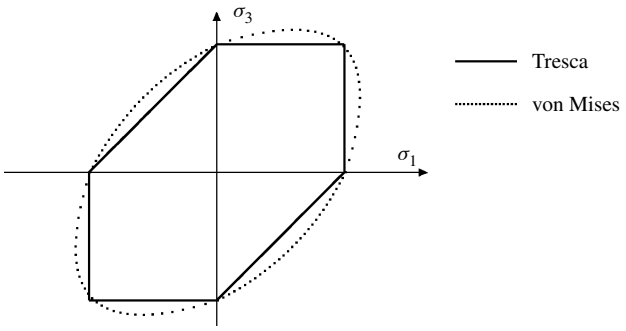

Figure 1.11: Tresca and von Mises yield criteria.

This criterion is shown in Figure 1.11. Experimental evidence for various states of stress attest that the maximum shear stress criterion is a good theory for predicting yield failure of ductile metals.

The total strain energy of an isotropic linear elastic material is often divided into two parts: the dilatation energy, which is associated with change of volume under a mean hydrostatic pressure, and the distortion energy, which is associated with change in shape. The energy of distortion theory states that yield is predicted to occur at a point in a material when the distortion energy at that point becomes equal to or exceeds the magnitude of the distortion energy at yield in a uniaxial tensile test of the same material. The critical yielding value of the distortion energy in a uniaxial test is

$$\mathcal{U}_{\mathrm{d}} = \frac{1+\nu}{6E}[2\sigma_Y^2]$$

This leads to the statement that yield will occur if

$$\sigma_{\mathrm{vm}} \equiv \sqrt{2[(\sigma_1-\sigma_2)^2+(\sigma_2-\sigma_3)^2+(\sigma_3-\sigma_1)^2]} \geq \sigma_Y$$

where σ_{vm} is called the *von Mises stress*. The behavior of this is shown in Figure 1.11. The predictions are close to those of the maximum shear stress criterion, but it has the slight advantage of using a single function for any state of stress. In 3-D complex stress states, the von Mises stress can be computed in terms of the component stresses through

$$\sigma_{\mathrm{vm}} = \sqrt{I_1^2 - 3I_2}$$

where I_1 and I_2 are the invariants computed from Equation (1.5).

Elastic Constitutive Relations

Because of our interest in structures, the elastic material is the one of most relevance to us. Furthermore, the situations that arise are usually of the type of Cases (b) and (c) of Figure 1.4 and we utilize this to make approximations.

Consider a small volume of material under the action of applied loads on its surface. Then one way to describe elastic behavior is as follows: *The work done by the applied forces is transformed completely into strain (potential) energy, and this strain energy is completely recoverable*. That the work is transformed into potential energy and that it is completely recoverable means the material system is conservative. Using Lagrangian variables, the increment of work done on the small volume is

$$\mathrm{d}W_e = \int_{V^o} \left[\sum\nolimits_{i,j} \sigma_{ij}^K \, \mathrm{d}E_{ij} \right] \mathrm{d}V^o$$

The potential is comprised entirely of the strain energy $\mathcal{U}$; the increment of strain energy is

$$\mathrm{d}\mathcal{U} = \mathrm{d}\mathcal{U}(E_{ij}) = \int_{V^o} \left[\sum\nolimits_{i,j} \frac{\partial \overline{\mathcal{U}}}{\partial E_{ij}} \, \mathrm{d}E_{ij} \right] \mathrm{d}V^o$$

where $\overline{\mathcal{U}}$ is the strain energy density. From the hypothesis, we can equate $\mathrm{d}W_e$ and $\mathrm{d}\mathcal{U}$, and because the volume is arbitrary, the integrands must be equal; hence we have

$$\sigma_{ij}^K = \frac{\partial \overline{\mathcal{U}}}{\partial E_{ij}} \tag{1.18}$$

A material described by this relation is called *hyperelastic*. Note that it is valid for large deformations and for anisotropic materials; however, rather than develop this general case, we will look at each of these separately.

Many structural materials (steel and aluminum, for example) are essentially isotropic in that the stiffness of a sheet is about the same in all directions. Consequently, the strain energy is a function of the strain invariants only; that is, $\overline{\mathcal{U}} = \overline{\mathcal{U}}(I_1, I_2, I_3)$, where the invariants are computed by

$$I_1 = \sum\nolimits_k E_{kk}, \qquad I_2 = \tfrac{1}{2} I_1^2 - \tfrac{1}{2} \sum\nolimits_{i,k} E_{ik} E_{ik}, \qquad I_3 = \det[\, E_{ij} \,]$$

On substituting these into the above constitutive relation, and rearranging them, we get

$$\sigma_{ij}^K = \beta_o \delta_{ij} + \beta_1 E_{ij} + \beta_2 \sum\nolimits_p E_{ip} E_{pj} \tag{1.19}$$

which is a nice compact relation. The coefficients β_i are functions of only the invariants [71].

Reinforced materials are likely to have directional properties and are therefore anisotropic. They are also more likely to have small operational strains, and we take advantage of this to effect another set of material approximations. Take the Taylor series expansion of the strain energy density function which, on differentiation, then leads to

$$\sigma_{pq}^K = \frac{\partial \overline{\mathcal{U}}}{\partial E_{pq}} \approx \left[\frac{\partial \overline{\mathcal{U}}}{\partial E_{pq}} \right]_0 + \sum_{r,s} \left[\frac{\partial^2 \overline{\mathcal{U}}}{\partial E_{pq} \partial E_{rs}} \right]_0 E_{rs} + \cdots = \sigma_{pq}^o + \sum_{r,s} D_{pqrs} E_{rs} + \cdots$$

where σ^o_{pq} corresponds to an initial stress. Because of symmetry in σ^K_{ij} and E_{ij}, C_{pqrs} reduces to 36 coefficients. But because of the explicit form of C_{pqrs} in terms of derivatives, we have the further restriction

$$D_{pqrs} = \left.\frac{\partial^2 \overline{\mathcal{U}}}{\partial E_{pq} \partial E_{rs}}\right|_0 = \left.\frac{\partial^2 \overline{\mathcal{U}}}{\partial E_{rs} \partial E_{pq}}\right|_0 = D_{rspq}$$

This additional symmetry reduces the elastic tensor to 21 constants. This is usually considered to be the most general linearly elastic material. We can write this relation in the matrix form

$$\{\sigma\} = [\ D\ ]\{E\}, \quad \{\sigma\} \equiv \{\sigma^K_{11}, \sigma^K_{22}, \sigma^K_{33}, \sigma^K_{23}, \ldots\}, \quad \{\epsilon\} \equiv \{E_{11}, E_{22}, E_{33}, 2E_{23}, \ldots\}$$

where $[\ D\ ]$ is of size $[6 \times 6]$. Because of the symmetry of both the stress and strain, we have $[\ D\ ]^{\mathrm{T}} = [\ D\ ]$. Special materials are reduced forms of this relation.

An *orthotropic* material has three planes of symmetry, and this reduces the number of material coefficients to nine; and the elastic matrix is given by

$$\begin{bmatrix} d_{11} & d_{12} & d_{13} & 0 & 0 & 0 \\ d_{12} & d_{22} & d_{23} & 0 & 0 & 0 \\ d_{13} & d_{23} & d_{33} & 0 & 0 & 0 \\ 0 & 0 & 0 & \frac{1}{2}(d_{11} - d_{12}) & 0 & 0 \\ 0 & 0 & 0 & 0 & \frac{1}{2}(d_{11} - d_{12}) & 0 \\ 0 & 0 & 0 & 0 & 0 & \frac{1}{2}(d_{11} - d_{12}) \end{bmatrix}$$

For a transversely isotropic material, this reduces to five coefficients because $d_{55} = d_{44}$ and $d_{66} = (d_{11} - d_{12})/2$. A thin fiber-reinforced composite sheet is usually considered to be transversely isotropic [100].

For the isotropic case, every plane is a plane of symmetry and every axis is an axis of symmetry. It turns out that there are only two independent elastic constants, and the elastic matrix is given as above but with

$$d_{11} = d_{22} = d_{33} = \lambda + 2\mu, \qquad d_{12} = d_{23} = d_{13} = \lambda$$

The constants λ and μ are called the Lamé constants. The stress/strain relation for isotropic materials (with no initial stress) are usually expressed in the form

$$\sigma^K_{ij} = 2\mu E_{ij} + \lambda \delta_{ij} \sum\nolimits_k E_{kk}, \qquad 2\mu E_{ij} = \sigma^K_{ij} - \frac{\lambda}{3\lambda + 2\mu} \delta_{ij} \sum\nolimits_k \sigma^K_{kk} \tag{1.20}$$

This is called *Hooke's law* and is the linearized version of Equation (1.19). The expanded form of the Hooke's law for strains in terms of stresses is

$$E_{xx} = \frac{1}{E}[\sigma^K_{xx} - \nu(\sigma^K_{yy} + \sigma^K_{zz})]$$

$$E_{yy} = \frac{1}{E}[\sigma^K_{yy} - \nu(\sigma^K_{zz} + \sigma^K_{xx})]$$

$$E_{zz} = \frac{1}{E}[\sigma^K_{zz} - \nu(\sigma^K_{xx} + \sigma^K_{yy})] \tag{1.21}$$
$$2E_{xy} = \frac{2(1+\nu)}{E}\sigma^K_{xy}, \quad 2E_{yz} = \frac{2(1+\nu)}{E}\sigma^K_{yz}, \quad 2E_{xz} = \frac{2(1+\nu)}{E}\sigma^K_{xz}$$

and for stresses in terms of strains

$$\begin{aligned}
\sigma^K_{xx} &= \frac{E}{(1+\nu)(1-2\nu)}[(1-\nu)E_{xx} + \nu(E_{yy} + E_{zz})] \\
\sigma^K_{yy} &= \frac{E}{(1+\nu)(1-2\nu)}[(1-\nu)E_{yy} + \nu(E_{zz} + E_{xx})] \\
\sigma^K_{zz} &= \frac{E}{(1+\nu)(1-2\nu)}[(1-\nu)E_{zz} + \nu(E_{xx} + E_{yy})] \\
\sigma^K_{xy} &= \frac{E}{2(1+\nu)}2E_{xy}, \quad \sigma^K_{yz} = \frac{E}{2(1+\nu)}2E_{yz}, \quad \sigma^K_{xz} = \frac{E}{2(1+\nu)}2E_{xz}
\end{aligned} \tag{1.22}$$

where E is the Young's modulus and ν is the Poisson's ratio related to the Lamé coefficients by

$$E = \frac{\mu(3\lambda + 2\mu)}{\lambda + \mu}, \quad \nu = \frac{\lambda}{2(\lambda + \mu)}, \quad \lambda = \frac{\nu E}{(1-2\nu)(1+\nu)}, \quad \mu = G = \frac{E}{2(1+\nu)}$$

The coefficient $\mu = G$ is called the shear modulus.

A special case that arises in the analysis of thin-walled structures is that of *plane stress*. Here, the stress through the thickness of the plate is approximately zero such that $\sigma^K_{zz} \approx 0$, $\sigma^K_{xz} \approx 0$, and $\sigma^K_{yz} \approx 0$. This leads to

$$E_{zz} = \frac{-\nu}{E}[\sigma^K_{xx} + \sigma^K_{yy}] = \frac{-\nu}{1-\nu}[E_{xx} + E_{yy}]$$

Substituting this into the 3-D Hooke's law then gives

$$\begin{aligned}
E_{xx} &= \frac{1}{E}[\sigma^K_{xx} - \nu\sigma^K_{yy}], \qquad \sigma^K_{xx} = \frac{E}{(1-\nu^2)}[E_{xx} + \nu E_{yy}] \\
E_{yy} &= \frac{1}{E}[\sigma^K_{yy} - \nu\sigma^K_{xx}], \qquad \sigma^K_{yy} = \frac{E}{(1-\nu^2)}[E_{yy} + \nu E_{xx}]
\end{aligned} \tag{1.23}$$

The shear relation is unaffected.

A final point to note is that, except for the isotropic material, the material coefficients are given with respect to a particular coordinate system. Hence, we must transform the coefficients into the new coordinate system when the axes are changed.

Strain Energy for Some Linear Elastic Structures

When the strains are small, we need not distinguish between the undeformed and deformed configurations. Under this circumstance, let the material obey Hooke's law

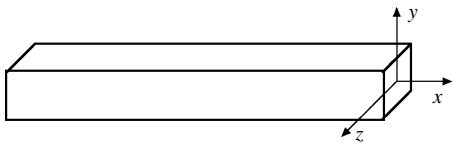

Figure 1.12: A slender structural member in local coordinates.

and be summarized in the matrix forms

$$\{\epsilon\} = [\ C\ ]\{\sigma\}, \qquad \{\sigma\} = [\ D\ ]\{\epsilon\}, \qquad [\ C\ ] = [\ D\ ]^{-1}$$

The general expression for the strain energy is

$$\mathcal{U} = \frac{1}{2}\int_V [\sigma_{xx}\epsilon_{xx} + \sigma_{yy}\epsilon_{yy} + \sigma_{xy}\gamma_{xy} + \cdots]\,\mathrm{d}V = \frac{1}{2}\int_V \{\sigma\}^{\mathrm{T}}\{\epsilon\}\,\mathrm{d}V$$

where $\gamma_{ij} = 2\epsilon_{ij} (i \neq j)$ is called the engineering shear strain. Using Hooke's law, the strain energy can be put in the alternate forms

$$\mathcal{U} = \frac{1}{2}\int_V \{\epsilon\}^{\mathrm{T}}[\ D\ ]\{\epsilon\}\,\mathrm{d}V = \frac{1}{2}\int_V \{\sigma\}^{\mathrm{T}}[\ C\ ][\ \sigma\ ]\,\mathrm{d}V \tag{1.24}$$

The above relations will now be particularized to some structural systems of interest by writing the distributions of stress and strain in terms of resultants and displacements, respectively.

For example, for the rod member of Figure 1.12, there is only an axial stress present and it is uniformly distributed on the cross section. Let F be the resultant force; then $\sigma_{xx} = F/A = E\epsilon_{xx}$ and

$$\text{axial:} \qquad \mathcal{U} = \frac{1}{2}\int_0^L \frac{F^2}{EA}\,\mathrm{d}x = \frac{1}{2}\int_0^L EA\left[\frac{\mathrm{d}u}{\mathrm{d}x}\right]^2 \mathrm{d}x$$

For the beam member in bending, there is only an axial stress, but it is distributed linearly on the cross section in such a way that there is no resultant axial force. Let M be the resultant moment; then $\sigma_{xx} = -My/I = E\epsilon_{xx}$ and

$$\text{bending:} \qquad \mathcal{U} = \frac{1}{2}\int_0^L \frac{M^2}{EI}\,\mathrm{d}x = \frac{1}{2}\int_0^L EI\left[\frac{\mathrm{d}^2v}{\mathrm{d}x^2}\right]^2 \mathrm{d}x$$

where I is the second moment of area. Other members are handled similarly [71].

1.5 The Finite Element Method

The discussions of the previous sections show that we can pose the solution of a solid mechanics problem in terms of extremizing a functional; this is known as the *weak*

form or *variational* form of the problem. What we wish to pursue in the following is approximation arising from the weak form; specifically, we will approximate the functional itself and use the variational principle to obviate consideration of the natural boundary conditions. This is called the Ritz method. The computational implementation will be in the form of the finite element method.

Ritz Method

In general, a continuously distributed deformable body consists of an infinity of material points and therefore has infinitely many degrees of freedom. The Ritz method is an approximate procedure by which continuous systems are reduced to systems with finite degrees of freedom. The fundamental characteristic of the method is that we operate on the functional corresponding to the problem. To fix ideas, consider the static case where the solution of $\delta\Pi = 0$ with prescribed boundary conditions on u is sought. Let

$$u(x, y, z) = \sum_{i=1}^{\infty} a_i g_i(x, y, z)$$

where $g_i(x, y, z)$ are independent known *trial functions*, and the a_i are unknown multipliers to be determined in the solution. The trial functions satisfy the essential (geometric) boundary conditions but not necessarily the natural boundary conditions. The variational problem states that

$$\Pi(u) = \Pi(a_1, a_2, \ldots) = \text{stationary}$$

Thus, $\Pi(a_1, a_2, \ldots)$ can be regarded as a function of the variables $a_1, a_2, \cdots$. To satisfy Π = stationary, we require that

$$\mathcal{F}_1 = \frac{\partial \Pi}{\partial a_1} = 0, \qquad \mathcal{F}_2 = \frac{\partial \Pi}{\partial a_2} = 0, \qquad \cdots$$

These equations are then used to determine the coefficients a_i. Normally, only a finite number of terms is included in the expansion.

An important consideration is the selection of the trial functions $g_i(x, y, z)$; but it must also be kept in mind that these functions need only satisfy the essential boundary conditions and not (necessarily) the natural boundary conditions. For practical analyses, this is a significant point and largely accounts for the effectiveness of the displacement-based finite element analysis procedure.

We will use the simple example of Figure 1.13 to illustrate some aspects of the Ritz method. To begin, we must have a compatible displacement field; this is achieved by imposing the geometric boundary conditions. For this problem, these conditions are $u = 0$ at both $x = 0$ and $x = L$. To satisfy these, assume a polynomial

$$u(x) = a_0 + a_1 x + a_2 x^2 + a_3 x^3 + \cdots$$

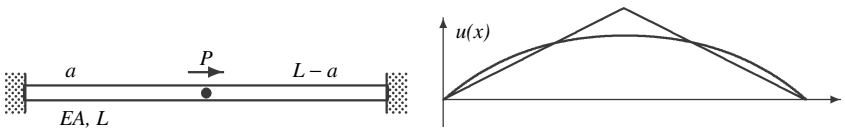

Figure 1.13: Fixed fixed rod with a concentrated load.

Imposing the boundary conditions allows a_0 and a_1 to be determined in terms of the other coefficients. This leads to the displacement representation

$$u(x) = a_2[x^2 - xL] + a_3[x^3 - xL^2] + \cdots = a_2 g_2(x) + a_3 g_3(x) + \cdots$$

that will satisfy the boundary conditions. Indeed, each of the functions separately satisfy the boundary conditions and therefore are individually acceptable Ritz functions.

The total potential energy of the rod problem is

$$\Pi = \frac{1}{2}\int_0^L EA\left(\frac{\mathrm{d}u}{\mathrm{d}x}\right)^2 \mathrm{d}x - Pu|_{x=a}$$

Substituting the assumed displacements and invoking the stationarity of Π with respect to the coefficients a_n, we obtain after differentiation

$$\frac{\partial \Pi}{\partial a_2} = \int_0^L EA\left[a_2[2x - L] + a_3[3x^2 - L^2] + \cdots\right][2x - L]\,\mathrm{d}x - P\left[[a^2 - aL]\right] = 0$$

$$\frac{\partial \Pi}{\partial a_3} = \int_0^L EA\left[a_2[2x - L] + a_3[3x^2 - L^2] + \cdots\right][3x^2 - L^2]\,\mathrm{d}x - P\left[[a^3 - aL^2]\right] = 0$$

Performing the required integrations gives

$$\frac{EA}{30}\begin{bmatrix} 10L^3 & 15L^4 & \cdots \\ 15L^4 & 24L^5 & \cdots \\ \vdots & \vdots & \vdots \end{bmatrix}\begin{Bmatrix} a_2 \\ a_3 \\ \vdots \end{Bmatrix} = P\begin{Bmatrix} a^2 - aL \\ a^3 - aL^2 \\ \vdots \end{Bmatrix}$$

It is typical to end up with a set of simultaneous equations. in these problems Note that the system matrix is symmetric; this too is usually the case.

Solving this system when only the a_2 term is used in the expansion gives the approximate solution

$$u(x) = \frac{P}{EAL^3}[a^2 - aL][x^2 - xL]$$

In the special case of $a = L/2$, the maximum deflection (also at $x = L/2$) is

$$u_{\max} = \frac{PL}{4EA}\frac{3}{4}, \qquad u_{\text{exact}} = \frac{PL}{4EA}$$

This underestimates the maximum as shown in Figure 1.13

We will now redo the problem but this time assume a compatible displacement field that is piecewise linear, that is, we let

$$u(x) = \left[\frac{x}{a}\right] u_o \qquad 0 \le x \le a\,, \qquad\qquad u(x) = \left[\frac{L-x}{L-a}\right] u_o \qquad a \le x \le L$$

where u_o is the displacement at the load application point. Since the displacement distribution is specified in a piecewise fashion, the integral for the strain energy must be divided up as

$$\mathcal{U} = \frac{1}{2}\int_0^L EA\left(\frac{\mathrm{d}u}{\mathrm{d}x}\right)^2 \mathrm{d}x = \frac{1}{2}\int_0^a EA\left[\frac{u_o}{a}\right]^2 \mathrm{d}x + \frac{1}{2}\int_a^L EA\left[\frac{-u_o}{L-a}\right]^2 \mathrm{d}x$$

This gives, after expanding and integrating,

$$\mathcal{U} = \frac{1}{2}EA\frac{u_o^2 a}{a^2} + \frac{1}{2}EA\frac{u_o^2(L-a)}{(L-a)^2} = \frac{1}{2}EA\frac{u_o^2 L}{a(L-a)}$$

The total potential for the problem is then

$$\Pi = \frac{1}{2}EA\frac{u_o^2 L}{a(L-a)} - Pu_o$$

Minimizing with respect to u_o gives

$$\frac{\partial \Pi}{\partial u_o} = EA\frac{u_o L}{a(L-a)} - P = 0 \qquad \text{or} \qquad u_o = \frac{P}{EA}\frac{a(L-a)}{L}$$

As it happens, this is the exact result.

This simple example is important in demonstrating the relationship between a Ritz analysis and a finite element analysis; that is, the classical Ritz method uses functions that cover the entire region, but as the example shows, we can alternatively use simpler functions, but limited to smaller regions. As discussed next, these smaller regions are actually the finite elements.

The Finite Element Discretization

One disadvantage of the conventional Ritz analysis is that the trial functions are defined over the whole region. This causes a particular difficulty in the selection of appropriate functions; in order to solve accurately for large stress gradients, say, we may need many functions. However, these functions are also defined over the regions in which the stresses vary rather slowly and where not many functions are required. Another difficulty arises when the total region is made up of subregions with different kinds of strain distributions. As an example, consider a building modeled by plates for the floors and beams for the

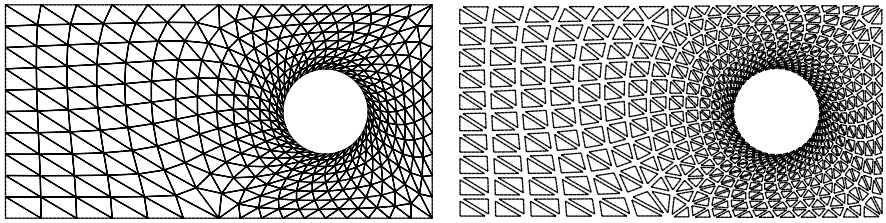

Figure 1.14: Continuous domain discretized as finite elements. Right figure has shrunk elements for easier viewing.

vertical frame. In this situation, the trial functions used for one region (e.g., the floor) are not appropriate for the other region (e.g., the frame), and special displacement continuity conditions and boundary relations must be introduced. We conclude that the conventional Ritz analysis is, in general, not particularly computer-oriented.

We can view the finite element method as an application of the Ritz method where, instead of the trial functions spanning the complete domain, the individual functions span only subdomains (the finite elements) of the complete region and are zero everywhere else. Figure 1.14 shows an example of a bar with a hole modeled as a collection of many triangular regions. The use of relatively many functions in regions of high strain gradients is made possible simply by using many elements as shown around the hole in the figure. The combination of domains with different kinds of strain distributions (e.g., a frame member connected to a plate) may be achieved by using different kinds of elements to idealize the domains.

In order that a finite element solution be a Ritz analysis, it must satisfy the essential boundary conditions. However, in the selection of the displacement functions, no special attention need be given to the natural boundary conditions, because these conditions are imposed with the load vector and are satisfied approximately in the Ritz solution. The accuracy with which these natural boundary conditions are satisfied depends on the specific trial functions employed and on the number of elements used to model the problem. This idea is demonstrated in the convergence studies of the next section.

The basic finite element procedure will now be described with reference to Figure 1.15. First, the structure is discretized into many subregions and for each subregion the displacement field is written in terms of nodal values. The total potential energy (which includes the strain energy and the potential of the nodal forces) is then minimized with respect to the nodal values to give the equilibrium relation

$$\{F_e\} = [\ k\ ]\{u\}$$

where $\{u\}$ is the *vector of nodal displacements*, $\{F_e\}$ is the *vector of element nodal forces*, and $[\ k\ ]$ is called the *element stiffness matrix*. We will also refer to $\{u\}$ as the *nodal degrees of freedom*.

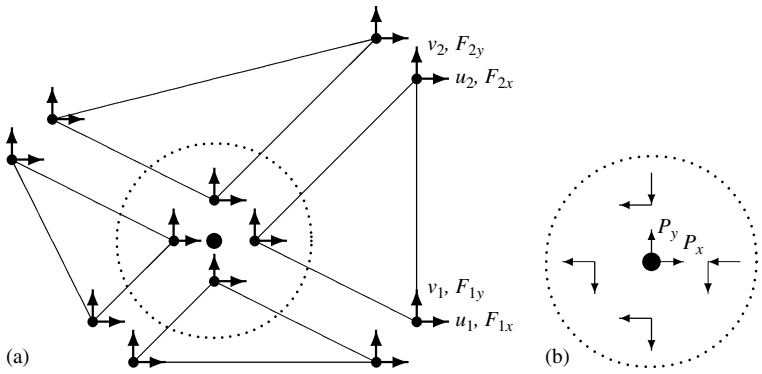

Figure 1.15: An assemblage of elements. (a) Nodal displacements and forces. (b) Equilibrium at common nodes.

When a continuous medium is discretized into a collection of piecewise simple regions, the issue of assemblage then arises. There are two aspects to this. The first is that there must be compatibility between the elements. This is achieved (in simple terms) through having neighboring elements share nodes and have common interpolations along shared interfaces. The second is that there must be equilibrium of the assembled elements. This can be viewed as either imposing equilibrium between the neighboring elements as depicted in Figure 1.15(b) or as adding the strain energies of elements. We will take the latter view.

Introduce the vector of all degrees of freedom (size $\{N \times 1\}$)

$$\{u\} \equiv \{u_1, u_2, u_3, \ldots\}^{\mathrm{T}}$$

The total potential of all the strain energies and applied loads is then

$$\Pi = \mathcal{U} + \mathcal{V} = \sum\nolimits_m \mathcal{U}_m - \{P\}^{\mathrm{T}}\{u\}$$

The applied loads vector $\{P\}$ is considered to comprise nodal applied loads, nodal loads arising from any load distributions $q(x)$, and inertia loads. Extremizing this with respect to the degrees of freedom then gives the equilibrium condition

$$\mathcal{F} = \frac{\partial \Pi}{\partial u} = 0 = \{P\} - \{F\}\,, \qquad \{F\} = \sum\nolimits_m \frac{\partial \mathcal{U}_m}{\partial u} = \sum\nolimits_m \{F_{\mathrm{e}}\}_m \tag{1.25}$$

The vector $\{F\}$ is the assemblage of element nodal forces. This relation (referred to as the *loading equation*) must be satisfied throughout the loading history and is valid for nonlinear problems.

We can give an alternate interpretation of the loading equation for linear problems. Augment each element stiffness with zeros to size $[N \times N]$ and call it $[\ K\ ]_m = [k_{\mathrm{augment}}]_m$. The total strain energy is

$$\mathcal{U} = \frac{1}{2}\sum\nolimits_m \{u\}^{\mathrm{T}}[\ K\ ]_m\{u\} = \{u\}^{\mathrm{T}}[\ K\ ]\{u\}$$

After extremizing, this leads to

$$[\ K\ ]\{u\} = \{P\}\,, \qquad [\ K\ ] \equiv \sum\nolimits_m [\ K\ ]_m = \sum\nolimits_m [k_{\text{augment}}]_m$$

The $[N \times N]$ square matrix $[\ K\ ]$ is called the *structural stiffness matrix*. Thus, the assemblage process (for linear problems) can be thought of as adding the element stiffnesses suitably augmented (with zeros) to full system size.

Convergence of the Approximate Solutions

Clearly, for the finite element method to be useful, its solutions must be capable of converging to the exact solutions.

As a Ritz procedure, it must satisfy the geometric boundary conditions and interelement compatibility. In addition, to insure convergence there are three more requirements. The essential requirement is that the element must be capable of modeling a constant state of strain and stress in the limit of small element size. For example, consider the following expansions for use in constructing a beam element:

$$v(x) = a_0 + a_1 x + a_2 x^2 + \cdots\,, \qquad v(x) = a_0 + a_1 x + a_3 x^3 \cdots$$

Both are adequate for ensuring compatibility between elements; however, since the strain in a beam is related to the second derivative of the deflection, the second expansion would not produce a state of constant strain in the limit of small elements (it would produce zero strain at one end of the element).

A subsidiary requirement is that the element should be capable of rigid-body displacements without inducing strains. This is actually an extreme case of the constant strain condition with $\epsilon_{ij} = 0$. The third requirement is that the assumed displacement functions should be complete up to orders required by the first criterion. In the expansions used for constructing a beam element, the first is complete, but the second is not.

We will have more to say about convergence as we construct particular elements for particular types of structures. In general, when the criteria are satisfied, a lower bound on the strain energy is assured, and convergence is monotonic.

1.6 Some Finite Element Discretizations

There are a great variety of elements documented in the literature; we consider just a few of them for illustrative purposes. We begin with the tetrahedron element; this 3-D element satisfies all convergence criteria and therefore it is suitable for computing accurate solutions for all problems. Unfortunately, it is not very practical in many situations because it requires too many elements to achieve the required accuracy. As a consequence, other elements which take advantage of the nature of the structure have been developed—we look at the frame and shell elements, but a great many more can be found in References [18, 45, 46, 71].

Tetrahedral Solid Element

Conceive of the 3-D solid as discretized into many tetrahedrons. Consider one of those tetrahedrons divided into four volumes where the common point is at (x, y, z) as shown in Figure 1.16. Define

$$h_1 = V_1/V, \qquad h_2 = V_2/V, \qquad h_3 = V_3/V, \qquad h_4 = V_4/V, \qquad h_i = h_i(x, y, z)$$

We have the obvious constraint that $h_1 + h_2 + h_3 + h_4 = 1$. The volumes of these tetrahedrons uniquely define the position of the common point.

The position of the point (x, y, z) in the tetrahedron can be written as

$$\begin{Bmatrix} 1 \\ x \\ y \\ z \end{Bmatrix} = \begin{bmatrix} 1 & 1 & 1 & 1 \\ x_1 & x_2 & x_3 & x_4 \\ y_1 & y_2 & y_3 & y_4 \\ z_1 & z_2 & z_3 & z_4 \end{bmatrix} \begin{Bmatrix} h_1 \\ h_2 \\ h_3 \\ h_4 \end{Bmatrix} \tag{1.26}$$

where the subscripts 1, 2, 3 refer to the counterclockwise nodes of the triangle as viewed from Node 4. We can invert this relation, but the expressions are rather lengthy.

In order for the four coordinates $\{h_1, h_2, h_3, h_4\}$ to describe the three coordinates (x, y, z), it must be supplemented by the constraint $h_1+h_2+h_3+h_4 = 1$. We can invoke this constraint explicitly by introducing *natural coordinates* as shown in Figure 1.16(b) and given as

$$h_1 = \xi\,, \qquad h_2 = \eta\,, \qquad h_3 = \zeta\,, \qquad h_4 = 1 - \xi - \eta - \zeta \tag{1.27}$$

These are volumes in (ξ, η, ζ) space. This notation is from Reference [35]. We have for a typical function

$$u(x, y, z) = \sum\nolimits_i^4 h_i(\xi, \eta, \zeta)u_i$$

where u_i are the nodal values of the function. The x coordinate, for example, is given from Equation (1.26) as

$$x = x_1h_1 + x_2h_2 + x_3h_3 + x_4h_4 = x_4 + x_{14}\xi + x_{24}\eta + x_{34}\zeta$$

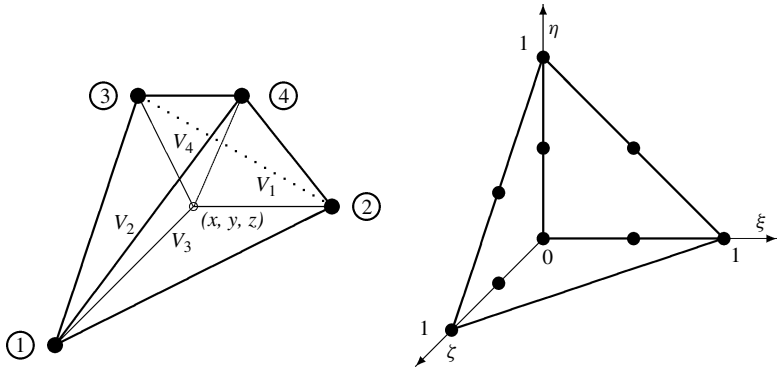

Figure 1.16: Volume and natural coordinates for a tetrahedron.

where $x_{14} = x_1 - x_4$, and so on. The strains are obtained in terms of derivatives of element displacements. Using the natural coordinate system, we get, for example,

$$\frac{\partial}{\partial x} = \frac{\partial}{\partial \xi}\frac{\partial \xi}{\partial x} + \frac{\partial}{\partial \eta}\frac{\partial \eta}{\partial x} + \frac{\partial}{\partial \zeta}\frac{\partial \zeta}{\partial x}$$

But, to evaluate the derivatives of (ξ, η, ζ) with respect to (x, y, z), we need to have the explicit relation between the two sets of variables. We obtain this as

$$\begin{Bmatrix} \frac{\partial}{\partial \xi} \\ \frac{\partial}{\partial \eta} \\ \frac{\partial}{\partial \zeta} \end{Bmatrix} = \begin{bmatrix} \frac{\partial x}{\partial \xi} & \frac{\partial y}{\partial \xi} & \frac{\partial z}{\partial \xi} \\ \frac{\partial x}{\partial \eta} & \frac{\partial y}{\partial \eta} & \frac{\partial z}{\partial \eta} \\ \frac{\partial x}{\partial \zeta} & \frac{\partial y}{\partial \zeta} & \frac{\partial z}{\partial \zeta} \end{bmatrix} \begin{Bmatrix} \frac{\partial}{\partial x} \\ \frac{\partial}{\partial y} \\ \frac{\partial}{\partial z} \end{Bmatrix} \qquad \text{or} \qquad \begin{Bmatrix} \frac{\partial}{\partial \xi} \end{Bmatrix} = [\ J\ ] \begin{Bmatrix} \frac{\partial}{\partial x} \end{Bmatrix}$$

where $[\ J\ ]$ is called the *Jacobian operator* relating the natural coordinates to the local coordinates and having the explicit form

$$[\ J\ ] = \begin{bmatrix} x_{14} & y_{14} & z_{14} \\ x_{24} & y_{24} & z_{24} \\ x_{34} & y_{34} & z_{34} \end{bmatrix}$$

The inverse relation for the derivatives

$$\begin{Bmatrix} \frac{\partial}{\partial x} \end{Bmatrix} = [J^{-1}] \begin{Bmatrix} \frac{\partial}{\partial \xi} \end{Bmatrix}$$

requires that $[J^{-1}]$ exists. In most cases, the existence is clear; however, in cases where the element is highly distorted or folds back on itself the Jacobian transformation can become singular. The inverse is given by

$$[J^{-1}] = \frac{1}{\det[\ J\ ]} \begin{bmatrix} y_{24}z_{34} - y_{34}z_{24} & y_{34}z_{14} - y_{14}z_{34} & y_{14}z_{24} - y_{24}z_{14} \\ z_{24}x_{34} - z_{34}x_{24} & z_{34}x_{14} - z_{14}x_{34} & z_{14}x_{24} - z_{24}x_{14} \\ x_{24}y_{34} - x_{34}y_{24} & x_{34}y_{14} - x_{14}y_{34} & x_{14}y_{24} - x_{24}y_{14} \end{bmatrix} = [\ A\ ]$$

where

$$\det[\ J\ ] = x_{14}[y_{24}z_{34} - y_{34}z_{24}] + y_{14}[z_{24}x_{34} - z_{34}x_{24}] + z_{14}[x_{24}y_{34} - x_{34}y_{24}] = 6|V|$$

The determinant of the Jacobian is related to the volume of the tetrahedron. Note that $[\ J\ ]$ and its inverse are constants related just to the coordinates of the tetrahedron.

The six components of strains are related to the displacements by

$$\epsilon_{xx} = \frac{\partial u}{\partial x}, \qquad \epsilon_{yy} = \frac{\partial v}{\partial y}, \qquad \epsilon_{zz} = \frac{\partial w}{\partial z}$$

$$2\epsilon_{yz} = \frac{\partial v}{\partial z} + \frac{\partial w}{\partial y}, \qquad 2\epsilon_{xz} = \frac{\partial u}{\partial z} + \frac{\partial w}{\partial x}, \qquad 2\epsilon_{xy} = \frac{\partial u}{\partial y} + \frac{\partial v}{\partial x}$$

We will place them, in this order, into the vector $\{\epsilon\}$. They are written in terms of the nodal DoF and inverse Jacobian components as

$$\{\epsilon\} = [\ B\ ]\{u\}$$

where

$$[\ B\ ] = \begin{bmatrix} A_{11} & 0 & 0 & A_{12} & 0 & 0 & A_{13} & 0 & 0 & -\overline{A}_1 & 0 & 0 \\ 0 & A_{21} & 0 & 0 & A_{22} & 0 & 0 & A_{23} & 0 & 0 & -\overline{A}_2 & 0 \\ 0 & 0 & A_{31} & 0 & 0 & A_{32} & 0 & 0 & A_{33} & 0 & 0 & -\overline{A}_3 \\ 0 & A_{31} & A_{21} & 0 & A_{32} & A_{22} & 0 & A_{33} & A_{23} & 0 & -\overline{A}_3 & -\overline{A}_2 \\ A_{31} & 0 & A_{11} & A_{32} & 0 & A_{12} & A_{33} & 0 & A_{13} & -\overline{A}_3 & 0 & -\overline{A}_1 \\ A_{21} & A_{11} & 0 & A_{22} & A_{12} & 0 & A_{23} & A_{13} & 0 & -\overline{A}_2 & -\overline{A}_1 & 0 \end{bmatrix}$$

and $\overline{A}_i = \sum_i A_{ij}$. The stresses are related to the strains by Hooke's law

$$\{\sigma\} = [\ D\ ]\{\epsilon\} = [\ D\ ][\ B\ ]\{u\}$$

with $\{\sigma\}$ organized the same as $\{\epsilon\}$.

The strain energy of the element is

$$\mathcal{U} = \frac{1}{2}\int_V \{\sigma\}^{\mathrm{T}}\{\epsilon\}\,\mathrm{d}V = \frac{1}{2}\int_V \{u\}^{\mathrm{T}}[\ B\ ]^{\mathrm{T}}[\ D\ ][\ B\ ]\{u\}\,\mathrm{d}V$$

Noting that none of the quantities inside the integral depends on the position coordinates, we have for the total potential

$$\Pi = \tfrac{1}{2}\{u\}^{\mathrm{T}}[\ B\ ]^{\mathrm{T}}[\ D\ ][\ B\ ]\{u\}V - \{F\}^{\mathrm{T}}\{u\}$$

The associated equilibrium equation is

$$\{F\} = [\ k\ ]\{u\}, \qquad [\ k\ ] \equiv [\ B\ ]^{\mathrm{T}}[\ D\ ][\ B\ ]V \tag{1.28}$$

The $[12 \times 12]$ square matrix $[\ k\ ]$ is called the stiffness matrix for the *Constant Strain Tetrahedron* (TET4) element. The coordinate system used to formulate the element (i.e., the local coordinate system) is also the global coordinate system; hence we do not need to do any rotation of the element stiffness before assemblage. The structural stiffness matrix is simply

$$[\ K\ ] = \sum\nolimits_m [\ k\ ]_m$$

where the element stiffnesses are suitably augmented to conform to the global system.

One of the most important characteristics of an element is its *convergence* properties, that is, it should converge to the exact result in the limit of small element size. When looking at convergence, it is necessary to change the mesh in a systematic way, preferably each time halving the element size in each dimension. The test problem we will use is that of the annulus shown in Figure 1.17 and loaded with an internal uniformly distributed traction. The mesh shown is made of $[32 \times 4 \times 1]$ modules where each module is a

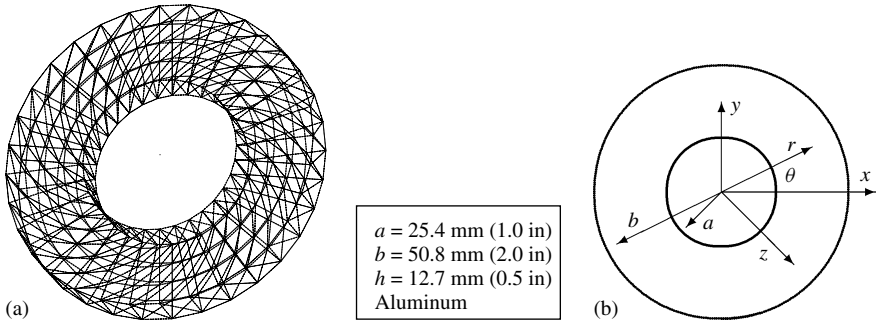

Figure 1.17: Annulus modeled with tetrahedral elements. (a) Properties of mesh with $[32 \times 4 \times 1]$ modules. (b) Cylindrical coordinates.

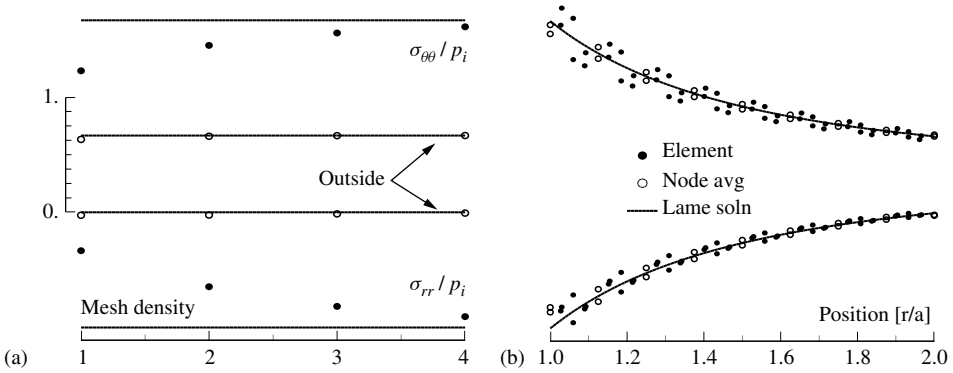

Figure 1.18: Annulus convergence results. (a) Boundary stresses for different mesh densities. (b) Stress distributions for mesh density 3.

hexahedron block made of six elements; the other meshes are similar except that the number of hoop and radial modules was changed by a factor of two each time.

Figure 1.18 shows the convergence behavior for the stresses on the inside and outside of the annulus. As expected, there is monotonic convergence from below. The mesh in Figure 1.17(a) is labeled as a density of "2"; the highest density tested was $[128 \times 16 \times 1]$ modules, which have 12,288 elements. It is easy to see how the number of elements can escalate as the mesh is refined.

It is interesting that the outside stresses converge to the exact solution much more rapidly than the inside ones. We can get a better insight into what is happening by looking at the distributions.

The exact radial and hoop stresses are given by the Lamé solution for thick cylinders [56]

$$\sigma_{rr} = \frac{p_i}{(1 - a^2/b^2)} \left[\frac{a^2}{b^2} - \frac{a^2}{r^2} \right], \qquad \sigma_{\theta\theta} = \frac{p_i}{(1 - a^2/b^2)} \left[\frac{a^2}{b^2} + \frac{a^2}{r^2} \right]$$

where p_i is the internal pressure. These distributions of stress are shown as the full line in Figure 1.18(b). The tetrahedral element has a constant stress distribution and these are shown as the full dots in Figure 1.18(b) plotted against the element centroidal radial position (they do not all lie on the same radial line). Even for mesh density 3, the values are spread about the exact solution, with the bigger spread occurring at the inside radius.

Typically, in an FEM analysis, the results are reported with respect to the nodal values. Therefore, some rule is needed to convert the element centroidal values into nodal values. A popular rule is to use nodal averages, that is, for a given node, the nodal value is the average value of all the elements attached to that node. These are shown in Figure 1.18(b) plotted as the empty circles, and for the most part they are very close to the exact solution. This rule is least accurate when the elements form a boundary with a stress gradient. In those cases, more sophisticated rules can be used (Reference [35] gives a nice scheme using least squares and the element interpolation functions) or the mesh can be designed to have a higher density in the vicinity of boundaries with stress gradients.

The tetrahedron element satisfies all convergence criteria, and therefore it is suitable for obtaining accurate solutions to all problems. Unfortunately, as just seen, it is usually not a very practical element because it requires too many elements to obtain sufficient accuracy. We now look at some other elements that *a priori* have built into them some structural simplifications.

Beam and Frame Element Stiffness

Consider a straight homogeneous beam element of length L as shown in Figure 1.19. Assume that there are no external loads applied between the two ends of Node 1 and Node 2 (i.e., $q(x) = 0$). At each node, there are two essential beam actions, namely, the bending moment and shear force. The corresponding nodal degrees of freedom are the rotation ϕ (or the slope of the deflection curve at the node) and the vertical displacement v. The positive directions of nodal forces and moments and the corresponding displacements and rotations are shown in the figure.

In this simple structural model, the 3-D distributions of displacement are reduced to the single displacement distribution $v(x)$ for the transverse deflection. We wish to write

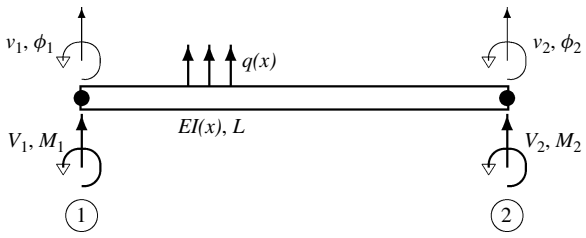

Figure 1.19: Sign convention for beam element.

this distribution in terms of the nodal displacements. There are four nodal values, so the simplest representation is

$$v(x) = a_0 + a_1 x + a_2 x^2 + a_3 x^3$$

where a_0, a_1, a_2, and a_3 are constants. By using the end conditions

$$v(0) = v_1, \qquad \frac{\mathrm{d}v(0)}{\mathrm{d}x} = \phi_1; \qquad v(L) = v_2, \qquad \frac{\mathrm{d}v(L)}{\mathrm{d}x} = \phi_2$$

we can rewrite the constants in terms of the nodal displacements v_1 and v_2, and the nodal rotations ϕ_1 and ϕ_2. Substitution of these into the expression for the deflection leads us to

$$\begin{aligned} v(x) &= \left[1 - 3\left(\frac{x}{L}\right)^2 + 2\left(\frac{x}{L}\right)^3\right] v_1 + \left(\frac{x}{L}\right)\left[1 - 2\left(\frac{x}{L}\right) + \left(\frac{x}{L}\right)^2\right] L\phi_1 \\ &\quad + \left(\frac{x}{L}\right)^2\left[3 - 2\left(\frac{x}{L}\right)\right] v_2 + \left(\frac{x}{L}\right)^2\left[-1 + \left(\frac{x}{L}\right)\right] L\phi_2 \\ &\equiv g_1(x)v_1 + g_2(x)L\phi_1 + g_3(x)v_2 + g_4(x)L\phi_2 \end{aligned} \tag{1.29}$$

The functions $g_n(x)$ are called the *beam shape functions*. The complete description of the element is captured in the four nodal degrees of freedom v_1, ϕ_1, v_2, and ϕ_2 (since the shape functions are known explicitly). For example, the curvature is obtained (in terms of the nodal degrees of freedom) simply by differentiation; that is,

$$\begin{aligned} \frac{\mathrm{d}^2 v}{\mathrm{d}x^2} &= [g_1''(x)v_1 + g_2''(x)L\phi_1 + g_3''(x)v_2 + g_4''(x)L\phi_2] \\ &= \frac{1}{L^3}[(-6L + 12x)v_1 + (-4L + 6x)L\phi_1 + (6L - 12x)v_2 + (-2L + 6x)L\phi_2] \end{aligned}$$

If, in any problem, these degrees of freedom can be determined, then the solution has been obtained.

The strain energy stored in the beam element is (neglecting shear)

$$\mathcal{U} = \frac{1}{2}\int_0^L EI\left[\frac{\mathrm{d}^2 v}{\mathrm{d}x^2}\right]^2 \mathrm{d}x = \frac{1}{2}\int_0^L EI[g_1''(x)v_1 + g_2''(x)L\phi_1 + g_3''(x)v_2 + g_4''(x)L\phi_2]^2\,\mathrm{d}x$$

The total potential for the problem is therefore

$$\Pi = \frac{1}{2}\int_0^L EI[g_1''(x)v_1 + g_2''(x)L\phi_1 + \cdots]^2\,\mathrm{d}x - V_1 v_1 - M_1\phi_1 - V_2 v_2 - M_2\phi_2$$

The element stiffness relation is obtained by extremizing the total potential to give, for example,

$$\mathcal{F}_{v_1} = \frac{\partial \Pi}{\partial v_1} = 0 = \int_0^L EIg_1''(x)g_1''(x)\,\mathrm{d}x - V_1$$

In general, the elements of the stiffness matrix are

$$k_{ij} = \frac{\partial^2 \Pi}{\partial u_i \partial u_j} = \int_0^L EIg_i''(x)g_j''(x)\,\mathrm{d}x$$

In the present form, these relations are applicable to nonuniform sections. Note that it is the symmetry of the terms $g_i''(x)g_j''(x)$ that insures the symmetry of the stiffness matrix.

Carrying out these integrations under the condition of constant EI gives the beam element stiffness matrix. Then, the nodal loads-displacement relations can be rearranged into the form

$$\begin{Bmatrix} V_1 \\ M_1 \\ V_2 \\ M_2 \end{Bmatrix} = \{F_e\} = [\ k\ ]\{u\} = \frac{EI}{L^3} \begin{bmatrix} 12 & 6L & -12 & 6L \\ 6L & 4L^2 & -6L & 2L^2 \\ -12 & -6L & 12 & -6L \\ 6L & 2L^2 & -6L & 4L^2 \end{bmatrix} \begin{Bmatrix} v_1 \\ \phi_1 \\ v_2 \\ \phi_2 \end{Bmatrix} \tag{1.30}$$

where $[\ k\ ]$ is the *beam element stiffness matrix*. Note that this stiffness matrix is symmetric. Also note that the nodal loads satisfy the equilibrium conditions for the free-body diagram of the element.

A typical member of a 3-D space frame can be thought of as having four actions: two bending actions, a twisting action, and an axial action. Thus, the displacement of each node is described by three translational and three rotational components of displacement, giving six degrees of freedom at each unrestrained node. Corresponding to these degrees of freedom are six nodal loads. The notations we will use for the displacement and force vectors at each node are, respectively,

$$\{u\} = \{u, v, w, \phi_x, \phi_y, \phi_z\}^{\mathrm{T}}, \qquad \{F_e\} = \{F_x, F_y, F_z, M_x, M_y, M_z\}^{\mathrm{T}}$$

On the local level, for each member, the forces are related to the displacements by the partitioned matrices

$$\{\overline{F}_e\} = \begin{bmatrix} \overline{k}_{11} & \overline{k}_{12} & \overline{k}_{13} & \overline{k}_{14} \\ \overline{k}_{21} & \overline{k}_{22} & \overline{k}_{23} & \overline{k}_{24} \\ \overline{k}_{31} & \overline{k}_{32} & \overline{k}_{33} & \overline{k}_{34} \\ \overline{k}_{41} & \overline{k}_{42} & \overline{k}_{43} & \overline{k}_{44} \end{bmatrix} \{\overline{u}\} = [\ \overline{k}\ ]\{\overline{u}\}$$

By way of example, the upper left quadrant is

$$\begin{bmatrix} \overline{k}_{11} & \overline{k}_{12} \\ \overline{k}_{21} & \overline{k}_{22} \end{bmatrix} = \frac{+1}{L} \begin{bmatrix} EA & 0 & 0 & 0 & 0 & 0 \\ 0 & 12EI_z/L^2 & 0 & 0 & 0 & 6EI_z/L \\ 0 & 0 & 12EI_y/L^2 & 0 & -6EI_y/L & 0 \\ 0 & 0 & 0 & GI_x & 0 & 0 \\ 0 & 0 & -6EI_y/L & 0 & 4EI_y & 0 \\ 0 & 6EI_z/L & 0 & 0 & 0 & 4EI_z \end{bmatrix}$$

where EA and GI_x are associated with the axial and torsional behaviors respectively. The other quadrants are similar. For example, the first quadrant of $[\ \overline{k}\ ]$ is the same as the fourth quadrant except for the signs of the off-diagonal terms.

The transformation of the components of a vector $\{v\}$ from the local to the global axes is given by

$$\{\overline{v}\} = [\ R\ ]\{v\}$$

where [R] is the transformation matrix. The same matrix will transform the vectors of nodal forces and displacements. To see this, note that the element nodal displacement vector is composed of four separate vectors, namely,

$$\{u\} = \{\{u_1, v_1, w_1\}; \{\phi_{x1}, \phi_{y1}, \phi_{z1}\}; \{u_2, v_2, w_2\}; \{\phi_{x2}, \phi_{y2}, \phi_{z2}\}\}$$

Each of these are separately transformed by the [3×3] rotation matrix [$\mathbf{R}$]. Hence, the complete transformation is

$$\{\overline{F}_e\} = [\ T\ ]\{F_e\}, \qquad \{\overline{u}\} = [\ T\ ]\{u\}, \qquad [\ T\ ] \equiv \begin{bmatrix} R & 0 & 0 & 0 \\ 0 & R & 0 & 0 \\ 0 & 0 & R & 0 \\ 0 & 0 & 0 & R \end{bmatrix}$$

where [$\mathbf{T}$] is a [12×12] matrix. Substituting for the barred vectors in the element stiffness relation allows us to obtain the global stiffness as

$$[\ k\ ] = [\ T\ ]^{\mathrm{T}}[\ \overline{k}\ ][\ T\ ]$$

For assemblage, each member stiffness is rotated to the global coordinate system and then augmented to the system size. The structural stiffness matrix is then

$$[\ K\ ] = \sum\nolimits_m [\ T\ ]_m^{\mathrm{T}}[\ \overline{k}\ ]_m[\ T\ ]_m$$

where the summation is over each member. It is important to realize that the transformation occurs before the assembly. The element stiffnesses just derived are exact for frames with uniform cross-sectional properties and therefore there need not be a discussion of convergence properties. It must be realized, however, that the beam model itself is an approximation to the actual 3-D case, and this discrepancy may need to be taken into account. We give an example of such a situation in Section 5.3.

Triangular Plate and Shell Elements

Plates and shells have one of their dimensions (the thickness) considerably smaller that the other two dimensions. In a manner similar to what is done for rods and beams, the behavior through the thickness is replaced in terms of resultants. We illustrate this for the membrane and flexural behavior.

Consider a triangle divided into three areas where the common apex is at location (x, y) as shown in Figure 1.20(a). Define

$$h_1 = A_1/A, \qquad h_2 = A_2/A, \qquad h_3 = A_3/A, \qquad h_i = h_i(x, y)$$

with the obvious constraint that $h_1 + h_2 + h_3 = 1$. The areas of these triangles define uniquely the position of the common apex.

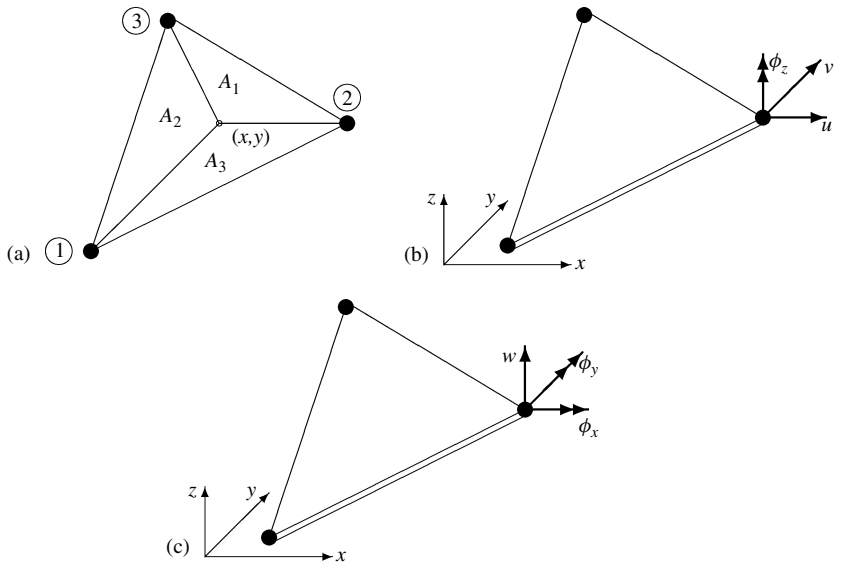

Figure 1.20: Triangular discretizations with nodal degrees of freedom. (a) Area coordinates for a triangle. (b) Membrane DoF. (c) Bending DoF.

The position of a point (x, y) in the triangle can be written as

$$\begin{Bmatrix} 1 \\ x \\ y \end{Bmatrix} = \begin{bmatrix} 1 & 1 & 1 \\ x_1 & x_2 & x_3 \\ y_1 & y_2 & y_3 \end{bmatrix} \begin{Bmatrix} h_1 \\ h_2 \\ h_3 \end{Bmatrix} \tag{1.31}$$

where the subscripts $1, 2, 3$ refer to the counterclockwise nodes of the triangle. We can invert this to get the expressions for the area coordinates

$$\begin{Bmatrix} h_1 \\ h_2 \\ h_3 \end{Bmatrix} = \frac{1}{2A} \begin{bmatrix} x_2y_3 - x_3y_2 & y_{23} & x_{32} \\ x_3y_1 - x_1y_3 & y_{31} & x_{13} \\ x_1y_2 - x_2y_1 & y_{12} & x_{21} \end{bmatrix} \begin{Bmatrix} 1 \\ x \\ y \end{Bmatrix} = \frac{1}{2A} \begin{bmatrix} a_1 & b_1 & c_1 \\ a_2 & b_2 & c_2 \\ a_3 & b_3 & c_3 \end{bmatrix} \begin{Bmatrix} 1 \\ x \\ y \end{Bmatrix} \tag{1.32}$$

with $2A \equiv x_{21}y_{31} - x_{31}y_{21}$, $x_{ij} \equiv x_i - x_j$, and so on. From this, it is apparent that functions of (x, y) can equally well be written as functions of (h_1, h_2, h_3); that is, any function of interest can be written as

$$u(x, y) = \sum\nolimits_i^3 h_i(x, y)u_i$$

where u_i are the nodal values.

Perhaps the simplest continuum element to formulate is that of the constant strain triangle (CST) element. We therefore begin with a discussion of this element. The basic assumption in the formulation is that the displacements are described by

$$u(x, y) = \sum\nolimits_i^3 h_i(x, y)u_i\,, \qquad v(x, y) = \sum\nolimits_i^3 h_i(x, y)v_i$$

The displacement gradients are given by

$$\frac{\partial u}{\partial x} = \sum \frac{\partial h_i}{\partial x} u_i = \frac{1}{2A} \sum\nolimits_i b_i u_i \,, \qquad \frac{\partial v}{\partial x} = \sum \frac{\partial h_i}{\partial x} v_i = \frac{1}{2A} \sum\nolimits_i b_i v_i$$
$$\frac{\partial u}{\partial y} = \sum \frac{\partial h_i}{\partial y} u_i = \frac{1}{2A} \sum\nolimits_i c_i u_i \,, \qquad \frac{\partial v}{\partial y} = \sum \frac{\partial h_i}{\partial y} v_i = \frac{1}{2A} \sum\nolimits_i c_i v_i$$

where the coefficients b_i and c_i are understood to be evaluated with respect to the original configuration. The strains are

$$\epsilon_{xx} = \frac{\partial u}{\partial x} \,, \qquad \epsilon_{yy} = \frac{\partial v}{\partial y} \,, \qquad 2\epsilon_{xy} = \gamma_{xy} = \frac{\partial u}{\partial y} + \frac{\partial v}{\partial x}$$

which are expressed in matrix form as

$$\begin{Bmatrix} \epsilon_{xx} \\ \epsilon_{yy} \\ 2\epsilon_{xy} \end{Bmatrix} = \frac{1}{2A} \begin{bmatrix} b_1 & 0 & b_2 & 0 & b_3 & 0 \\ 0 & c_1 & 0 & c_2 & 0 & c_3 \\ c_1 & b_1 & c_2 & b_2 & c_3 & b_3 \end{bmatrix} \begin{Bmatrix} u_1 \\ v_1 \\ u_2 \\ v_2 \\ u_3 \\ v_3 \end{Bmatrix} \quad \text{or} \quad \{\epsilon\} = [\, B_L \,]\{u\}$$

The stresses are related to the strains by the plane stress Hooke's law

$$\begin{Bmatrix} \sigma_{xx} \\ \sigma_{yy} \\ \sigma_{xy} \end{Bmatrix} = \frac{E}{1-\nu^2} \begin{bmatrix} 1 & \nu & 0 \\ \nu & 1 & 0 \\ 0 & 0 & (1-\nu)/2 \end{bmatrix} \begin{Bmatrix} \epsilon_{xx} \\ \epsilon_{yy} \\ 2\epsilon_{xy} \end{Bmatrix} \quad \text{or} \quad \{\sigma\} = [\, \mathbf{D} \,]\{\epsilon\}$$

The virtual work for a plate in plane stress is

$$\delta W = \int_V \left[\sigma_{xx}\delta\epsilon_{xx} + \sigma_{yy}\delta\epsilon_{yy} + \sigma_{xy}\delta\gamma_{xy}\right] \mathrm{d}V \qquad \text{or} \qquad \delta W = \int_V \{\sigma\}^{\mathrm{T}} \delta\{\epsilon\} \, \mathrm{d}V$$

Substituting for the stresses and strains in terms of the degrees of freedom gives

$$\delta W = \int_V \{u\}^{\mathrm{T}} [\, B_L \,]^{\mathrm{T}} [\, D \,] [\, B_L \,] \delta\{u\} \, \mathrm{d}V$$

Noting that none of the quantities inside the integral depends on the position coordinates, we have

$$\delta W = \{u\}^{\mathrm{T}} [\, B_L \,]^{\mathrm{T}} [\, D \,] [\, B_L \,] \delta\{u\} V$$

The virtual work of the nodal loads is

$$\delta W = \{F_{\mathrm{e}}\}^{\mathrm{T}} \delta\{u\}$$

From the equivalence of the two, we conclude that the nodal forces are related to the degrees of freedom through

$$\{F_{\mathrm{e}}\} = [\, k \,]\{u\} \,, \qquad [\, k \,] \equiv [\, B_L \,]^{\mathrm{T}} [\, D \,] [\, B_L \,] V \tag{1.33}$$

The [6 × 6] square matrix [k] is called the stiffness matrix for the *Constant Strain Triangle* (CST) element.

The CST element has only two displacements in its formulation and is generally overstiff in situations involving rotations. A three-noded triangular element (which we will label as MRT) is discussed in Reference [71] and taken from References [25, 26]. This element is shown to have superior in-plane performance over the CST element. The DoF at each node are $\{u\} = \{u, v, \phi_z\}$. A similar element was developed in Reference [9], and a nice comparison of the performance of these elements is given in Reference [135].

The convergence study is for the deep cantilever beam shown in Figure 1.21; the basic mesh is also shown in the figure—other meshes are similar except that the number of modules per side was changed by factors of two.

The results for the tip deflection at B and stresses at A are shown in Figure 1.22 where they are compared with the exact solution. The normalizations are with respect to the exact solution for v_B and σ_A. Both elements show a nice convergence to the exact solution.

The basic idea of the discrete Kirchhoff triangular (DKT) element is to treat the plate element in flexure as composed of a series of plane stress triangular laminas stacked on top of each other. From the previous discussion, we know that we can describe each lamina adequately using the CST or higher element; hence, it then only remains to impose the

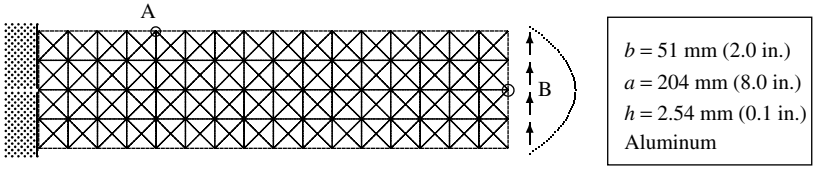

Figure 1.21: Mesh geometry [4 × 16] for a cantilever beam.

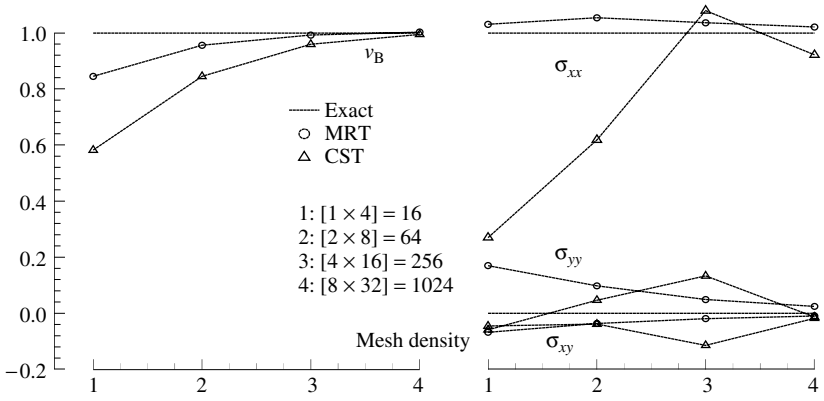

Figure 1.22: Convergence of membrane displacements and stresses.

constraints that the laminas form a structure in flexure. An explicit formulation is given in Reference [20] and coding is given in References [45, 96].

This element, now called the Discrete Kirchhoff Triangular (DKT) element was first introduced by Stricklin, Haisler, Tisdale, and Gunderson in 1968 [162]. It has been widely researched and documented as being one of the more efficient flexural elements. Batoz, Bathe, and Ho [19] performed extensive testing on three different elements including the hybrid stress model (HSM), DKT element, and a selective reduced integration (SRI) element. Comparisons between the different element types were made based on the results from different mesh orientations and different boundary and loading conditions. The authors concluded that the DKT and HSM elements are the most effective elements available for bending analysis of thin plates. Of these two elements, the DKT element was deemed superior to the HSM element based on the comparison between the experimental and theoretical results [19].

We now look at the convergence properties of the DKT element. The problem considered is that of a simply supported plate (with mesh as shown in Figure 1.23) and the transverse load applied uniformly. When looking at convergence, it is necessary to change the mesh in a systematic way. The mesh shown is made of [4 × 8] modules, where each module is made of four elements. The other meshes are variations of this mesh, obtained by uniformly changing the number of modules.

The results are shown in Figure 1.24 where it is compared with the exact solution. The normalizations for the displacements and moments are

$$w_{\mathrm{o}} = \frac{16 q_{\mathrm{o}} b^4}{D\pi^6}, \qquad M_{\mathrm{o}} = \frac{q_{\mathrm{o}} b^2}{4\pi^2}$$

The DKT element exhibits excellent convergence. It is pleasing to see that it gives good results even for relatively few modules.

The performance of the DKT element for the moments is also very good. These reported moments are nodal averages. Because a lumped load was used in this example, we conclude that a lumped representation is adequate when a suitably refined mesh is used.

In our formulation, the displacement of each node of a space frame or shell is described by three translational and three rotational components of displacement, giving

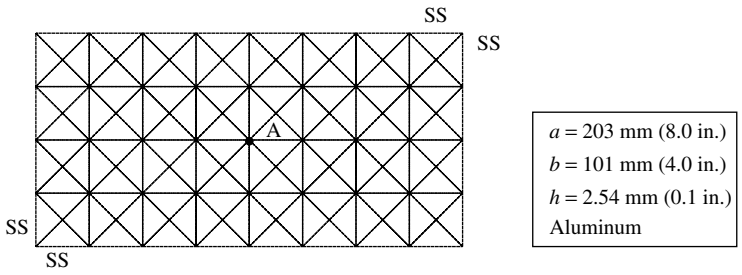

Figure 1.23: Generic [4 × 8] mesh used in the plate flexure convergence study.

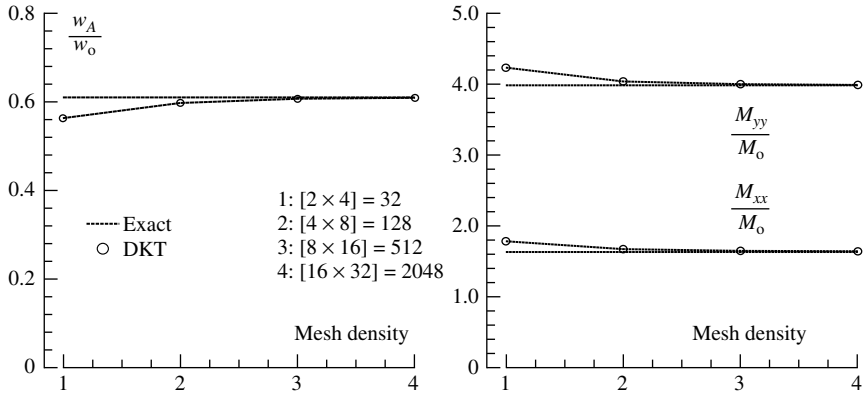

Figure 1.24: Convergence study for displacements and moments.

six degrees of freedom at each unrestrained node. Corresponding to these degrees of freedom are six nodal loads. The notations for the shell are identical to those of the space frame. For each element in local coordinates, the forces are related to the displacements by

$$\{\overline{F}_e\} = \{\overline{u}\} = [\ \overline{k}\ ]\{\overline{u}\}$$

where $[\ \overline{k}\ ]$ is of size $[18 \times 18]$. It is comprised of a combination of the $[9 \times 9]$ MRT and $[9 \times 9]$ DKT elements. Just as for the frame, we can write the element stiffness of the shell in global coordinates as a transformation of the local stiffness

$$[\ k\ ] = [\ T\ ]^T[\ \overline{k}\ ][\ T\ ]$$

Here, however, $[\ T\ ]$ is of size $[18 \times 18]$ and its construction is given in Reference [71]. The assemblage procedure is the same as for the frame.

Applied Body and Traction Loads

The applied loads fall into two categories. The first are point forces and moments; these do not need any special treatment since they are already in nodal form. The others arise from distributed loads in the form of body loads such as weight and applied tractions such as pressures; these are the loads of interest here. We want to develop a scheme that converts the distributed loads into equivalent concentrated forces and moments. In this process, this adds another level of approximation to the FEM solution; but keep in mind that any desired degree of accuracy can always be achieved by increasing the number of nodes. (This is at the expense of computing time, but has the advantage of being simple.) The question now is as follows: is there a best way to convert a distributed load into a set of concentrated loads? We will investigate two approximate ways of doing this.

To get the equivalent nodal loads, we will equate the virtual work of the nodal loads to that of the distributed load. The virtual work is the load times the virtual displacement,

we will take the displacement as represented (interpolated) by

$$\{\overline{u}(x, y, z)\} = [N(x, y, z)]\{u\}$$

where $\{\overline{u}\}$ is the collection of relevant displacements.

Consider the body forces first. The virtual work is

$$\{P\}^{\mathrm{T}}\{\delta u\} = \int_V \{\rho\overline{b}(x, y, z)\}^{\mathrm{T}}\{\delta\overline{u}(x, y, z)\}\,\mathrm{d}V = \int_V \{\rho\overline{b}(x, y, z)\}^{\mathrm{T}}[N(x, y, z)]\{\delta u\}\,\mathrm{d}V$$

This leads to

$$\{P\} = \int_V [N(x, y, z)]^{\mathrm{T}}\{\rho\overline{b}(x, y, z)\}\,\mathrm{d}V$$

If, furthermore, the body force distribution is discretized similar to the displacements, that is,

$$\{\rho\overline{b}(x, y, z)\} = [N(x, y, z)]\{\rho b\}$$

then the equivalent nodal forces are given by

$$\{P\} = \left\{\int_V [N(x, y, z)]^{\mathrm{T}}[N(x, y, z)]\,\mathrm{d}V\right\}\{\rho b\}$$

We will gives a few examples of this.

Consider the beam shown in Figure 1.25. The virtual work of the equivalent system is

$$\delta W_{\mathrm{e}} = P_1\delta v_1 + T_1\delta\phi_1 + P_2\delta v_2 + T_2\delta\phi_2$$

The displacements are interpolated as

$$v(x) = g_1(x)v_1 + g_2(x)L\phi_1 + g_3(x)v_2 + g_4(x)L\phi_2 = [g_1, g_2L, g_3, g_4L]\{u\} = [\ N\ ]\{u\}$$

If the body force per unit length is uniform such that $\rho b = q_0 =$ constant, then the integrations lead to

$$\{P\} = \{P_1, T_1, P_2, T_2\}^{\mathrm{T}} = \tfrac{1}{2}q_0AL\{1, \tfrac{1}{6}L, 1, -\tfrac{1}{6}L\}^{\mathrm{T}}$$

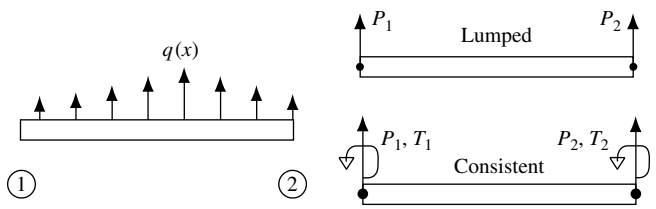

Figure 1.25: Replacement of an arbitrary load distribution by equivalent nodal values.

It is interesting to note the presence of the moments. Consider the triangular membrane element with displacements represented by

$$\begin{Bmatrix} u(x,y) \\ v(x,y) \end{Bmatrix} = \frac{1}{2A} \begin{bmatrix} h_1 & 0 & h_2 & 0 & h_3 & 0 \\ 0 & h_1 & 0 & h_2 & 0 & h_3 \end{bmatrix} \begin{Bmatrix} u_1 \\ \vdots \\ v_3 \end{Bmatrix} = [\ N\ ]\{u\}$$

Assuming $\rho b_i = q_{i0} =$ constant leads to

$$\{P\} = \{P_{x1}, P_{y1}, \ldots, P_{y3}\}^{\mathrm{T}} = \tfrac{1}{3} Ah\{q_{x0}, q_{y0}; q_{x0}, q_{y0}; q_{x0}, q_{y0}\}^{\mathrm{T}}$$

The other elements are treated in a similar fashion. The next section, when dealing with the mass matrix, shows examples of using linear interpolations on the body forces.

Traction distributions are treated similar to the body forces except that the equivalent loads act only on the loaded section of the element. The virtual work is

$$\{P\}^{\mathrm{T}}\{\delta u\} = \int_A \{\bar{t}(x,y,z)\}^{\mathrm{T}}\{\delta \overline{u}(x,y,z)\}\,\mathrm{d}A = \int_A \{\bar{t}(x,y,z)\}^{\mathrm{T}}[N(x,y,z)]\{\delta u\}\,\mathrm{d}A$$

where A is the loaded surface. This leads to

$$\{P\} = \int_A [N(x,y,z)]^{\mathrm{T}}\{\bar{t}(x,y,z)\}\,\mathrm{d}A$$

If, furthermore, the body force distribution is discretized similar to the displacements, then the equivalent nodal forces are given by

$$\{P\} = \left\{ \int_A [N(x,y,z)]^{\mathrm{T}}[N(x,y,z)]\,\mathrm{d}A \right\} \{\, t\,\}$$

We will give just a single example of this.

Consider the triangle shown in Figure 1.26. Let the tractions at the end points be t_{x1}, t_{y1} and so on, and let them be linearly interpolated with the same interpolation functions

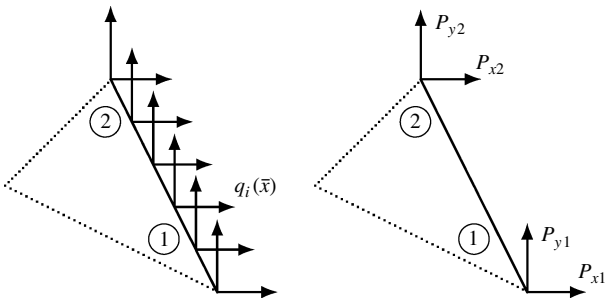

Figure 1.26: Replacement of an arbitrary traction load by equivalent nodal values.

as for the element. Then, the nodal forces are

$$\begin{Bmatrix} P_{x1} \\ P_{y1} \\ P_{x2} \\ P_{y2} \end{Bmatrix} = \frac{hL_{12}}{6} \begin{bmatrix} 2 & 0 & 1 & 0 \\ 0 & 2 & 0 & 1 \\ 1 & 0 & 2 & 0 \\ 0 & 1 & 0 & 2 \end{bmatrix} \begin{Bmatrix} t_{x1} \\ t_{y1} \\ t_{x2} \\ t_{y2} \end{Bmatrix}$$

We see that these replace the load distribution with nodal values that are weighted averages of the distribution. Because the weighting functions are the shape functions for the element displacements this representation is called the *consistent* load representation. Notice that the consistent loads in the case of the beam have moments even though the applied distributed load does not.

The consistent loads are a statically equivalent load system. This can be shown in general, but we demonstrate it with the following special cases. For a uniform distributed load q_0 acting on a beam, for example,

$$P_1 = \tfrac{1}{2}q_0 L, \qquad P_2 = \tfrac{1}{2}q_0 L$$
$$T_1 = +\tfrac{1}{12}q_0 L^2, \quad T_2 = -\tfrac{1}{12}q_0 L^2$$

The resultant vertical force is $P_1 + P_2 = q_0 L$, which is in agreement with the total distributed load. The resultant moment about the first node is $T_1 + T_2 + P_2 L = \frac{1}{2}q_0 L^2$ again in agreement with the value from the distributed load.

An alternative loading scheme is to simply lump the loads at the nodes, that is, for the beam, let

$$P_i = \tfrac{1}{2}\int_L q \, \mathrm{d}x \,, \qquad T_i = 0$$

A triangular plate element with a distributed pressure would put one-third of the resultant on each node. As shown in the example of Figure 1.23 for the rectangular plate, this is usually adequate when reasonable mesh refinements are used; the difference in the performance is only noticeable for coarse meshes. There is also another reason for preferring the lumped approach: during nonlinear deformations, the applied moments are nonconservative loads and therefore would require special treatment.

1.7 Dynamic Considerations

We showed earlier that the linearized version of Lagrange's equations leads to

$$[\ M\ ]\{\ddot{u}\} + [\ C\ ]\{\dot{u}\} + [\ K\ ]\{u\} = \{P\} \tag{1.34}$$

The computer solution of the structural equations of motion is discussed in more detail in later chapters, but it is of value now to consider some of the major problem types originating from this set. The above equations of motion are to be interpreted as a system of differential equations in time for the unknown nodal displacements $\{u\}$, subject to the known forcing histories $\{P\}$, and a set of boundary and initial conditions. The categorizing of problems is generally associated with the type of applied loading. But first we will establish the mass and damping matrices.

Mass and Damping Matrices

By D'Alembert's principle, we can consider the body force loads as comprising the applied force loads and the inertia loads, that is

$$\rho b_i \Rightarrow \rho b_i - \rho \ddot{u}_i - \eta \dot{u}_i$$

Thus, we can do a similar treatment as used for the body forces above. This leads to

$$-\sum_i \int_{V^o} (\rho \ddot{u}_i + \eta \dot{u}_i)\delta u_i \, \mathrm{d}V^o \Rightarrow -[\ m\ ]\{\ddot{u}\} = -\left[\int_{V^o} \rho [N]^{\mathrm{T}}[N] \, \mathrm{d}V^o\right]\{\ddot{u}\}$$

$$\Rightarrow -[\ c\ ]\{\dot{u}\} = -\left[\int_{V^o} \eta [N]^{\mathrm{T}}[N] \, \mathrm{d}V^o\right]\{\dot{u}\}$$

where $[\ m\ ]$ is called the element mass matrix and $[\ c\ ]$ is called the element damping matrix. Note that the integrations are over the original geometry. When the shape functions $[\ N\ ]$ are the same as used in the stiffness formulation, the mass and damping matrices are called *consistent*.

The assemblage process for the mass and damping matrices is done in exactly the same manner as for the linear elastic stiffness. As a result, the mass and damping matrices will exhibit all the symmetry and bandedness properties of the stiffness matrix. When the structural joints have concentrated masses, we need only amend the structural mass matrix as follows

$$[\ M\ ] = \sum_i [m^{(i)}] + \lceil M_{\mathrm{c}} \rfloor$$

where $\lceil M_{\mathrm{c}} \rfloor$ is the collection of joint concentrated masses. This is a diagonal matrix.

Note that the resulting matrix forms for $[\ m\ ]$ and $[\ c\ ]$ are identical, that is,

$$[\ c\ ] = \frac{\eta}{\rho}[\ m\ ]$$

This is an example of the damping matrix being proportional to the mass matrix on an element level. For proportional damping at the structural level, we assume

$$[\ C\ ] = \alpha[\ M\ ] + \beta[\ K\ ]$$

where α and β are constants chosen to best represent the physical situation. Note that this relation is not likely to hold for structures composed of different materials. However, for lightly damped structures it can be a useful approximation.

We will establish the mass matrix for the beam. The accelerations are represented by

$$\{\ddot{v}\} = [\ g_1 \ \ g_2 L \ \ g_3 \ \ g_4 L\ ] \begin{Bmatrix} \ddot{v}_1 \\ \vdots \\ \ddot{\phi}_2 \end{Bmatrix} \qquad \text{or} \qquad \{\ddot{u}\} = [\ N\ ]\{\ddot{u}\}$$

with [N] being a [1×4] matrix. The consistent mass matrix for a uniform beam is

$$m_{ij} = \int_0^L \rho A g_i(x) g_j(x)\,\mathrm{d}x \qquad \text{or} \qquad [\ m\ ] = \frac{\rho AL}{420}\begin{bmatrix} 156 & 22L & 54 & -13L \\ 22L & 4L^2 & 13L & -3L^2 \\ 54 & 13L & 156 & -22L \\ -13L & -3L^2 & -22L & 4L^2 \end{bmatrix}$$

The mass matrix of the frame is a composition of that of the rod and beam suitably augmented, for example, to [6×6] for a plane frame.

For the membrane behavior, we use the shape functions associated with the constant strain triangle. The accelerations are represented as

$$\begin{Bmatrix} \ddot{u} \\ \ddot{v} \end{Bmatrix} = \begin{bmatrix} h_1 & 0 & h_2 & 0 & h_3 & 0 \\ 0 & h_1 & 0 & h_2 & 0 & h_3 \end{bmatrix} \begin{Bmatrix} \ddot{u}_1 \\ \ddot{v}_1 \\ \vdots \\ \ddot{v}_3 \end{Bmatrix} \qquad \text{or} \qquad \{\ddot{u}\} = [\ N\ ]\{\ddot{u}\}$$

Then the mass matrix is

$$[\ m\ ] = \int_{V^o} \rho [\ N\ ]^{\mathrm{T}} [\ N\ ]\,\mathrm{d}V^o \Longrightarrow [\ m\ ] = \frac{\rho Ah}{12}\begin{bmatrix} 2 & 0 & 1 & 0 & 1 & 0 \\ 0 & 2 & 0 & 1 & 0 & 1 \\ 1 & 0 & 2 & 0 & 1 & 0 \\ 0 & 1 & 0 & 2 & 0 & 1 \\ 1 & 0 & 1 & 0 & 2 & 0 \\ 0 & 1 & 0 & 1 & 0 & 2 \end{bmatrix}$$

For the bending behavior, let the displacements be represented by

$$\{w(x, y)\} = [\ N\ ]\{u\}, \qquad \{u\} = \{w_1, \phi_{x1}, \phi_{y1}; w_2, \phi_{x2}, \phi_{y2}; w_3, \phi_{x3}, \phi_{y3}\}$$

where the shape functions $N(x, y)$ are appropriately selected. Again, we get

$$[\ m\ ] = \int \rho h [\ N\ ]^{\mathrm{T}} [\ N\ ]\,\mathrm{d}A$$

The expressions are too lengthy to write here. We will generally find it more beneficial, anyway, to use the lumped mass matrix.

It is useful to realize that because the mass matrix does not involve derivatives of the shape function, we can be more lax about the choice of shape function than for the stiffness matrix. In fact, in many applications, we will find it preferable to use a lumped mass (and damping) approximation where the only nonzero terms are on the diagonal. We show some examples here.

The simplest mass model is to consider only the translational inertias, which are obtained simply by dividing the total mass by the number of nodes and placing this value of mass at the node. Thus, the diagonal terms for the 3-D frame and plate are

$$\lceil\ m\ \rfloor = \tfrac{1}{2}\rho AL\lceil 1, 1, 1, 0, 0, 0; 1, 1, 1, 0, 0, 0\rfloor$$

$$\lceil\ m\ \rfloor = \tfrac{1}{3}\rho Ah\lceil 1, 1, 1, 0, 0, 0; 1, 1, 1, 0, 0, 0; 1, 1, 1, 0, 0, 0\rfloor$$

respectively. These neglect the rotational inertias of the flexural actions. Generally, these contributions are negligible and the above are quite accurate especially when the elements are small. There is, however, a very important circumstance when a zero diagonal mass is unacceptable and reasonable nonzero values are needed. Later in this section, we develop an explicit numerical integration scheme where the time step depends on the highest resonant frequencies of the structure; these frequencies in turn are dictated by the rotational inertias—a zero value would imply an infinitesimally small Δt.

First consider the frame. We will use the diagonal terms of the consistent matrix to form an estimate of the diagonal matrix. Note that the translation diagonal terms add up to only $\rho AL312/420$. Hence, by scaling each diagonal term by $420/312$ we get

$$\lceil\ m\ \rfloor = \tfrac{1}{2}\rho AL\lceil 1, 1, 1, 2\beta, \beta, \beta; 1, 1, 1, 2\beta, \beta, \beta\rfloor\,, \qquad \beta = \alpha L^2/40$$

where α is typically taken as unity. This scheme has the merit of correctly giving the translational inertias. We treat the plate in an analogous manner as

$$\lceil\ m\ \rfloor = \tfrac{1}{3}\rho Ah\lceil 1, 1, 1, \beta, \beta, 20\beta; 1, 1, 1, \beta, \beta, 20\beta; 1, 1, 1, \beta, \beta, 20\beta\rfloor$$

with $\beta = \alpha L^2/40$. We estimate the effective length $L \approx \sqrt{A/\pi}$ as basically the radius of a disk of the same area as the triangle. Again, α is typically taken as unity.

Types of Linear Dynamic Problems

For *transient* dynamic problems, the applied load $P(t)$ are general functions of time. Typically, the equations require some numerical scheme for integration over time and become computationally intensive in two respects. First, a substantial increase in the number of elements must be used in order to model the mass and stiffness distributions accurately. The other is that the complete system of equations must be solved at each time increment. When the applied load is short lived, the resulting problem gives rise to *free wave propagation*.

For the special case when the excitation force is time harmonic, that is,

$$\{P\} = \{\hat{P}\}\mathrm{e}^{\mathrm{i}\omega t} \qquad \text{or} \qquad \begin{Bmatrix} P_1 \\ \vdots \\ P_n \end{Bmatrix} = \begin{Bmatrix} \hat{P}_1 \\ \vdots \\ \hat{P}_n \end{Bmatrix} \mathrm{e}^{\mathrm{i}\omega t}$$

where ω is the angular frequency and many of the P_n could be zero, then the response is also harmonic and given by

$$\{u\} = \{\hat{u}\}\mathrm{e}^{\mathrm{i}\omega t} \qquad \text{or} \qquad \begin{Bmatrix} u_1 \\ \vdots \\ u_n \end{Bmatrix} = \begin{Bmatrix} \hat{u}_1 \\ \vdots \\ \hat{u}_n \end{Bmatrix} \mathrm{e}^{\mathrm{i}\omega t}$$

This type of analysis is referred to as *forced frequency* analysis. Substituting these forms into the differential equations gives

$$[\ K\ ]\{\hat{u}\}\mathrm{e}^{\mathrm{i}\omega t} + \mathrm{i}\omega[\ C\ ]\{\hat{u}\}\mathrm{e}^{\mathrm{i}\omega t} - \omega^2[\ M\ ]\{\hat{u}\}\mathrm{e}^{\mathrm{i}\omega t} = \{\hat{P}\}\mathrm{e}^{\mathrm{i}\omega t}$$

or, after canceling through the common time factor,

$$\Big[[\ K\ ] + \mathrm{i}\omega[\ C\ ] - \omega^2[\ M\ ]\Big]\{\hat{u}\} = \{\hat{P}\} \qquad \text{or} \qquad [\ \hat{K}\ ]\{\hat{u}\} = \{\hat{P}\}$$

Thus, the solution can be obtained analogous to the static problem; the difference is that the stiffness matrix is modified by the inertia term $\omega^2[\ M\ ]$ and the complex damping term $\mathrm{i}\omega[\ C\ ]$. This is the discrete approximation of the dynamic structural stiffness. It is therefore frequency dependent as well as complex. This system of equations is now recognized as the spectral form of the equations of motion of the structure. One approach, then, to transient problems is to evaluate the above at each frequency and use the FFT [31] for time domain reconstructions. This is feasible, but a more full-fledged spectral approach based on the exact dynamic stiffness is developed in References [70].

A case of very special interest is that of free vibrations. When the damping is zero this case gives the mode shapes that are a very important aspect of modal analysis [76, 82]. For free vibrations of the system, the applied loads $\{P\}$ are zero giving the equations of motion as

$$[[\ K\ ] - \omega^2[\ M\ ]]\{\hat{u}\} = 0$$

This is a system of homogeneous equations for the nodal displacements $\{\hat{u}\}$. For a nontrivial solution, the determinant of the matrix of coefficients must be zero. We thus conclude that this is an eigenvalue problem, ω^2 are the eigenvalues, and the corresponding $\{\hat{u}\}$ are the eigenvectors of the problem. Note that the larger the number of elements (for a given structure), the larger the system of equations; consequently, the more eigenvalues we can obtain.

In the remainder of this section, and in some of the forthcoming chapters, we will be primarily concerned with the transient dynamic problem.

Time Integration Methods

This section introduces some time integration methods for finding the dynamic response of structures; that is, the dynamic equilibrium equations are integrated directly in a step-by-step fashion.

To construct the central difference algorithm, we begin with finite difference expressions for the nodal velocities and accelerations at the current time t

$$\{\dot{u}\}_t = \frac{1}{2\Delta t}\{u_{t+\Delta t} - u_{t-\Delta t}\}, \qquad \{\ddot{u}\}_t = \frac{1}{\Delta t^2}\{u_{t+\Delta t} - 2u_t + u_{t-\Delta t}\} \tag{1.35}$$

Substitute these into the equations of motion written at time t to get

$$[\ K\ ]\{u\}_t + [\ C\ ]\frac{1}{2\Delta t}\{u_{t+\Delta t} - u_{t-\Delta t}\} + [\ M\ ]\frac{1}{\Delta t^2}\{u_{t+\Delta t} - 2u_t + u_{t-\Delta t}\} = \{P\}_t$$

We can rearrange this equation so that only quantities evaluated at time $t + \Delta t$ are on the left-hand side

$$\left[\frac{1}{2\Delta t}C + \frac{1}{\Delta t^2}M\right]\{u\}_{t+\Delta t} = \{P\}_t - \left[K - \frac{2}{\Delta t^2}M\right]\{u\}_t - \left[\frac{1}{\Delta t^2}M - \frac{1}{2\Delta t}C\right]\{u\}_{t-\Delta t} \tag{1.36}$$

This scheme is therefore explicit. Note that the stiffness is on the right-hand side in the effective load vector; therefore, these equations cannot recover the static solution in the limit of large Δt. Furthermore, if the mass matrix is not positive definite (that is, if it has some zeros on the diagonal) then the scheme does not work, because the square matrix on the left-hand side is not invertible.

The algorithm for the step-by-step solution operates as follows: we start at $t = 0$; initial conditions prescribe $\{u\}_0$ and $\{\dot{u}\}_0$. From these and the equation of motion we find the acceleration $\{\ddot{u}\}_0$ if it is not prescribed. These equations also yield the displacements $\{u\}_{-\Delta t}$ needed to start the computations; that is, from the differences for the velocity and acceleration we get

$$\{u\}_{-\Delta t} = \{u\}_0 - (\Delta t)\{\dot{u}\}_0 + \tfrac{1}{2}(\Delta t)^2\{\ddot{u}\}_0$$

The set of Equations (1.35) and (1.36) are then used repeatedly; the equation of motion gives $\{u\}_{\Delta t}$, then the difference equations give $\{\ddot{u}\}_{\Delta t}$ and $\{\dot{u}\}_{\Delta t}$, and then the process is repeated.

We now derive a different integration scheme by considering the equations of motion at the time step $t + \Delta t$. Assume that the acceleration is constant over the small time step Δt and is given by its average value, that is,

$$\ddot{u}(t) \approx \tfrac{1}{2}(\ddot{u}_t + \ddot{u}_{t+\Delta t}) = \text{constant} = \alpha$$

Integrate this to give the velocity and displacement as

$$\dot{u}(t) = \dot{u}_t + \alpha t\,, \qquad u(t) = u_t + \dot{u}_t t + \tfrac{1}{2}\alpha t^2$$

We estimate the average acceleration by evaluating the displacement at time $t + \Delta t$ to give

$$\tfrac{1}{2}(\ddot{u}_t + \ddot{u}_{t+\Delta t}) = \alpha = \frac{2}{\Delta t^2}\{u_{t+\Delta t} - u_t - \dot{u}_t\Delta t\}$$

These equations can be rearranged to give difference formulas for the new acceleration and velocity (at time $t + \Delta t$) in terms of the new displacement as

$$\begin{aligned}\{\ddot{u}\}_{t+\Delta t} &= 2\{\alpha\} - \{\ddot{u}\}_t = \frac{4}{\Delta t^2}\{u_{t+\Delta t} - u_t\} - \frac{4}{\Delta t}\{\dot{u}\}_t - \{\ddot{u}\}_t \\ \{\dot{u}\}_{t+\Delta t} &= \{\alpha\}\Delta t + \{\dot{u}\}_t = \frac{2}{\Delta t}\{u_{t+\Delta t} - u_t\} - \{\dot{u}\}_t\end{aligned} \tag{1.37}$$

Substitute these into the equations of motion at the new time $t + \Delta t$ and shift all terms that have been evaluated at time t to the right-hand side to obtain the scheme

$$\left[K + \frac{2}{\Delta t}C + \frac{4}{\Delta t^2}M\right]\{u\}_{t+\Delta t} = \{P\}_{t+\Delta t} + [\ C\ ]\left\{\frac{2}{\Delta t}u + \dot{u}\right\}_t + [\ M\ ]\left\{\frac{4}{\Delta t^2}u + \frac{4}{\Delta t}\dot{u} + \ddot{u}\right\}_t \tag{1.38}$$

The new displacements are obtained by solving this system of simultaneous equations, which makes it an implicit scheme. This scheme is a special case of Newmark's method [18].

The algorithm operates very similar to the explicit scheme: We start at $t = 0$; initial conditions prescribe $\{u\}_0$ and $\{\dot{u}\}_0$. From these and the equations of motion (written at time $t = 0$) we find $\{\ddot{u}\}_0$ if it is not prescribed. Then the above system of equations are solved for the displacement $\{u\}_{\Delta t}$, from which estimates of the accelerations $\{\ddot{u}\}_{\Delta t}$ and the velocities $\{\dot{u}\}_{\Delta t}$ can also be obtained. These are used to obtain current values of the right-hand side. Then solving the equation of motion again yields $\{u\}_{2\Delta t}$, and so on. The solution procedure for $\{u\}_{t+\Delta t}$ is not trivial, but the coefficient matrix need to be reduced to $[\ U\ ]^{\mathrm{T}}\lceil\ D\ \rfloor[\ U\ ]$ form only once if Δt and all of the system matrices do not change during the integration. Note that in the limit of large ΔT we recover the static solution.

Explicit Versus Implicit Schemes

The computational cost for the explicit method is approximately

$$\text{cost} = \tfrac{1}{2}NB_{\mathrm{m}}^2 + [2N(2B_{\mathrm{m}} - 1) + N2B]q$$

where q is the number of time increments, B is the semibandwidth of the stiffness matrix, and B_{m} is the semibandwidth of the mass (and damping) matrix. When the mass matrix is diagonal this reduces to

$$\text{cost} = 2NBq$$

Thus, there is a considerable reduction when the mass and damping matrices are diagonal.

By contrast, the computational cost for the implicit method is approximately

$$\text{cost} = \tfrac{1}{2}NB^2 + [2NB + 2N(2B_{\mathrm{m}} - 1)]q$$

where the first term is the cost of the matrix decomposition. When the mass matrix is diagonal this reduces to

$$\text{cost} = \tfrac{1}{2}NB^2 + 2NBq$$

Except for the cost of the initial decomposition, the total cost is the same as for the central difference method.

Numerical integration schemes are susceptible to (numerical) instabilities, a symptom of which is that the solution diverges at each time step. For the central difference algorithm, we require that [71]

$$\Delta t < \frac{2}{\omega} = \frac{T}{\pi} \tag{1.39}$$

where T is the period associated with the frequency ω. Therefore, for numerical stability, the step size must be less than one-third of the period. Hence, the method is only *conditionally stable*, since it is possible for this criterion to not be satisfied in some circumstances. For the average acceleration method, we get that the system is *unconditionally stable* [71], gives no amplitude decay, but will exhibit a phase shift.

The foregoing analysis shows that the computational cost for the explicit central difference scheme can be less than the implicit average acceleration method. Further, the stability criterion of Equation (1.39) will be automatically satisfied for the explicit scheme because of accuracy considerations; that is, this seems easily achieved since it is generally considered [24, 45] that the step size should be less than one-tenth the period for an accurate solution. Hence, we could conclude that the explicit scheme is preferable of the two.

A very important factor was overlooked in the above discussion: a multiple degree of freedom system will have many (vibrational) modes, and when direct integration is used, this is equivalent to integrating each mode with the same time step Δt. Therefore, the above stability criterion must be applied to the highest modal frequency of the system even if our interest is in the low frequency response. In other words, if we energize the system in such a way as to excite only the lower frequencies, we must nonetheless choose an integration step corresponding to the highest possible mode. The significance of this is that the matrix analyses of structures produce so-called *stiff equations*. In the present context, stiff equations characterize a structure whose highest natural vibration frequencies are much greater than the lowest. Especially stiff structures therefore include those with a very fine mesh, and a structure with near-rigid support members. If the conditionally stable algorithm is used for these structures, Δt must be very small, usually orders of magnitude smaller than for the implicit scheme.

In summary, explicit methods are conditionally stable and therefore require a small Δt but produce equations that are cheap to solve. The implicit methods are (generally) unconditionally stable and therefore allow a large Δt but produce equations that are more expensive to solve. The size of Δt is governed by considerations of accuracy rather than stability; that is, we can adjust the step size appropriate to the excitation force or the number of modes actually excited. The difference factor can be orders of magnitude and will invariably outweigh any disadvantage in having to decompose the system matrices. On the basis of these considerations, the implicit scheme is generally the method of choice for general structural dynamics problems that are linear and where the frequency content is relatively low. The explicit scheme is generally the method of choice for wave-type dynamic problems where the frequency content is relatively high. A schematic of this division is shown in Figure 1.27. Additional considerations come into play when we look at nonlinear systems. More discussions can be found in References [24, 71].

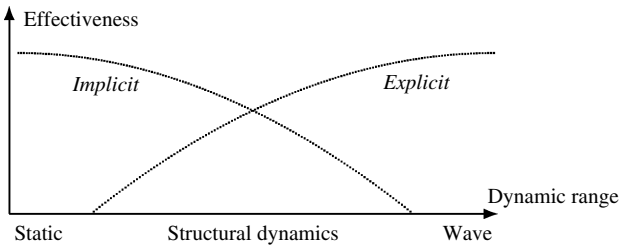

Figure 1.27: Overlap of effectiveness of implicit and explicit integration methods.

1.8 Geometrically Nonlinear Problems

In this section, using some simple examples taken from Reference [71], we lay out the basic difficulties inherent in directly solving nonlinear problems. All nonlinear problems are solved in an incremental/iterative manner with some sort of linearization done at each time or load step; that is, we view the deformation as occurring in a sequence of steps associated with time increments Δt, and at each step it is the increment of displacements that are considered to be the unknowns. We first consider this incremental aspect to the solution.

Incremental Solution Scheme

Consider the loading equation (1.25) at time step t_{n+1}

$$\{\mathcal{F}\}_{n+1} = \{P\}_{n+1} - \{F(u)\}_{n+1} = \{0\}$$

where $\{P\}$ are the applied loads, $\{F(u)\}$ are the deformation dependent element nodal forces, $\{\mathcal{F}\}$ is the vector of out-of-balance forces; all are of size $\{M_u \times 1\}$. For equilibrium, we must have that $\{\mathcal{F}\} = \{0\}$, but as we will see this is not necessarily (numerically) true during an incremental approximation of the solution.

We do not know the displacements $\{u\}_{n+1}$; hence we cannot compute the nodal forces $\{F\}_{n+1}$. As is usual in such nonlinear problems, we linearize about a known state; that is, assume we know everything at time step t_n, then write the Taylor series approximation for the element nodal forces

$$\{F(u)\}_{n+1} \approx \{F(u)\}_n + \left[\frac{\partial F}{\partial u}\right]_n \{\Delta u\} + \cdots = \{F(u)\}_n + [K_{\mathrm{T}}]_n\{\Delta u\} + \cdots \qquad (1.40)$$

The square matrix $[K_{\mathrm{T}}]$ is called the *tangent stiffness matrix*. It is banded, symmetric of size $[M_u \times B]$.

We are now in a position to solve for the increments of displacement; rearrange the approximate equilibrium equation into a loading equation as

$$\{P\}_{n+1} - \{F\}_n - [K_{\mathrm{T}}]\{\Delta u\} \approx 0 \Longrightarrow [K_{\mathrm{T}}]\{\Delta u\} = \{P\}_{n+1} - \{F\}_n$$

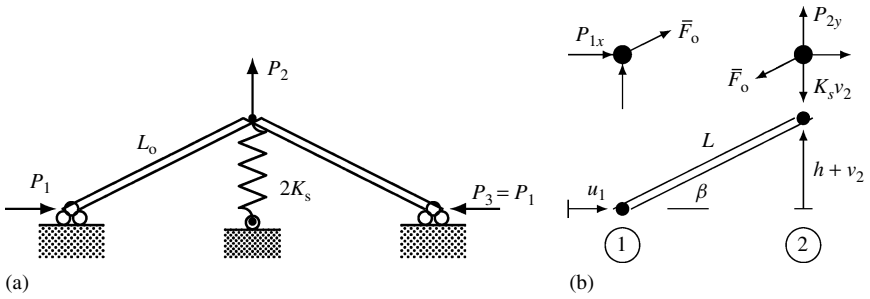

Figure 1.28: Simple pinned truss with a grounded spring. (a) Geometry. (b) Free-body diagrams.

The basic procedure is to compute the increment $\{\Delta u\}$, update the displacement and element nodal forces, and move to the next load level.

To make the ideas explicit, consider the simple truss whose geometry is shown in Figure 1.28. The members are of original length L_o and the unloaded condition has the apex at a height of h. The two ends are on pinned rollers. When h is zero, this problem gives rise to a static instability (buckling); nonzero h acts as a geometric imperfection. This problem is considered in greater depth in Reference [71].

Let the height h be small relative to the member length, and let the deflections be somewhat small; then we have the geometric approximations

$$L_x = L\cos\alpha \approx L_o - u_1\,, \qquad L_y = L\sin\alpha \approx h + v_2\,, \qquad u_1 \ll v_2$$

The deformed length of the member is

$$L = \sqrt{(L_o - u_1)^2 + (h + v_2)^2} \approx L_o - u_1 + \frac{h}{L_o}v_2 + \frac{1}{2}L_o\left(\frac{v_2}{L_o}\right)^2$$

The axial force is computed from the axial strain as

$$\overline{F}_o = EA_o\overline{\epsilon} = EA_o\frac{L - L_o}{L_o} = EA_o\left[-\frac{u_1}{L_o} + \frac{h}{L_o}\frac{v_2}{L_o} + \tfrac{1}{2}\left(\frac{v_2}{L_o}\right)^2\right]$$

Note that we consider the parameters of the constitutive relation to be unchanged during the deformation.

Look at equilibrium in the deformed configuration as indicated in Figure 1.28; specifically, consider the resultant horizontal force at Node 1 and vertical force at Node 2 giving

$$0 = P_{1x} + \overline{F}_o\cos\beta \approx P_{1x} + \overline{F}_o$$
$$0 = P_{2y} - \overline{F}_o\sin\beta - K_s v_2 \approx P_{2y} - \beta\overline{F}_o - K_s v_2\,, \qquad \beta \equiv (h + v_2)/L_o$$

Rewrite these in vector form as

$$\begin{Bmatrix} 0 \\ 0 \end{Bmatrix} = \begin{Bmatrix} P_{1x} \\ P_{2y} \end{Bmatrix} + \begin{Bmatrix} \overline{F}_o \\ -\beta\overline{F}_o \end{Bmatrix} - \begin{Bmatrix} 0 \\ K_s v_2 \end{Bmatrix} \qquad \text{or} \qquad \{\mathcal{F}\} = \{P\} - \{F\} = \{0\}$$

We can solve these equations explicitly for the special case $P_{1x} = P$, $P_{2y} = 0$. This leads to $\overline{F}_o = -P$ and the two deflections

$$u_1 = \left[\frac{P}{EA} + \left(\frac{h}{L_o}\right)^2 \frac{P}{K_s L_o - P} + \frac{1}{2}\left(\frac{h}{L_o}\right)^2 \left(\frac{P}{K_s L_o - P}\right)^2 \right] L_o$$

$$v_2 = \left[\frac{h}{L_o} \frac{P}{K_s L_o - P} \right] L_o$$

The load/deflection relations are nonlinear even though the deflections are assumed to be somewhat small. Indeed, when the applied load is close to $K_s L_o$, we get very large deflections. (This is inconsistent with our above stipulation that the deflections are "somewhat small," let us ignore that issue for now and accept the results as indicated.) These results, for different values of h, are shown in Figure 1.29 as the continuous lines. The effect of a decreasing h is to cause the transition to be more abrupt. Also shown are the behaviors for $P > K_s L_o$. These solutions could not be reached using monotonic loading, but they do in fact represent equilibrium states that can cause difficulties for a numerical scheme that seeks the equilibrium path approximately, that is, it is possible to accidentally converge on these spurious equilibrium states.

The tangent stiffness for our truss problem takes the explicit form

$$[K_T]_n = \left[\frac{\partial F}{\partial u}\right]_n = \begin{bmatrix} \frac{\partial F_{1x}}{\partial u_1} & \frac{\partial F_{1x}}{\partial v_2} \\ \frac{\partial F_{2x}}{\partial u_1} & \frac{\partial F_{2x}}{\partial v_2} \end{bmatrix}_n = \begin{bmatrix} \frac{\partial \overline{F}_o}{\partial u_1} & -\frac{\partial \overline{F}_o}{\partial v_2} \\ \beta \frac{\partial \overline{F}_o}{\partial u_1} & \frac{1}{L_o}\overline{F}_o + \beta \frac{\partial \overline{F}_o}{\partial u_2} + K_s \end{bmatrix}_n$$

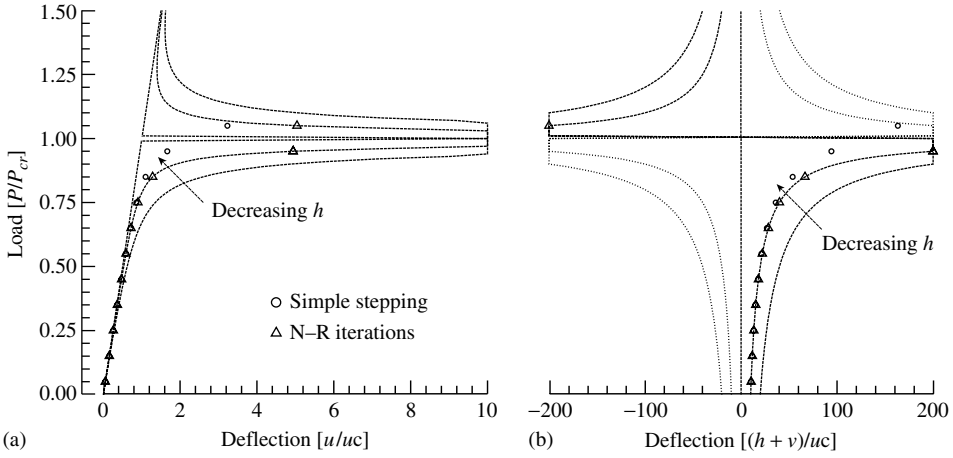

Figure 1.29: Load/deflection behavior for the simple truss. (a) Horizontal displacement u_1. (b) Vertical displacement v_2.

Performing the differentiations

$$\frac{\partial \overline{F}_{\mathrm{o}}}{\partial u_1} = EA\left[-\frac{1}{L_{\mathrm{o}}}\right], \qquad \frac{\partial \overline{F}_{\mathrm{o}}}{\partial v_2} = EA\left[\frac{h}{L_{\mathrm{o}}^2} + \frac{v_2}{L_{\mathrm{o}}^2}\right]$$

then leads to the stiffness

$$[K_{\mathrm{T}}] = \left[\frac{\partial F}{\partial u}\right] = \frac{EA}{L_{\mathrm{o}}}\begin{bmatrix} 1 & -\beta \\ -\beta & \beta^2 + \frac{K_{\mathrm{s}}L_{\mathrm{o}}}{EA} \end{bmatrix} + \frac{\overline{F}_{\mathrm{o}}}{L_{\mathrm{o}}}\begin{bmatrix} 0 & 0 \\ 0 & 1 \end{bmatrix} = [K_{\mathrm{E}}] + [K_{\mathrm{G}}]$$

Note that both matrices are symmetric. The first matrix is the elastic stiffness—the elastic stiffness of a truss member oriented slightly off the horizontal by the angle $\beta = (h + v_2)/L_{\mathrm{o}}$. The second matrix is called the *geometric stiffness matrix* because it arises due to the rotation of the member; note that it depends on the axial load $\overline{F}_{\mathrm{o}}$.

Continuing the special case when $P_{1x} = P$, $P_{2y} = 0$, the system of equations to be solved is

$$\left[\frac{EA}{L_{\mathrm{o}}}\begin{bmatrix} 1 & -\beta \\ -\beta & \beta^2 + \gamma \end{bmatrix} + \frac{\overline{F}_{\mathrm{o}}}{L_{\mathrm{o}}}\begin{bmatrix} 0 & 0 \\ 0 & 1 \end{bmatrix}\right]_n \begin{Bmatrix} \Delta u_1 \\ \Delta v_2 \end{Bmatrix} = \begin{Bmatrix} P \\ 0 \end{Bmatrix}_{n+1} - \begin{Bmatrix} -\overline{F}_{\mathrm{o}} \\ -\beta\overline{F}_{\mathrm{o}} + K_{\mathrm{s}}v_2 \end{Bmatrix}_n$$

with $\gamma = K_{\mathrm{s}}L_{\mathrm{o}}/EA$. A simple solution scheme, therefore, involves computing the increments at each step and updating the displacements as

$$u_{1(n+1)} = u_{1(n)} + \Delta u_1, \qquad v_{2(n+1)} = v_{2(n)} + \Delta v_2$$

The axial force and orientation β also need to be updated as

$$\overline{F}_{\mathrm{o}}|_{n+1} = EA\left[-\frac{u_1}{L_{\mathrm{o}}} + \frac{h}{L_{\mathrm{o}}}\frac{v_2}{L_{\mathrm{o}}} + \frac{1}{2}\left(\frac{v_2}{L_{\mathrm{o}}}\right)^2\right]_{n+1}, \qquad \beta_{n+1} = \frac{h + v_2}{L_{\mathrm{o}}}|_{n+1}$$

Table 1.3 and Figure 1.29 shows the results using this simple stepping scheme where $P_{cr} = K_{\mathrm{s}}L_{\mathrm{o}}$ and $u_{cr} = P_{cr}/EA$.

Table 1.3 also shows the out-of-balance force

$$\{\mathcal{F}\}_{n+1} = \{P\}_{n+1} - \{F\}_{n+1}$$

computed at the end of each step. Clearly, nodal equilibrium is not being satisfied and it deteriorates as the load increases. In order for this simple scheme to give reasonable results, it is necessary that the increments be small. This can be computationally prohibitive for large systems because at each step, the tangent stiffness must be formed and decomposed. A more refined incremental version that uses an iterative scheme to enforce nodal equilibrium will now be developed.

Newton–Raphson Equilibrium Iterations

The increments in displacement are obtained by solving

$$\{K_{\mathrm{T}}\}_n\{\Delta u\} = \{P\}_{n+1} - \{F\}_n$$

Table 1.3: Incremental results using simple stepping.

P/P_{cr}	u_1/u_{cr}	$(h+v_2)/u_{cr}$	P	$\mathcal{F}_{1x}$	$\mathcal{F}_{2y}$
0.0500	0.051000	10.5000	100.00	0.050003	0.989497E−02
0.1500	0.153401	11.6315	300.00	0.256073	0.446776E−01
0.2500	0.257022	13.1329	500.00	0.450836	0.589465E−01
0.3500	0.362372	15.0838	700.00	0.761169	0.759158E−01
0.4500	0.470656	17.7037	900.00	1.37274	0.100333
0.5500	0.584416	21.3961	1100.0	2.72668	0.137041
0.6500	0.709589	26.9600	1300.0	6.19165	0.192208
0.7500	0.862467	36.1926	1500.0	17.0481	0.257334
0.8500	1.09898	53.8742	1700.0	62.5275	0.938249E−01
0.9500	1.66455	94.1817	1900.0	324.939	-4.00430
1.050	3.23104	163.411	2100.0	958.535	-24.0588

from which an estimate of the displacements is obtained as

$$\{u\}_{n+1} \approx \{u\}_n + \{\Delta u\}$$

As just pointed out, if these estimates for the new displacements are substituted into Equation (1.8) then this equation will not be satisfied because the displacements were obtained using only an approximation of the nodal forces given by Equation (1.40). What we can do, however, is repeat the above process at the same applied load level until we get convergence; that is, with i as the iteration counter, we repeat

$$\begin{aligned} \text{solve:} \quad & \{K_{\mathrm{T}}\}_{n+1}^{i-1}\{\Delta u\}^i = \{P\}_{n+1} - \{F\}_{n+1}^{i-1} \\ \text{update:} \quad & \{u\}_{n+1}^{i} = \{u\}_{n+1}^{i-1} + \{\Delta u\}^i \\ \text{update:} \quad & \{K_{\mathrm{T}}\}_{n+1}^{i}, \qquad \{F\}_{n+1}^{i} \end{aligned}$$

until $\{\Delta u\}^i$ becomes less than some tolerance value. The iteration process is started (at each increment) using the starter values

$$\{u\}_{n+1}^{0} = \{u\}_n, \qquad \{K_{\mathrm{T}}\}_{n+1}^{0} = \{K_{\mathrm{T}}\}_n, \qquad \{F\}_{n+1}^{0} = \{F\}_n$$

This basic algorithm is known as the *full Newton–Raphson method*.

Combined incremental and iterative results are also given in Figure 1.29. We see that it gives the exact solution. Iteration results for a single load step equal to $0.95\,P_{cr}$ are given in Table 1.4 in which the initial guesses correspond to the linear elastic solution. We see that convergence is quite rapid, and the out-of-balance forces go to zero.

It is worth pointing out the converged value above P_{cr} in Figure 1.29; this corresponds to a vertical deflection where the truss has "flipped" over to the negative side. Such a situation would not occur physically, but does occur here due to a combination of linearizing the problem (i.e., the small angle approximation) and the nature of the iteration process (i.e., no restriction is placed on the size of the iterative increments).

Table 1.4: Newton–Raphson iterations for a load step 0.95 P_{cr}.

i	u_1	v_2	$u_1 - u_{1ex}$	$v_2 - v_{2ex}$	$\mathcal{F}_{1x}$	$\mathcal{F}_{2y}$
1	−3.02304	76.0009	−3.12184	72.2009	10.3207E+7	−0.244E+7
2	29.0500	75.9986	28.9512	72.1986	0.21923	−72.3657
3	−25.8441	3.95793	−25.9429	0.157933	0.2594E+7	−107896.
4	0.105242	3.95793	0.64416E-2	0.157926	0.6835E-2	−0.158213
5	0.09867	3.80001	−0.12436E-3	0.8344E-5	12.4694	−0.498780
6	0.09880	3.80000	0.15646E-6	0.4053E-5	0.000000	−0.3948E-5
7	0.09880	3.80000	0.000000	0.000000	−0.4882E-3	0.1878E-4
exact	0.09880	3.80000				

The full Newton–Raphson method has the disadvantage that during each iteration, the tangent stiffness matrix must be formed and decomposed. The cost of this can be quite prohibitive for large systems. Thus, effectively, the computational cost is like that of the incremental solution with many steps. It must be realized, however, that because of the quadratic convergence, six Newton–Raphson iterations, say, is more effective than six load increments.

The *modified Newton–Raphson method* is basically as above except that the tangent stiffness is not updated during the iterations but only after each load increment. This generally requires more iterations and sometimes is less stable, but it is less computationally costly.

Both schemes are illustrated in Figure 1.30 where the starting point is from the zero load state—it is clear why the modified method will take more iterations. The plot for the modified method has the surprising implication that we do not need to know the actual tangent stiffness in order to compute correct results—what must be realized in the incremental/iterative scheme is that we are imposing equilibrium (iteratively) in terms

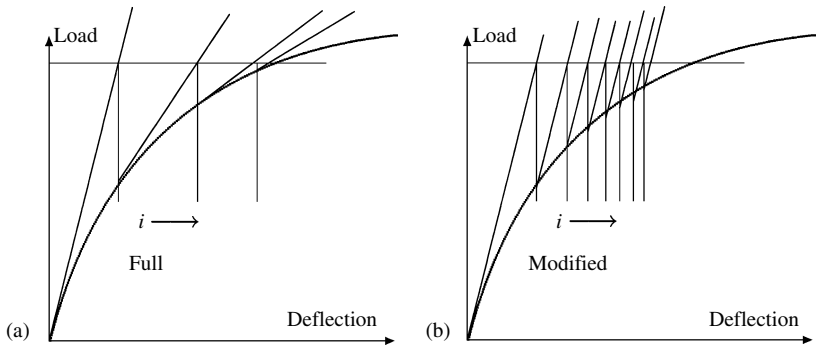

Figure 1.30: Full and modified Newton–Raphson methods for a single load step. (a) The tangent stiffness is updated at each iteration. (b) The tangent stiffness remains the same at each iteration.

of the applied loads and resultant nodal forces; we need good quality *element* stiffness matrices in order to get the good quality element nodal forces, but the assembled tangent stiffness matrix is used only to suggest a direction for the iterative increments; that is, to get the correct converged results we need to have good element stiffness relations, but not necessarily a good assembled tangent stiffness matrix. Clearly, however, a good quality tangent stiffness will give more rapid convergence as well as increase the radius of convergence.

The Corotational Scheme

A particularly effective method for handling the analysis of structures, which undergo large deflections and rotations is the corotational scheme [23, 46, 71]. In this, a local coordinate system moves with each element, and constitutive relations and the like are written with respect to this coordinate system. Consequently, for linear materials, all of the nonlinearities of the problem are shifted into the description of the moving coordinates. We will review just the essentials of the scheme here.

The main objectives are establishing the relation between the local variables and the global variables, from which we can establish the stiffness relations in global variables. To help in the generalization, assume that each element has N nodes with three components of force at each node.

There are $2N$ position variables we are interested in: the global position of each node before deformation ($\hat{x}_{oj}$), and after deformation ($\hat{x}_j$), where the subscript j enumerates the nodes as illustrated in Figure 1.31 for a triangular element. The local positions are given by

$$\hat{\bar{x}}_{oj} = [\, E_{\mathrm{o}}^{\mathrm{T}}]\{\hat{x}_{oj} - \hat{x}_{o1}\}\,, \qquad \hat{\bar{x}}_j = [\, E^{\mathrm{T}}]\{\hat{x}_j - \hat{x}_{o1}\}$$

where $[\, E_{\mathrm{o}} \,]$ and $[\, E \,]$ are the triads describing the orientation of the element before and after deformation, respectively. The local displacements are defined as

$$\hat{\bar{u}}_j = \hat{\bar{x}}_j - \hat{\bar{x}}_{oj}$$

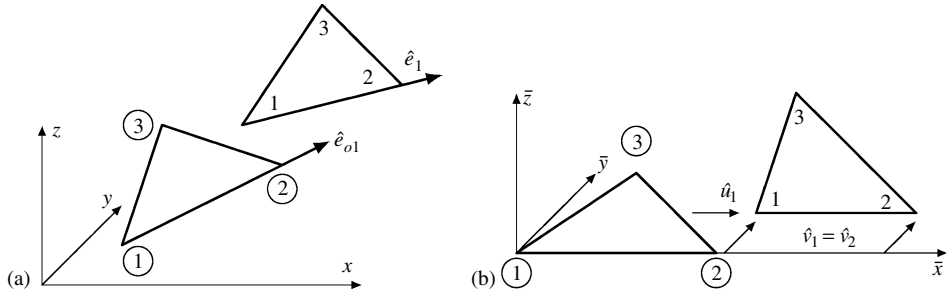

Figure 1.31: The corotational concept. (a) Global positions of an element. (b) Local positions of an element.

The local virtual displacements are related to the global variables by

$$\delta\{\hat{\overline{u}}\}_j = \delta\{[\,E^{\mathrm{T}}\,]\{\hat{x}_j - \hat{x}_{o1}\} - \hat{\overline{x}}_{oj}\} = [\,E^{\mathrm{T}}\,]\{\delta\hat{u}_j\} + \delta[\,E^{\mathrm{T}}\,]\{\hat{x}_j - \hat{x}_{o1}\}$$

Note that, for some vector $\hat{v}$,

$$\delta[\,E^{\mathrm{T}}\,]\{\,v\,\} = [\,E^{\mathrm{T}}\,][S(\hat{v})]\{\delta\beta\}$$

where $\{\beta\}$ is the small rotation spin and the notation $[S(\hat{v})]$ means the skew-symmetric rotation matrix [71] obtained with the components of the corresponding vector; that is, put the components of the vector $\hat{v}$ (i.e., v_x, v_y, v_z) into the rotation array. Using this, we get

$$\{\delta\hat{\overline{u}}\}_j = [\,E^{\mathrm{T}}\,]\{\delta u\}_j + [\,E^{\mathrm{T}}\,][S(\hat{x}_j - \hat{x}_{o1})]\{\delta\beta\}$$

This shows how the local displacements $\{\delta\overline{u}\}_j$, global spin $\{\delta\beta\}$, and global displacements $\{\delta u\}_j$ are interrelated. However, the spin is not independent of the displacements because we require that the local spin be zero (since it is rotating with the element).

Establishing this constraint [71] then leads to

$$\{\delta\overline{u}\} = [\;T\;]\{\delta u\}\,, \qquad [\;T\;] = [\;P\;][\,E^{\mathrm{T}}\,]$$

where we refer to $[\;P\;]$ as a *projector matrix*; it depends only on the local coordinates. Discussions of the projector matrix can be found in References [130, 134, 135].

The virtual work in global variables must equal the virtual work in local variables, hence

$$\{F_{\mathrm{e}}\}^{\mathrm{T}}\{\delta u\} = \{\overline{F}\}^{\mathrm{T}}\{\delta\overline{u}\} = \{\overline{F}\}^{\mathrm{T}}[\;T\;]\{\delta u\}$$

From this we conclude that

$$\{F_{\mathrm{e}}\} = [\;T\;]^{\mathrm{T}}\{\overline{F}\} = [\;E\;][\;P\;]^{\mathrm{T}}\{\overline{F}_{\mathrm{e}}\}$$

What this highlights is the possibility (at least when equilibrium is achieved as part of an iterative process) that local quantities (including the stiffness matrix) have a simple coordinate rotation relation to their global counterparts. We will keep that in mind when we develop the stiffness relations.

At the global level, the variation of the nodal forces leads to

$$\{\delta F_{\mathrm{e}}\} = \left[\frac{\partial F_{\mathrm{e}}}{\partial u}\right]\{\delta u\} = [\,K_{\mathrm{T}}\,]\{\delta u\}$$

where $[\,K_{\mathrm{T}}\,]$ is the element tangent stiffness matrix in global coordinates. Substituting for $\{F_{\mathrm{e}}\}$ in terms of local variables, we get

$$\{\delta F_{\mathrm{e}}\} = [\;T\;]^{\mathrm{T}}\{\delta\overline{F}_{\mathrm{e}}\} + \delta[\;T\;]^{\mathrm{T}}\{\overline{F}_{\mathrm{e}}\} = [\;T\;]^{\mathrm{T}}[\;\overline{k}\;]\{\delta\overline{u}\} + \delta[\;T\;]^{\mathrm{T}}\{\overline{F}_{\mathrm{e}}\}$$

We see that the tangent behavior is comprised of two parts: one is related to the elastic stiffness properties of the element, the other is related to the rotation of the element. Replacing the local variables in terms of the global variables gives

$$\{\delta F_{\mathrm{e}}\} = [\ T\ ]^{\mathrm{T}}[\ \overline{k}\ ][\ T\ ]\{\delta u\} + [\cdots]\{\delta u\}$$

Each term is postmultiplied by $\{\delta u\}$, and therefore we can associate each term with a stiffness matrix. The latter contribution (which is relatively complex) is the geometric stiffness matrix.

The first set of terms

$$[\ k_{\mathrm{E}}\ ] \equiv [\ T\ ]^{\mathrm{T}}[\ \overline{k}\ ][\ T\ ] = [\ E\ ][\ P\ ]^{\mathrm{T}}[\ \overline{k}\ ][\ P\ ][\ E\ ]^{\mathrm{T}}$$

gives the elastic stiffness. We therefore recognize the global stiffness matrix as the components of the local stiffness matrices transformed to the current orientation of the element. However, it is not just the local stiffness itself but the local stiffness times the projector matrix. The remaining set of terms gives the geometric contribution to the stiffness matrix. The contributions to the geometric stiffness reduce to

$$[\ k_{\mathrm{G}}\ ] = [\ E\ ][[\overline{k}_{\mathrm{G1}}] + [\overline{k}_{\mathrm{G2}}] + [\overline{k}_{\mathrm{G3}}]][\ E^{\mathrm{T}}\ ]$$

The core terms are referred only to the local coordinates.

An important point learned from the earlier simple results is that the more accurate the tangent stiffness, the better the convergence rate, but a consequence of using Newton–Raphson equilibrium iterations is that it is not essential that the actual exact tangent stiffness be used. Consequently, if it is convenient to approximate the tangent stiffness, then the basic nonlinear formulation is not affected, only the convergence rate (and radius of convergence) of the algorithm is affected. With this in mind, the geometric stiffness for a frame with member loads $\overline{F}_{\mathrm{o}}$, $\overline{V}_{\mathrm{o}}$, $\overline{V}_{\mathrm{o}}$, is

$$[\ \overline{k}_{\mathrm{G}}\ ]_{11} = \frac{\overline{F}_{\mathrm{o}}}{L}\begin{bmatrix} 0 & 0 & 0 \\ 0 & 1 & 0 \\ 0 & 0 & 1 \end{bmatrix} + \frac{\overline{V}_{\mathrm{o}}}{L}\begin{bmatrix} 0 & -1 & 0 \\ -1 & 0 & 0 \\ 0 & 0 & 0 \end{bmatrix} + \frac{\overline{W}_{\mathrm{o}}}{L}\begin{bmatrix} 0 & 0 & -1 \\ 0 & 0 & 0 \\ -1 & 0 & 0 \end{bmatrix}$$

with the remainder of the $[6 \times 6]$ array given by

$$[\ \overline{k}_{\mathrm{G}}\ ]_{12} = [\ \overline{k}_{\mathrm{G}}\ ]_{21} = -[\ \overline{k}_{\mathrm{G}}\ ]_{22} = -[\ \overline{k}_{\mathrm{G}}\ ]_{11}$$

The contributions associated with the rotational DoF are zero. The $[3 \times 3]$ submatrix of the $[9 \times 9]$ geometric stiffness for a plate with in-plane loads $\overline{N}_{xx}$, $\overline{N}_{xy}$, $\overline{N}_{yy}$, is

$$[\ \overline{k}_{\mathrm{G}}\ ]_{ij} = \frac{\overline{N}_{xx}}{4A}\begin{bmatrix} 0 & 0 & 0 \\ 0 & 0 & 0 \\ 0 & 0 & b_i b_j \end{bmatrix} + \frac{\overline{N}_{xy}}{4A}\begin{bmatrix} 0 & 0 & 0 \\ 0 & 0 & 0 \\ 0 & 0 & b_i c_j + b_j c_i \end{bmatrix} + \frac{\overline{N}_{yy}}{4A}\begin{bmatrix} 0 & 0 & 0 \\ 0 & 0 & 0 \\ 0 & 0 & c_i c_j \end{bmatrix}$$

where the coefficients are those of the triangular interpolations Again, the contributions associated with the rotational DoF are zero. Thus, in both cases, we ignore flexural effects on the geometric stiffness and say it depends only on the axial/membrane behavior.

Nonlinear Dynamics

When inertia effects are significant in nonlinear problems, as in such problems as wave propagation, we have the choice of using either an explicit integration scheme or an implicit scheme. We will see that the explicit scheme is simpler to implement (primarily because it does not utilize the tangent stiffness matrix) and therefore is generally the more preferable of the two.

We assume the solution is known at time t and wish to find it at time $t + \Delta t$. The applied loads in this case include the inertia and damping forces. For the explicit scheme, we begin with the dynamic equilibrium equation at time t

$$[\ M\ ]\{\ddot{u}\}_t + [\ C\ ]\{\dot{u}\}_t = \{P\}_t - \{F\}_t$$

Using difference expressions for the nodal velocities and accelerations at the current time leads to

$$\left[\frac{1}{2\Delta t}C + \frac{1}{\Delta t^2}M\right]\{u\}_{t+\Delta t} = \{P\}_t - \{F\}_t - \left[-\frac{2}{\Delta t^2}M\right]\{u\}_t - \left[\frac{1}{\Delta t^2}M - \frac{1}{2\Delta t}C\right]\{u\}_{t-\Delta t} \tag{1.41}$$

Generally, the mass and damping matrices are arranged to be diagonal and hence the solution for the displacements is a trivial computational effort (a simple division). Furthermore, there are no equilibrium iteration loops as will be needed in the implicit schemes.

A very important feature of this scheme is that the structural stiffness matrix need not be formed [22]; that is, we can assemble the element nodal forces directly for each element. This is significant in terms of saving memory and also has the advantage that the assemblage effort can be easily distributed on a multiprocessor computer. Furthermore, since the nodal forces $\{F\}$ are obtained directly for each element, there is flexibility in the types of forces that can be allowed. For example, Reference [175] uses a cohesive stress between element sides in order to model the dynamic fracture of brittle materials. In this context, we can also model deformation dependent loading effects (such as follower forces or sliding friction) without changing the basic algorithm.

As indicated in Figure 1.27, our meaning of structural dynamics is the frequency range that begins close to zero and extends a moderate way, perhaps 5 to 50 of the modal frequencies. Since this encompasses nearly static problems, we see that we must use some sort of implicit integration scheme that utilizes the tangent stiffness [71]. The dynamic equilibrium equation at time $t + \Delta t$ is

$$[\ M\ ]\{\ddot{u}\}_{t+\Delta t} + [\ C\ ]\{\dot{u}\}_{t+\Delta t} = \{P\}_{t+\Delta t} - \{F\}_{t+\Delta t} \tag{1.42}$$

The element nodal loads are not known but, as was done in the static case, can be approximated as

$$\{F\}_{t+\Delta t} \approx \{F\}_t + \{\Delta F\} = \{F\}_t + [\ K_{\mathrm{T}}\ ]\{\Delta u\}\,, \qquad [\ K_{\mathrm{T}}\ ] \equiv \left[\frac{\partial F}{\partial u}\right] \tag{1.43}$$

where $\{\Delta F\}$ is the increment in element nodal loads due to an increment in the displacements. Using the finite differences of the constant acceleration method allows the increment in displacements to be obtained by solving

$$\left[K_{\mathrm{T}} + \frac{4}{\Delta t}C + \frac{4}{\Delta t^2}M\right]\{\Delta u\} = \{P\}_{t+\Delta t} - \{F\}_t + [\ C\ ]\left\{\frac{2}{\Delta t}u + \dot{u}\right\}_t + [\ M\ ]\left\{\frac{4}{\Delta t^2}u + \frac{4}{\Delta t}\dot{u} + \ddot{u}\right\}_t \tag{1.44}$$

Just as in the static case, we need Newton–Raphson iterative improvements to the solution; these are obtained by

$$\left[K_{\mathrm{T}} + \frac{4}{\Delta t}C + \frac{4}{\Delta t^2}M\right]^{i-1}\{\Delta u\}^i = \{P\}_{t+\Delta t} - \{F\}^{i-1}_{t+\Delta t} + [\ C\ ]\left\{\frac{-2}{\Delta t}\left(u^{i-1}_{t+\Delta t} - u_t\right) + \dot{u}\right\}_t + [\ M\ ]\left\{\frac{-4}{\Delta t^2}\left(u^{i-1}_{t+\Delta t} - u_t\right) + \frac{4}{\Delta t}\dot{u} + \ddot{u}\right\}_t \tag{1.45}$$

The iteration process is started (at each increment) using the starter values

$$\{u\}^0_{t+\Delta t} = \{u\}_t\,, \qquad [\,K_{\mathrm{T}}\,]^0_{t+\Delta t} = [\,K_{\mathrm{T}}\,]_t\,, \qquad \{F\}^0_{t+\Delta t} = \{F\}_t$$

This basic algorithm is essentially the same as for the static case.

The implicit integration scheme, when applied to nonlinear problems, has a step size restriction much more restrictive than for the corresponding linear problem [71]. Schemes for improving the algorithm are discussed in References [46, 84, 111], but all require additional computations at the element level and therefore are not readily adapted to general-purpose finite element programs. The best that can be done at present is to always test convergence with respect to step size and tolerance.

As done for linear problems, generally, we take the damping as proportional in the form

$$[\ C\ ] = \alpha[\ M\ ] + \beta[\ K\ ]$$

The easiest way to see the effect of damping is to observe the attenuation behavior of a wave propagating in a structure. From this it becomes apparent that when $\alpha \neq 0$, $\beta = 0$ (mass proportional), the low frequencies are attenuated, whereas, when $\alpha = 0$, $\beta \neq 0$ (stiffness proportional), the high frequencies are attenuated.

These results have an important implication for our choice of time integration scheme. If we choose an explicit integration scheme, then the stiffness matrix is not readily available and we must use a mass proportional damping. Consequently, the high-frequency components will not be attenuated. If, in order to get some sort of high-frequency attenuation, $[\ C\ ]$ is approximated somehow in terms of an initial stiffness matrix, then we loose the advantage of dealing with diagonal matrices, and the computational cost increases significantly.

1.9 Nonlinear Materials

Figure 1.32 shows two examples of nonlinear behavior: one is nonlinear elastic, and the other is elastic/plastic. We elaborate on both of these in this section.

The key to the FEM formulation for nonlinear materials is to write the element stiffness relations for the increment of strain rather than the total strain. In this sense, it has a good deal in common with the incremental formulation of the geometrically nonlinear problem. For the explicit integration scheme where equilibrium is imposed at step n to get the displacement at $n+1$, we need to know the element nodal forces $\{F\}_n$. These are obtained as part of the updating after the new displacements are computed. For example, for each element

$$\{F_{\mathrm{e}}\}_n = \{F_{\mathrm{e}}\}_{n-1} + \{\Delta F_{\mathrm{e}}\} = \{F_{\mathrm{e}}\}_{n-1} + [\,K_{\mathrm{T}}\,]\{u_n - u_{n-1}\}$$

If the stresses change significantly over the step, then $\{\Delta F_{\mathrm{e}}\}$ is obtained by integrating over the step. For the implicit integration scheme, $\{u\}_{n+1}$ and $\{F_{\mathrm{e}}\}_{n+1}$ are obtained simultaneously as part of the Newton–Raphson iterations.

The constitutive description is simplest in the corotational context (because the rotations are automatically accounted for) and that is the one used here. We consider both nonlinear elastic and elastic-plastic materials and the task is to establish $[\ \overline{k}\ ]$.

Hyperelastic Materials

Hyperelastic materials are elastic materials for which the current stresses are some (nonlinear) function of the current total strains; a common example is the rubber materials. For these materials, the stresses are derivable from an elastic potential, which can be written (from Equation (1.18)) for small strain as

$$\sigma_{ij} = \frac{\partial \mathcal{U}}{\partial \epsilon_{ij}}$$

A simple 1-D example is

$$\mathcal{U} = E[\tfrac{1}{2}\epsilon^2 - \tfrac{1}{6}\epsilon^3/\epsilon_o]\,, \qquad \sigma = f(\epsilon) = E[\epsilon - \tfrac{1}{2}\epsilon^2/\epsilon_o]\,, \qquad E_{\mathrm{T}} = E[1 - \epsilon/\epsilon_o]$$

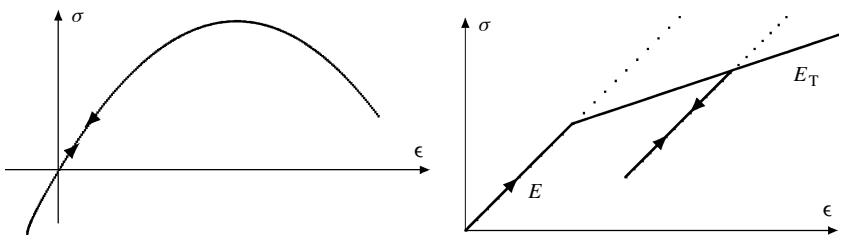

Figure 1.32: Examples of nonlinear material behavior. (a) Elastic. (b) Elastic-plastic.

and is depicted in Figure 1.32(a). Even this simple example shows a characteristic of nonlinear materials (and nonlinear problems in general), namely, the possibility of (static) instabilities. This would occur when $\epsilon = \epsilon_o$ giving a zero tangent modulus and hence a zero tangent stiffness; we will not be considering these cases.

In an incremental formulation over many steps n, given $\{\Delta u\}$, we compute the increment of strain as

$$\{\Delta\epsilon\} = \{\epsilon_{n+1} - \epsilon_n\}, \qquad \epsilon_{n+1} = \epsilon(u_{n+1}) \quad \epsilon_n = \epsilon(u_n)$$

It is necessary to store the previous strain $\{\epsilon\}_n$ at each time step. The tangent modulus relationship can be written, in general, as

$$\Delta\sigma_{ij} = \sum_{p,q} \frac{\partial^2 \mathcal{U}}{\partial\epsilon_{ij}\partial\epsilon_{pq}}\Delta\epsilon_{pq} = \sum_{p,q} D_{Tijpq}\Delta\epsilon_{pq} \qquad \text{or} \qquad \{\Delta\sigma\} = [\,D_{\mathrm{T}}\,]\{\Delta\epsilon\}$$

Note that the fourth-order tensor $[\,D_{\mathrm{T}}\,]$ is symmetric but generally not constant, being a function of the current strains. We need it to form the tangent stiffness matrix for an element, but the stresses (when needed) will be computed from the total strain relationship. The element stiffness in local coordinates is

$$[\,\overline{k}_{\mathrm{T}}\,] = \int_V [\;B\;]^{\mathrm{T}}[\,D_{\mathrm{T}}\,][\;B\;]\,\mathrm{d}V$$

and therefore has the same structure as the corresponding linear element—only the appropriate tangent modulus need be used. For example, the nonlinear rod has

$$[\,\overline{k}_{\mathrm{T}}\,] = \frac{\hat{E}_{\mathrm{T}}A}{L}\begin{bmatrix} 1 & -1 \\ -1 & 1 \end{bmatrix}, \qquad \hat{E}_{\mathrm{T}} \equiv \int_{\epsilon}^{\epsilon+\Delta\epsilon} E_{\mathrm{T}}(\epsilon)\,\mathrm{d}\epsilon$$

If $\Delta\epsilon$ is large, then numerical methods may be used to compute the integral.

Elastic-Plastic Materials

Thin-walled structures, for example, have a plane state of stress where σ_{zz}, σ_{xz}, and σ_{yz} are all approximately zero; we will derive explicit elastic-plastic relations for this case.

Plasticity is a phenomenon that occurs beyond a certain stress level called the yield stress. The von Mises yield function, for example, is

$$f = [\sigma_{xx}^2 + \sigma_{yy}^2 - \sigma_{xx}\sigma_{yy} + 3\sigma_{xy}^2]^{1/2} - \sigma_Y \equiv \overline{\sigma} - \sigma_Y$$

where σ_Y is the yield stress for a uniaxial specimen. In this relation, $\overline{\sigma}$ is called the *effective stress*, which is a scalar measure of the level of stress. We would like to have a similar effective measure of the plastic strain.

The basic assumptions of the Prandtl–Reuss theory of plasticity [99, 101] is that plasticity is a distortion (no volume change) dominated phenomenon and that the plastic strain increments are proportional to the current stress deviation. Thus

$$\frac{\Delta\epsilon_{xx}^p}{\sigma_{xx} - \sigma_{\mathrm{m}}} = \frac{\Delta\epsilon_{yy}^p}{\sigma_{yy} - \sigma_{\mathrm{m}}} = \frac{\Delta\epsilon_{zz}^p}{\sigma_{zz} - \sigma_{\mathrm{m}}} = \frac{\Delta\epsilon_{xy}^p}{\sigma_{xy}} = \frac{\Delta\epsilon_{yz}^p}{\sigma_{yz}} = \frac{\Delta\epsilon_{zx}^p}{\sigma_{zx}} = \mathrm{d}\lambda \qquad (1.46)$$

where

$$\sigma_{\mathrm{m}} = (\sigma_{xx} + \sigma_{yy} + \sigma_{zz})/3$$

is the mean hydrostatic stress. Specializing this for plane stress gives

$$\begin{Bmatrix} \Delta\epsilon^p_{xx} \\ \Delta\epsilon^p_{yy} \\ 2\Delta\epsilon^p_{xy} \end{Bmatrix} = \frac{\mathrm{d}\lambda}{3} \begin{Bmatrix} 2\sigma_{xx} - \sigma_{yy} \\ 2\sigma_{yy} - \sigma_{xx} \\ 6\sigma_{xy} \end{Bmatrix} = \frac{\mathrm{d}\lambda}{3}\{ s \}, \qquad \begin{Bmatrix} \sigma_{xx} \\ \sigma_{yy} \\ \sigma_{xy} \end{Bmatrix} = \frac{1}{\mathrm{d}\lambda} \begin{Bmatrix} 2\Delta\epsilon^p_{xx} + \Delta\epsilon_{yy} \\ 2\Delta\epsilon^p_{yy} + \Delta\epsilon_{xx} \\ \Delta\epsilon^p_{xy} \end{Bmatrix}$$

The plastic work performed during an increment of plastic strain is

$$\Delta W^p = \sigma_{xx}\Delta\epsilon^p_{xx} + \sigma_{yy}\Delta\epsilon^p_{yy} + \sigma_{xy}2\Delta\epsilon^p_{xy} \equiv \overline{\sigma}\Delta\overline{\epsilon}^p$$

We can substitute for the strain increments in terms of the stresses to get

$$\Delta W^p = \tfrac{2}{3}\mathrm{d}\lambda \left[\sigma^2_{xx} + \sigma^2_{yy} - \sigma_{xx}\sigma_{yy} + 3\sigma^2_{xy}\right] = \tfrac{2}{3}\mathrm{d}\lambda\overline{\sigma}^2$$

Comparing the two work terms leads to the measure of effective plastic strain

$$\Delta\overline{\epsilon}^p = \tfrac{2}{3}\mathrm{d}\lambda\overline{\sigma} \qquad \text{and} \qquad \Delta W^p = \frac{3}{2\mathrm{d}\lambda}\Delta\overline{\epsilon}^{p2}$$

It remains now to determine $\Delta\overline{\epsilon}^p$ in terms of its components. Substitute for the stresses in terms of the strain increments in the plastic work expression to get

$$\Delta W^p = \frac{2}{\mathrm{d}\lambda}[\Delta\epsilon^{p2}_{xx} + \Delta\epsilon^{p2}_{yy} + \Delta\epsilon^p_{xx}\Delta\epsilon^p_{yy} + \Delta\epsilon^{p2}_{xy}] = \frac{3}{2\mathrm{d}\lambda}\Delta\overline{\epsilon}^{p2}$$

from which we conclude that

$$\Delta\overline{\epsilon}^p = \frac{2}{\sqrt{3}}[\Delta\epsilon^{p2}_{xx} + \Delta\epsilon^{p2}_{yy} + \Delta\epsilon^p_{xx}\Delta\epsilon^p_{yy} + \Delta\epsilon^{p2}_{xy}]^{1/2}$$

We also have the interpretation, analogous to Equation (1.46),

$$\mathrm{d}\lambda = \frac{3}{2}\frac{\Delta\overline{\epsilon}^p}{\overline{\sigma}}$$

Thus, $\mathrm{d}\lambda$ relates the increment of plastic stress to the current stress state. For uniaxial stress, these plasticity relations reduce to

$$\overline{\sigma} = \sigma_{xx}, \qquad \Delta\overline{\epsilon} = \Delta\epsilon_{xx}$$

and the plastic parameters become

$$\mathrm{d}\lambda = \frac{\frac{3}{2}E\sigma_{xx}\Delta\epsilon_{xx}}{[E\sigma^2_{xx} + H']}, \qquad \Delta\epsilon_{xx} = \frac{3}{2}\mathrm{d}\lambda\sigma_{xx}, \qquad \Delta\sigma_{xx} = E\left[1 - \frac{E}{E + H'}\right]\Delta\epsilon_{xx}$$

This elastic-plastic behavior is shown in Figure 1.32(b).

Most structural materials increase their yield stress under increased loading or straining; this is called *strain hardening* or *work hardening*. Let the yield stress change according to

$$f = \overline{\sigma}(\sigma) - \sigma_Y(\overline{\epsilon}^p)\,, \qquad \overline{\epsilon}^p = \sum \Delta\overline{\epsilon}^p$$

Under uniaxial tension with σ_{xx} as the only nonzero stress, we have $\overline{\sigma} = \sigma_{xx} = \sigma_Y$. This leads to $\Delta\epsilon^p_{yy} = -\frac{1}{2}\Delta\epsilon^p_{xx}$ giving $\Delta\overline{\epsilon}^p = \Delta\epsilon^p_{xx}$; consequently, the relationship between $\overline{\epsilon}$ and $\overline{\sigma}$ can be taken directly off the uniaxial stress/strain curve. In particular,

$$\sigma_Y = \sigma_{Y0} + H'\overline{\epsilon}^p \qquad \text{or} \qquad H' = \frac{\partial\sigma_Y}{\partial\overline{\epsilon}^p} = \frac{\partial\sigma_{xx}}{\partial\epsilon^p_{xx}} = \frac{E_{\mathrm{T}}}{1 - E_{\mathrm{T}}/E}$$

This is shown in Figure 1.32(b).

With increasing stress, plastic flow occurs, and the yield surface expands so that the stresses always remain on the yield surface. This means that

$$\Delta f = \Delta\overline{\sigma}(\sigma) - \Delta\sigma_Y(\overline{\epsilon}^p) = \left\{\frac{\partial\overline{\sigma}}{\partial\sigma}\right\}^{\mathrm{T}}\{\Delta\sigma\} + \frac{\partial\sigma_Y}{\partial\overline{\epsilon}^p}\Delta\overline{\epsilon}^p = \frac{1}{2\overline{\sigma}}\{s\}^{\mathrm{T}}\{\Delta\sigma\} - H'\frac{2}{3}\overline{\sigma}\mathrm{d}\lambda = 0$$

Solving for $\mathrm{d}\lambda$, we then have an alternative expression for the increments of plastic strain

$$\{\Delta\epsilon^p\} = \left[\frac{\{s\}\{s\}^{\mathrm{T}}}{\overline{\sigma}^2 H'}\right]\{\Delta\sigma\} = [\,C_{\mathrm{p}}\,]\{\Delta\sigma\}$$

The $[3 \times 3]$ square bracket term is like an (inverse) modulus; in this case, however, it is a stress-dependent modulus.

At each stage of the loading, the increment of stress is related to the increment of strain. To establish this incremental stiffness relation, we need to replace the plastic strain increments with total strains. The elastic strain increment and the stresses are related by Hooke's law

$$\{\Delta\sigma\} = [\,D_{\mathrm{e}}\,]\{\Delta\epsilon^e\}\,, \qquad [\,D_{\mathrm{e}}\,] = \frac{E}{1-\nu^2}\begin{bmatrix} 1 & \nu & 0 \\ \nu & 1 & 0 \\ 0 & 0 & (1-\nu)/2 \end{bmatrix}$$

Replace the elastic strains with total strains

$$\{\Delta\sigma\} = [\,D_{\mathrm{e}}\,]\{\Delta\epsilon - \Delta\epsilon^p\} = [\,D_{\mathrm{e}}\,]\{\{\Delta\epsilon\} - \tfrac{1}{3}\lambda\{s\}\}$$

and substitute this into the strain-hardening relation to solve for $\mathrm{d}\lambda$ as

$$\mathrm{d}\lambda = \frac{3\{s\}^{\mathrm{T}}[\,D_{\mathrm{e}}\,]\{\Delta\epsilon\}}{\{s\}^{\mathrm{T}}[\,D_{\mathrm{e}}\,]\{s\} + 4H'\overline{\sigma}^2}$$

The incremental stress relation thus becomes

$$\{\Delta\sigma\} = [\,D_{\mathrm{e}}\,]\left[\lceil\ 1\ \rfloor - \frac{\{s\}\{s\}^{\mathrm{T}}[\,D_{\mathrm{e}}\,]}{\{s\}^{\mathrm{T}}[\,D_{\mathrm{e}}\,]\{s\} + 4H'\overline{\sigma}^2}\right]\{\Delta\epsilon\} = [\,D_{\mathrm{T}}\,]\{\Delta\epsilon\}$$

The element tangent stiffness for the increments is then

$$[\, k_{\mathrm{T}} \,] = \int_V [\, B \,]^{\mathrm{T}} [\, D_{\mathrm{T}} \,][\, B \,]\, \mathrm{d}V = [\, B \,]^{\mathrm{T}} [\, D_{\mathrm{T}} \,][\, B \,]\, V$$

In the case of the CST element, it is thus just a matter of replacing the elastic material stiffness with the elastic/plastic stress-dependent relation. From a programming point of view, it is necessary to remember the state of stress and elastic strain from the previous step.

Discussion of Nonlinear Materials in FEM Codes

The purpose of this section, as is so with many other sections, is to give an intimation of the issues addressed in actual FEM codes. It is not intended to be a primer on how to program these codes—this is best left to specialist books. Indeed, as we will see in the ensuing chapters, we will develop inverse methods whereby we use FEM programs as stand-alone external processes such that FEM code is not part of the inverse methods. In this way, essentially, if an FEM program can handle a certain nonlinear material behavior, then the inverse method also can handle that material behavior and the particular implementation details are not especially relevant. This also applies to special material implementations such as those for composite materials.